UNCLASSIFIED

AD NUMBER
AD801025
NEW LIMITATION CHANGE
TO Approved for public release, distribution unlimited
FROM Distribution authorized to U.S. Gov't. agencies and their contractors; Critical Technology; JUN 1966. Other requests shall be referred to Air Force Flight Dynamics Laboratory, ATTN: FDTR, Wright-Patterson AFB, OH 45433.
AUTHORITY
AFFDL ltr dtd 15 Feb 1973

THIS PAGE IS UNCLASSIFIED

AFFDL-TR-66-92

AD801025

A STUDY OF THE INFLUENCE OF GEOMETRY ON THE STRENGTH OF FATIGUE CRACKED PANELS

E. K. Walker

NOTICES

When Government drawings, specifications, or other data are used for any purpose other than in connection with a definitely related Government procurement operation, the United States Government thereby incurs no responsibility nor any obligation whatsoever; and the fact that the Government may have formulated, furnished, or in any way supplied the said drawings, specifications, or other data, is not to be regarded by implication or otherwise as in any manner licensing the holder or any other person or corporation, or conveying any rights or permission to manufacture, use, or sell any patented invention that may in any way be related thereto.

BEST AVAILABLE COPY

Copies of this report should not be returned [illegible] nology Division unless return is required by security [illegible] contractual obligations, or notice on a specific [illegible]

AFFDL-TR-66-92

A STUDY OF THE INFLUENCE OF GEOMETRY ON THE STRENGTH OF FATIGUE CRACKED PANELS

E. K. Walker

FOREWORD

This report was prepared by Northrop Norair, a Division of Northrop Corporation, Hawthorne, California, under Air Force Contract AF 33(615)-2522. The effort reported herein is a part of an advanced development effort under Project 1467, "Structural Analysis Methods," Task 146704, "Structural Fatigue Analysis." The work was administered under the direction of the Air Force Flight Dynamics Laboratory, Research and Technology Division, Wright-Patterson Air Force Base, Ohio, by Mr. V. E. Kearney, FDTR, Project Engineer.

The research reported herein was conducted between June 1965 and May 1966. The report was submitted by the author for review by the AFFDL on 1 June 1966. This report has been assigned NOR 66-131 for internal control at Northrop Norair.

The author expresses appreciation for technical support provided throughout the program by Mr. D. P. Wilhem, the valuable contributions of Mr. John Spratt, Test Engineer, and Mr. Mark Welever, Laboratory Technician, and to the many other Norair personnel who contributed to the program. The aforementioned program was under the technical direction of Mr. R. D. Hayes.

Publication of this report does not constitute Air Force approval of the report's findings or conclusions. It is published only for the exchange and stimulation of ideas.

FRANCIS J. JANIK, JR.
Chief, Theoretical Mechanics Branch
Structures Division

ABSTRACT

The objectives of the study program were to define and verify a synthesis of strength-limiting parameters for fatigue cracked panels which would be applicable to the wide range of conditions of interest in the engineering problem of strength analysis and to present this synthesis in a form that would lead to a better conceptual understanding of the interaction between parameters.

The program consisted of an analytical study and a supporting experimental study. The analytical study, governed by the above objectives, considered fracture in the elastic range with buckling restraint provided, fracture combined with net section and gross section yielding, and fracture in the elastic range for unrestrained panels. The design problem involving appreciable amounts of slow tear was also considered. The experimental program provided supporting information on the behavior of fatigue cracks for bare 2024-T3 aluminum. Limited test data were also obtained for duplex annealed titanium 8Al-1Mo-1V. The aluminum alloy crack lengths ranged from .5 inch to over 10 inches. Panel widths were thirty, twenty, twelve and nine inches, and nominal panel thicknesses were .080 inch, .063 inch, and .032 inch. The titanium alloy panel widths were twelve and nine inches, and thicknesses were .045 inch and .020 inch. Buckling restraints were used for approximately half of the panels tested.

Test information from other sources was used to illustrate specific points in theory and to show the generality of conclusions.

TABLE OF CONTENTS

TABLE OF CONTENTS (Cont.)

TABLE OF CONTENTS (Cont.)

TABLE OF CONTENTS (Cont.)

LIST OF ILLUSTRATIONS

LIST OF ILLUSTRATIONS (Cont.)

LIST OF ILLUSTRATIONS (Cont.)

LIST OF ILLUSTRATIONS (Cont.)

LIST OF TABLES

LIST OF SYMBOLS

A	area	inches^2
C	boundary influence coefficient	
c	spring constant for elastic restraint of column	psi
E	Young's modulus	ksi
e_B	critical column strain for buckling	inches/inch
Esec	secant modulus	ksi
e_{py}	component of plastic strain normal to a crack	inches/inch
e_u	ultimate crack tip strain	inches/inch
e_x	component of elastic strain parallel to a crack	inches/inch
e_y	component of elastic strain normal to a crack	inches/inch
I	moment of inertia	inches^4
k	crack tip stress intensity parameter	ksi $\sqrt{\text{inch}}$
k_2	crack tip stress intensity parameter corresponding to the beginning of unstable tear	ksi $\sqrt{\text{inch}}$
ℓ	crack length	inches
ℓ_1	initial crack length	inches
m	interaction exponent	
P_B	critical column load for buckling	kips
r_p	radius of plastic zone	inches
s	$\sqrt{1 + \frac{\Delta\ell}{\ell_1}}$	
t	panel thickness	inches
w	panel width	inches
β	$\sqrt[4]{c/4EI}$	inches^{-1}

LIST OF SYMBOLS (Cont.)

γ	A lumped multiplying parameter for comparison between crack buckling and an Euler column	
δ	buckling deflection measured at crack centerline	inches
μ	Poisson's ratio	
μ_p	Poisson's ratio for plastic strain	
ρ'	effective crack tip radius	inches
$\bar{\sigma}$	width adjusted stress	ksi
σ_B	critical column stress for buckling	ksi
σ_o	gross uniaxial stress normal to and away from a crack	ksi
σ_{ox}	gross panel stress away from and parallel to a crack (biaxial stress)	ksi
σ_{oy}	gross panel stress away from and normal to a crack (biaxial stress)	ksi
σ_n	net cross section stress	ksi
σ_u	ultimate gross panel stress corresponding to e_u	ksi
σ_y	yield stress	ksi

I INTRODUCTION

During the past several years, there has been considerable advancement in the concepts of fracture mechanics and in the application of these concepts to the problems of material evaluation[1]. In those design cases where relatively small flaws are present at the onset of fracture, a fracture mechanics approach has also proven valuable[2]. However, for design and strength evaluations for those relatively ductile materials of most interest for aircraft structure, larger flaws or fatigue cracks are more likely to be of interest. For these larger flaws, parameters not normally considered as part of the materials evaluation can have a significant influence on the resulting strength. Thus, while materials evaluation studies have for the most part employed the fracture mechanics concepts, many of the studies more directly concerned with structural evaluation have chosen alternate approaches which permit the introduction of additional variables[3,4,5,6]. One of these alternate methods, the notch-strength analysis method[5,6] has found favor for its ability to evaluate the strength reduction resulting from fatigue cracks for those cases where general yielding accompanies fracture and also for those cases where buckling occurs due to the presence of a fatigue crack. The notch analysis method makes use of an effective radius concept[7] and, thus, the information usually gathered during material evaluation studies based on fracture mechanics concepts is not useable. Data from which the influence of general yielding and panel buckling can be determined are seldom available.

In order that the bulk of information now being compiled on fracture strength be more applicable to design oriented problems, further understanding of the influence of geometric variables must be attained and design methods using this understanding in conjunction with fracture mechanics concepts should be explored. The program reported herein has been undertaken with this objective in mind.

II SUMMARY

The influences of gross section yielding and panel buckling on the stress intensity for the end of stable tear in wide panels is presented in the form of a diagram (Figure 29) having three non-dimensional axes representing ultimate strength failure, elastic fracture and the influences of panel buckling. Three zones of behavior are designated on the diagram as follows:

Zone I Short Cracks - The beginning of unstable tear occurs due to a combination of fracture and gross section yielding. The suggested equation for predicting the stress intensity at the beginning of unstable tear is

$$\left\langle \frac{\sigma_c - 0.8\,\sigma_y}{\sigma_u - 0.8\,\sigma_y} \right\rangle^m + \frac{\bar{\sigma} \ell^{\frac{1}{2}}}{k_2} = 1$$

Zone II Intermediate Cracks - The beginning of unstable tear occurs with gross panel stress in the elastic range. The influence of panel buckling in 2024-T3 aluminum can be assumed constant, with the stress intensity k_2 at the onset of unstable tear correspondingly less than in guided panels. The quantity, $\left\langle \frac{\sigma_o - .8\,\sigma_y}{\sigma_u - .8\,\sigma_y} \right\rangle^m$, is negative and, thus, assumed as zero so that the equation for predicting unstable tear becomes

$$\frac{\bar{\sigma} \ell^{\frac{1}{2}}}{k_2} = 1$$

Zone III Long Cracks - Cracks whose length to panel width ratio exceeds 1/3 can be expected to show further reduction in the stress intensity, k_2, resulting from the influence of panel width on buckling.

The use of the interaction diagram is illustrated by data from 20 and 30 inch wide panels of 2024-T3 aluminum. Trends and behavior of fatigue cracks in 9 inch wide and 12 inch wide 2024-T3 aluminum and titanium 8Al-1Mo-1V are explained in terms of components of the interaction diagram and by curves showing strength reduction in narrow panels beyond that predicted by elastic analysis methods.

III PREFACE

The discussion and theory are presented in the following sections. Section IV deals with the problem of panels to which sufficient lateral support is provided so that the panel remains essentially flat at failure (guided panels) and the net cross section remains elastic. These limitations in behavior currently define the problem area in which linear elastic fracture mechanics have proven relatively successful[1]. In approaching the presentation of theory for this range of behavior, the need to incorporate problems involving stable crack growth led to the choice of static considerations of ultimate strain at the crack tip as a failure criterion rather than the more standard energy approach. The first section of theory thus represents an attempt to restate basic concepts of fracture mechanics in terms of static considerations insofar as practical. An attempt has also been made to define limitations of current theory and thus define the limits of panel geometries to which the extensions of theory explored in subsequent sections are applicable.

The sections that follow consider extensions of theory for problems of general yielding accompanying fracture, failure of unrestrained panels that distort from a flat panel prior to failure (panel buckling) and finally, the synthesis of the strength reducing influences of fracture, yielding, and panel buckling into a single failure diagram.

An additional section discusses the problem of predicting the amount of slow tear preceding final rupture and includes suggestions of how this additional variable can be introduced into failure considerations.

Because of the complex nature of the fracture problem, many of the formulations suggested are empirical in nature. In each case, however, an attempt has been made to retain at least a qualitative theoretical base and to provide for growth potential within the basic formulation as understanding is increased. It is hoped that the resulting compilation will thus both add to the basic understanding of the interaction between strength influencing parameters and encourage additional studies to explore details which were of necessity left unresolved by the scope of the present program.

The experimental data for 2024-T3 aluminum and titanium 8Al-1Mo-1V used in the development of curves and illustration of theory, unless specifically noted, were obtained during the supporting test program. A tabulated summary of these data along with stress vs crack length curves are found in the Appendix.

IV GUIDED PANELS WITH ELASTIC BEHAVIOR AWAY FROM CRACK

COMPARISON OF FAILURES IN MATERIALS WITH LOW AND HIGH DUCTILITY

The definition of failure in a brittle material is a relatively simple matter due to the lack of significant amounts of slow tear. Thus, the initial crack length and the stress corresponding to the maximum load are all that need be considered. Additionally, plastic deformation is not a significant consideration and an elastic formulation of stress concentration or energy is reasonably applicable. For a relatively ductile material, however, the problem becomes more complex. Stable slow tear initiates at a load level considerably below the ultimate load. In this stable slow tear phase, the tearing can be stopped by stopping the loading process. Eventually, a maximum load is reached. If this maximum load is approached through a process of small increments of loading, successively longer increments of tear can be observed as the maximum load is approached. At the maximum load, an additional increment in load will result in a continued slow extension of the crack, indicating an unstable condition. Near the end of this unstable phase of crack extension, noticeable acceleration occurs ending in an explosive and almost instantaneous separation of the remainder of the uncracked section.

POSSIBLE FAILURE CRITERIA

From the above failure sequence for a relatively ductile material containing a crack, two different methods of measuring or defining failure criteria are currently used.

1. The initial crack length and stress at maximum load[5].

2. The crack length and stress at maximum load [1].

Two additional criteria could be of interest.

3. The crack length and load at the onset of crack acceleration.

4. The crack length and load at rupture.

Each of the above criteria properly have a place in the overall problem of strength evaluation and analysis. The typical sequence of these four possible criteria are shown diagramatically in Figure 1. From Figure 1, it can be seen that with the exception of the first criterion, each criterion could be represented by some instantaneous condition of stress, strain, or energy within the panel during the failure sequence. The first criterion of initial crack length and maximum load is not subject to rigorous stress, strain or energy interpretation. It is a combination of two quantities occurring at distinctly different times during the failure sequence. It can also be seen that only the first criterion permits the determination of the maximum load associated with a known initial crack length. A criterion relating initial crack length to maximum load is definitely needed. A possible method for developing this criterion, through parameters of stress or strain, is through the definition of the amount of stable crack extension[3]. This is also shown on Figure 1.

For the purposes of this report, the second criterion, crack length and

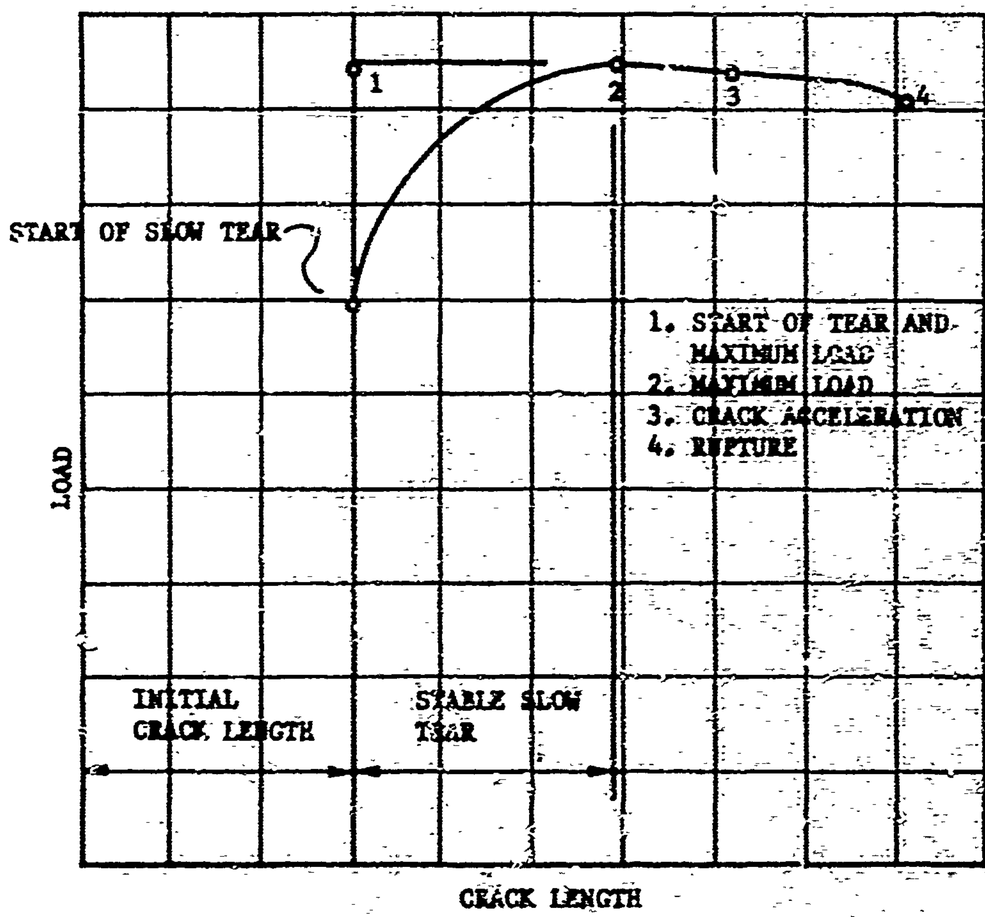

FIGURE 1 TYPICAL STAGES OF TEAR FOR A FATIGUE CRACK IN DUCTILE MATERIAL

stress at maximum load, will be used as a definition of crack instability. Whenever reference is made to one of the four points shown on the Figure 1, the appropriate subscript will be used.

CRACK TIP STRESS INTENSITY PARAMETER

Because of the need to consider stable tear as well as the critical crack length - maximum load relationship, a crack tip stress or strain approach is most applicable. This approach can be presented in the form of a stress intensity parameter for wide panels

$$k = \sigma_0 \ell^{\frac{1}{2}} \tag{1}$$

where: k = a measure of crack tip stress intensity

σ_o = gross panel stress

ℓ = the total crack length

In applying the stress intensity approach to the critical crack length - maximum load point, the upper limit of the stable crack lengths can be considered to be the same as the lower limit of unstable crack lengths defined by a critical energy release rate. This resolves to the fact that either a critical crack tip stress or strain, or a critical energy release rate is sufficient criteria for the definition of instability[9,10]. It is thus possible to use a stress intensity approach and still be compatible with fracture mechanics concepts of instability and energy release rates.

STRAIN INTERPRETATION OF THE STRESS INTENSITY PARAMETER

For the purposes of explanation of slow tear phenomena and the consideration of failure under combined conditions of fracture and yielding, it is desirable to appraise at least qualitatively the components of the stress intensity parameter k. This can be accomplished by considering the equation for elastic stress or strain at the tip of a crack in an infinitely wide panel:

$$e_u = \frac{\sigma_u}{E} = \frac{\sigma_o}{E}\left(1 + \sqrt{\frac{2\ell}{\rho'}}\right) \tag{2}$$

where: e_u = critical or ultimate crack tip strain (actually, this is a physically undefinable quantity as neither the gage length nor stress condition is known to the extent that it can be derived from present methods of measuring strain on unnotched tensile coupons)

σ_u = Ultimate gross panel stress corresponding to e_u

E = Young's modulus

ℓ = crack length

ρ' = Effective crack tip radius similar to that defined by Neuber[7]

Equation (2) involves two unknowns, e_u and ρ'. In order to use equation (2) without solving independently for e_u and ρ', it is necessary to assume that ρ' will be small so that $\sqrt{\frac{2\ell}{\rho'}} \gg 1$. With this assumption, equation (2) becomes

$$\sigma_0 \ell^{\frac{1}{2}} = e_u \, E \sqrt{\frac{\rho'}{2}} = k \tag{3}$$

Equation (3) is most applicable to problems involving elastic behavior. For those cases where the observed critical crack lengths occur at a near constant value of k_2 with local plastic deformation adjacent to the notch tip, equation (3) can be used provided the quantity ρ' is assumed as a lumped parameter used to account for the influences of local plasticity.

The stress intensity parameter can thus be considered a parameter having two unmeasurable components e_u and ρ'. Of these two, e_u must be at some critical or limiting value whenever tear initiates. Instability may or may not follow as instability depends on incremental changes in crack tip conditions as well as on the instantaneous condition of critical crack tip strain. These incremental changes can be qualitatively explained by variance of the quantity ρ'.

RELATIONSHIP BETWEEN THE STRESS INTENSITY PARAMETER AND CRACK TIP STRAIN

During the slow tear phase, an interesting relationship between the stress intensity parameter, k, and true crack tip strain can be observed (see Figures 44 and 45). The onset of slow tear indicates that a maximum or critical crack tip condition has been reached. After the first increment of tear at constant load, the crack remains stationary until additional load is applied. With sufficient additional load, additional tear occurs which will again halt if the load is held constant. Thus, it can be observed that the critical strain level at the crack tip can be reached many times between onset of tear and instability; each time at an increased value of k. Referring to equation (3), for a given value of k, the maximum crack tip strain is dependent upon the value of the effective radius ρ' which is assumed to account for the influences of local plasticity. While this interpretation of equation (3) is not rigorous, some useful qualitative evaluations can be made.

In terms of equation (3), the range of stable tearing that takes place prior to instability of a crack can be interpreted to mean that once the crack tip strain reaches some critical value, additional stable tear is possible only with an increase in ρ'. Instability is thus considered to occur whenever the crack tip strain has reached a critical value for tear and ρ' can no longer increase sufficiently to compensate for additional increases in k. For changes in k with the load held constant, equation (3) could be written for an incremental increase in the length ℓ up to the critical crack length at which instability occurs.

$$\frac{dk}{d\ell} = \frac{e_u E}{\sqrt{2}} \frac{d\sqrt{\rho'}}{d\ell} \qquad (4)$$

For the first unstable increment of crack extension, equation (4) becomes

$$\frac{dk}{d\ell} > \frac{e_u E}{\sqrt{2}} \frac{d\sqrt{\rho'}}{d\ell} \qquad (5)$$

It has been suggested that the increase in ρ' can be attributed to the development of the shear mode of fracture[13]; however, observations on 2024-T3[13] which were substantiated during this program showed the development of the tear resistance to occur with fully developed shear surfaces throughout. Thus, a more general dependence of tear resistance on plastic deformation is indicated.

THE INFLUENCE OF PANEL WIDTH

The influence of free panel boundaries near a stress concentration such as a fatigue crack causes stress in the vicinity of the crack tip to be higher than would be the case if the boundaries were remote. To account for this influence, a stress correction is usually employed. The stress correction used throughout this report is that proposed by Dixon [11].

$$\bar{\sigma} = \sigma_0 \left[\frac{1}{1 - \left(\frac{\ell}{w}\right)^2}\right]^{\frac{1}{2}} \qquad (6)$$

where w = panel width

$\bar{\sigma}$ = width adjusted stress

The Dixon correction has found favor in engineering studies [6,12] and is within 3 percent of the Westergard width correction used in the current fracture toughness formulation[12]

$$\left[\frac{1}{1 - \left(\frac{\ell}{w}\right)^2}\right]^{\frac{1}{2}} \approx \sqrt{\frac{w}{\pi \frac{\ell}{2}} \tan \frac{\pi \frac{\ell}{2}}{w}} \qquad (7)$$

In addition to the elastic width correction (equation 6), an additional width influence has been illustrated [1,13] which, when significant, would cause the stress intensity at the beginning of unstable tear (k_2) to be a variable with width. An easy way to explain qualitatively this width influence can be obtained by rewriting equation (4) for a panel of finite width using equations (1) and (6)

$$\frac{dk}{d\ell} = \frac{d\left(\sigma_0 \ell^{\frac{1}{2}} \left[\frac{1}{1-\left(\frac{\ell}{w}\right)^2}\right]^{\frac{1}{2}}\right)}{d\ell} = \frac{e_u E}{\sqrt{2}} \quad \frac{d\sqrt{\rho'}}{d\ell} \tag{8}$$

Equation (8) shows that the rate of change of k with respect to ℓ increases with the ℓ/w ratio thus agreeing with the observations of Reference 1. Since the rate of change of $\sqrt{\rho'}$ with respect to ℓ seems to diminish near the instability point, the last possible equilibrium solution of equation (8) tends to be at lesser values of k for increasing values of ℓ/w. For values of ℓ/w less than 0.5 in 2024-T3 aluminum, the change in instability from that of an infinitely wide panel is relatively small as shown by the tangency of effective stress and tear curves, Figure 2a, and in the k^2 vs ℓ plot, Figure 2b. Figure 2b can easily be compared to the energy release rate form of presentation. Figure 2a is however considerably easier to construct.

The two width corrections discussed above, equations (6) and (8), are both based on elastic theory and are thus increasingly inaccurate as local plastic deformation near the notch increases. However, as long as the local plastic deformation reaches approximately the same extent at the beginning of unstable tear over the range of geometries of interest, predictions of tear instability based on these elastic equations can be relatively successful. In this respect, there is an additional width influence that must be considered. This is the possibility that local plastic deformation at the crack tip can be significantly influenced by the proximity of the panel boundaries. In actuality, the plastic deformation should be influenced by boundary conditions whenever the boundaries are close enough to influence the elastic stresses. For a given crack length, this influence should generally increase as ductility increases and as width decreases. The panel widths for which this influence causes significant error in unstable tear predictions based on elastic equations can usually be avoided by following recommended fracture mechanics practice[1]. Particular problems arise, however, when elevated temperature testing is involved.

To illustrate the nature of the influence of panel width on guided panels of varied materials, Figure 3 shows the fraction of wide panel fracture strength $\left(\frac{k_2}{k_{2\infty}}\right)$ attained in successively smaller widths for a variety of materials. Width corrections were made using equation (6). Width corrections of the type illustrated by equation (8) were considered to be small as the ℓ/w ratios of the test panels were generally 0.4 or less. The yield/ultimate ratio of the several materials is also shown to indicate the general influence of ductility. Figures 4 and 5 show similar behavior as a function of temperature in test panel data selected from the same heats of materials tested at ambient and elevated temperatures.

DEFINITION OF WIDE AND NARROW PANELS

From Figure 3, it can be seen that for each material, there is a width of panels above which further increase in width will cause little if any change in the stress intensity at instability. Panels having widths equal to or above this limiting value will be referred to as wide panels in this report. Panels having widths less than this limiting value will be referred to as

FIGURE 2a ILLUSTRATING USE OF TANGENCY OF $\bar{\sigma}$ VS ℓ CURVE AND TEAR CURVE FOR 2024-T3 ALUMINUM

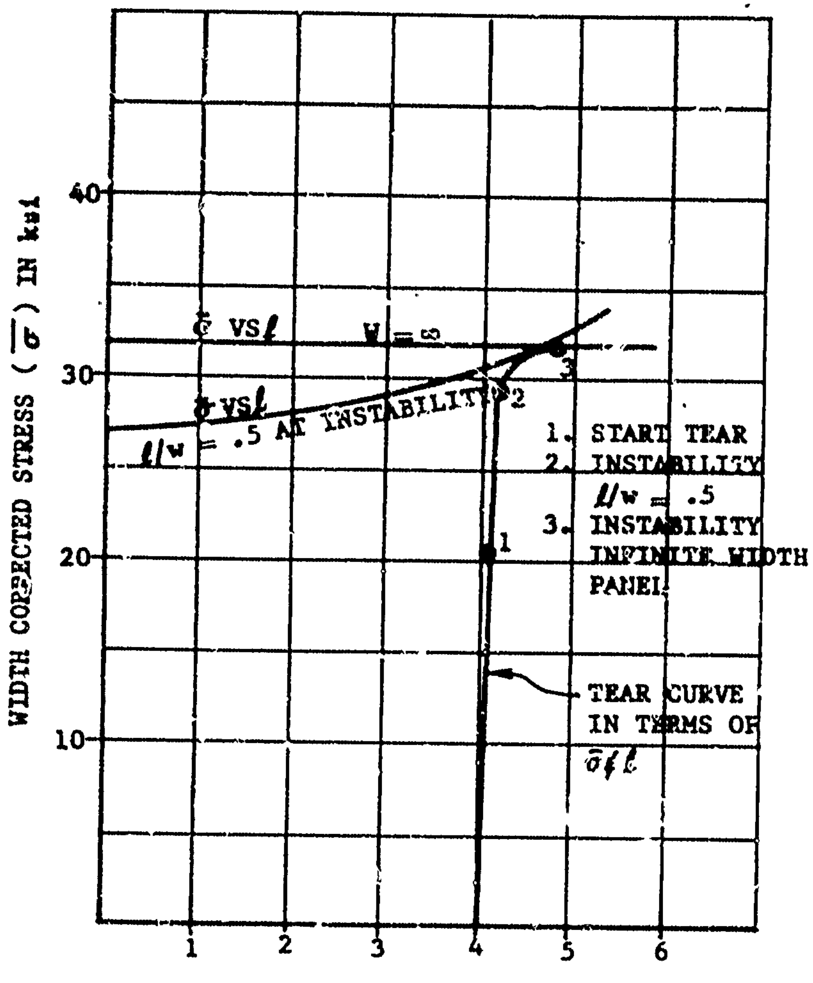

FIGURE 2b ILLUSTRATING USE OF TANGENCY OF k^2 VS ℓ CURVE AND TEAR CURVE FOR 2024-T3 ALUMINUM

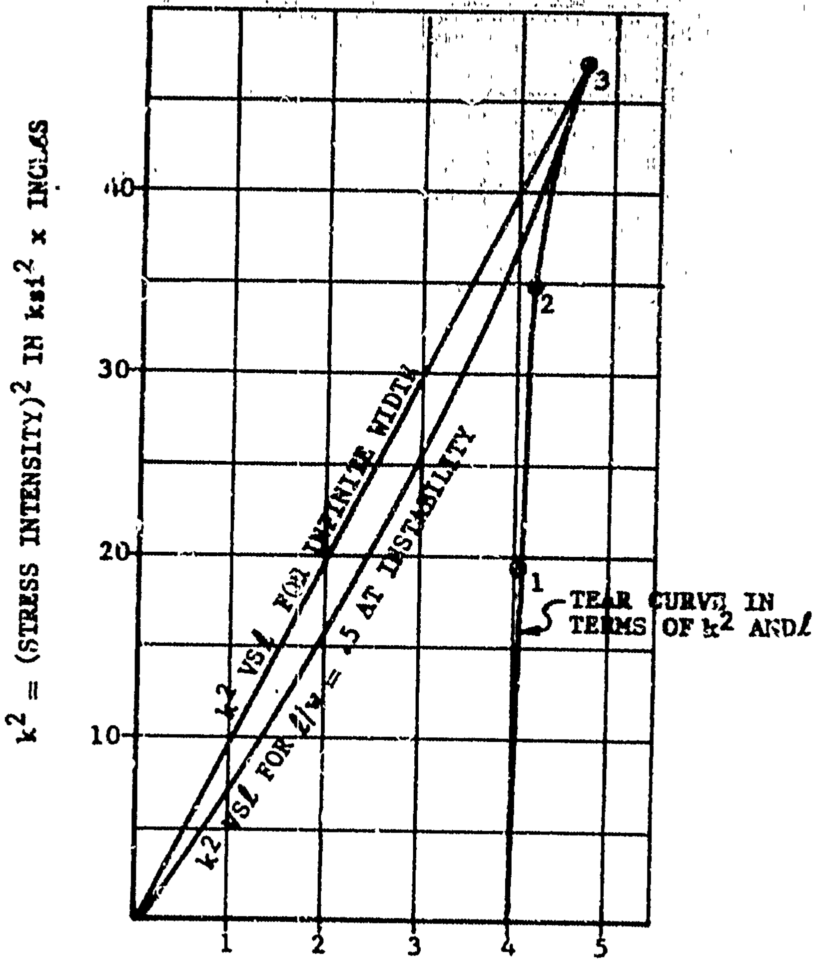

FIGURE 2 RELATIONSHIP BETWEEN RATE OF CHANGE OF STRESS INTENSITY AND STRESS INTENSITY FOR UNSTABLE CRACK EXTENSIONS

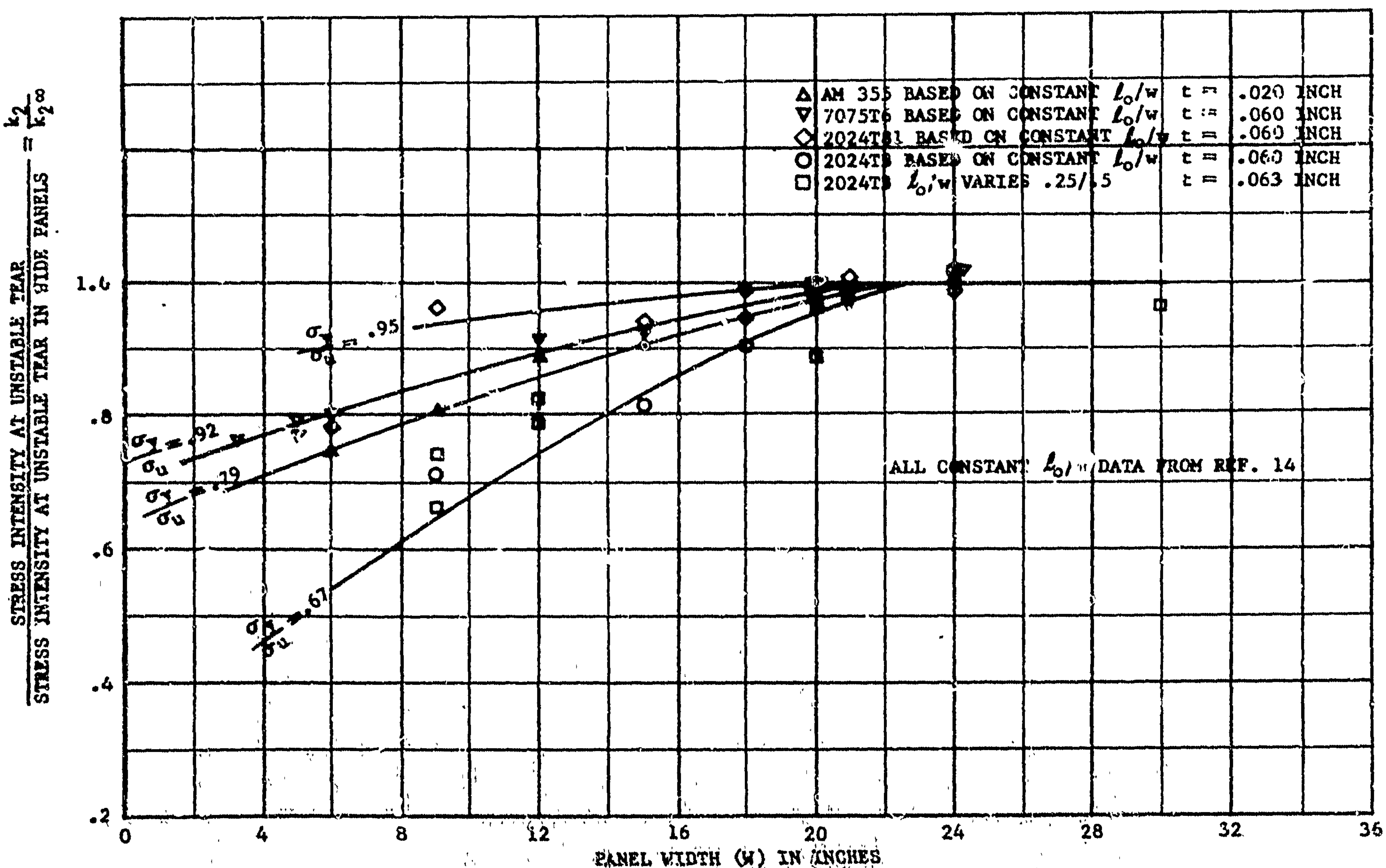

FIGURE 3 RELATIONSHIP BETWEEN YIELD/ULTIMATE RATIO, STRESS INTENSITY, AND WIDTH FOR GUIDED PANELS

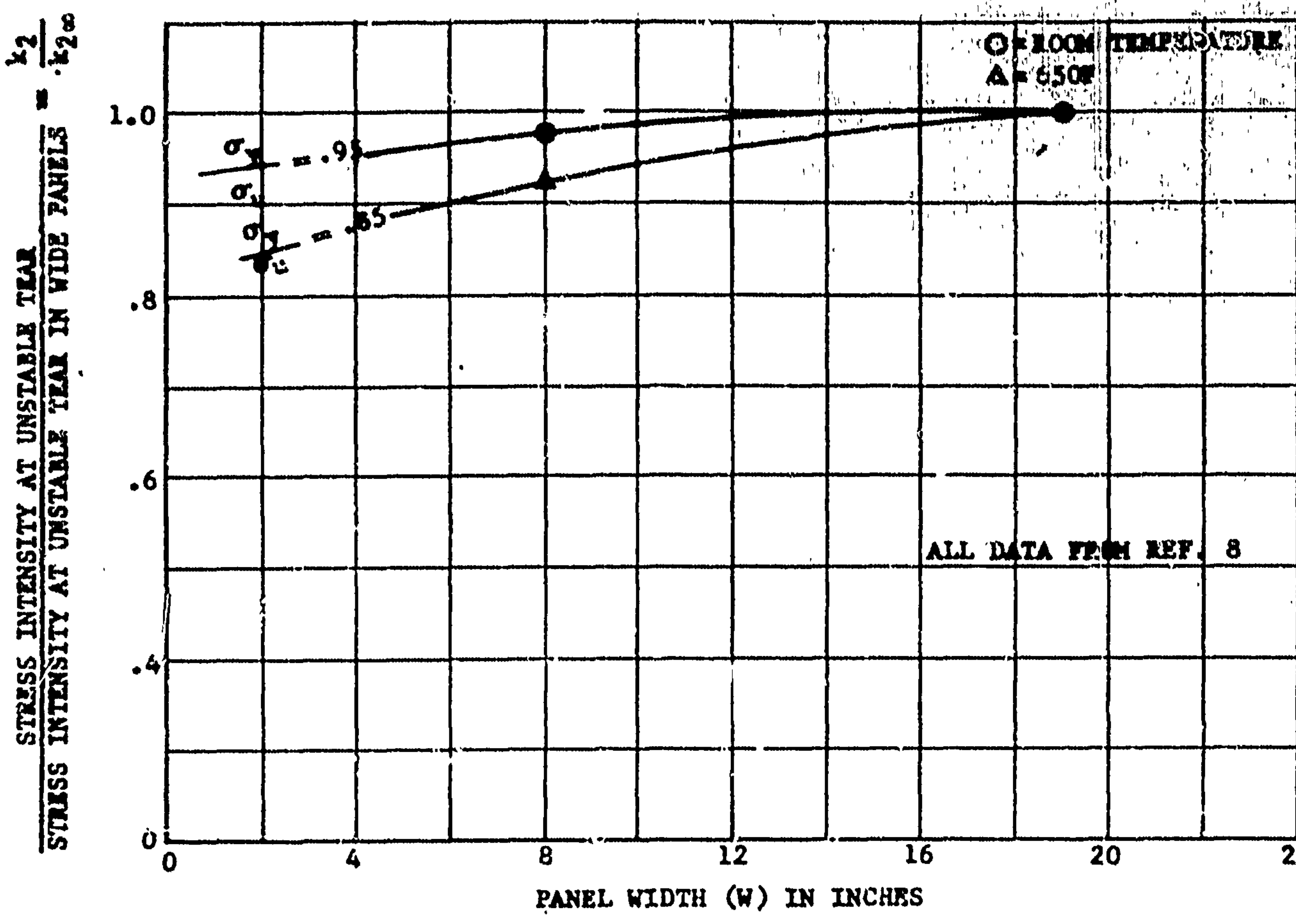

FIGURE 4 INFLUENCE OF TEMPERATURE ON STRENGTH/WIDTH RELATIONSHIP FOR TITANIUM 6A1-4V

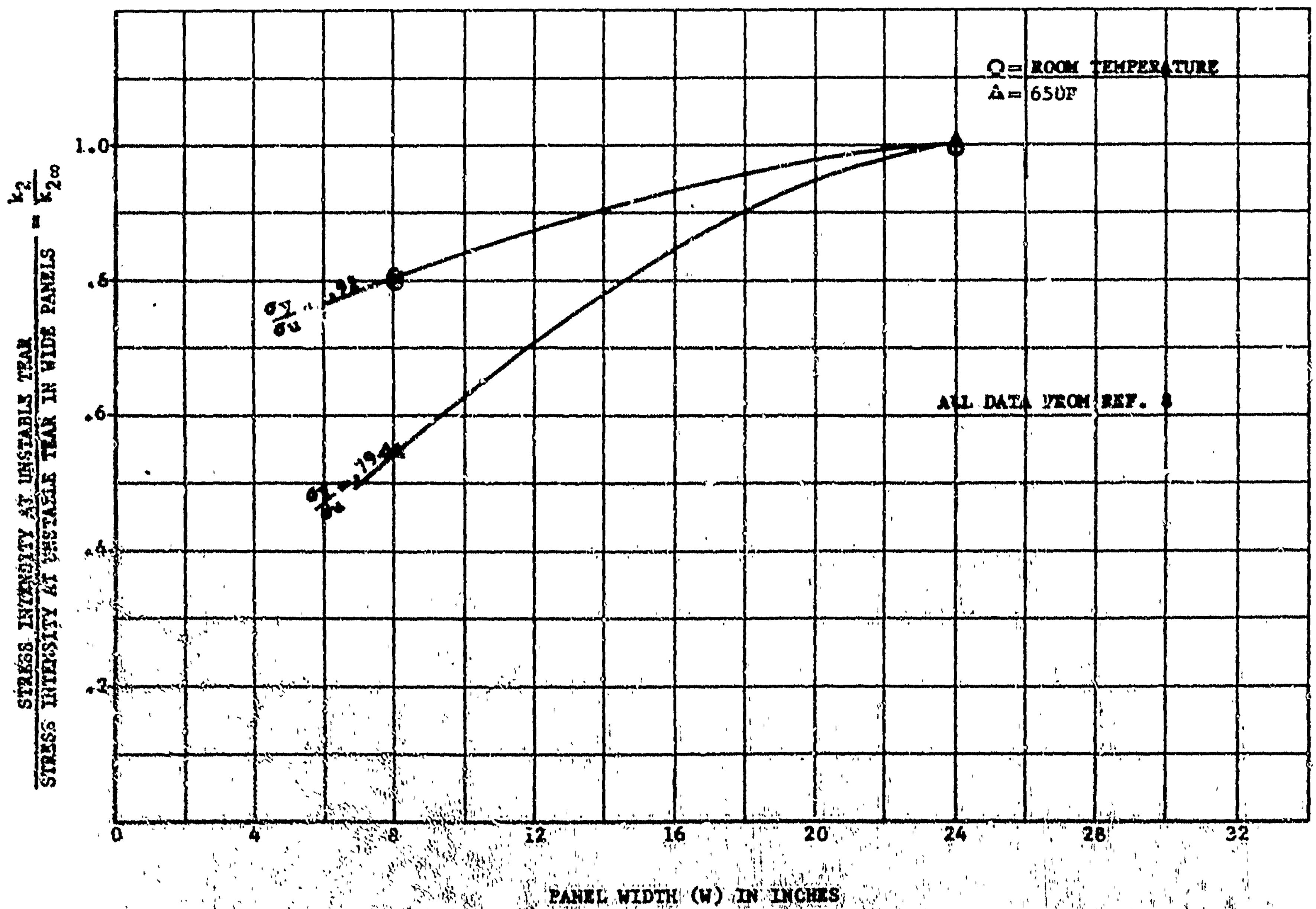

FIGURE 5 INFLUENCE OF TEMPERATURE ON STRENGTH/WIDTH RELATIONSHIP FOR TITANIUM 8A1-1Mo-1V

narrow panels.

For the present, strength prediction of narrow panels can best be handled by use of curves such as Figures 3, 4, and 5. While this catagory of panels is generally known to exist, it is significant that much of the available data falls within this range. It is possible that correlations such as shown will lead to a better understanding of this phenomena and to methods of interpreting wide panel strength from data obtained from narrow panels. Before this can be done, however, a considerably more complex means of ranking materials must be devised to account for ultimate strain differences and strain hardening characteristics.

Because of the limitations in using the stress intensity parameter in conjunction with narrow panels, the discussion of stress intensity applications in this report is limited to wide panels for which elastic considerations of width correction are sufficient.

PLASTIC ZONE CORRECTIONS TO STRESS INTENSITY

At this point in discussion, wide panels have been defined as those panels whose tear behavior can be correlated in terms of parameters based on elastic considerations (equations 1, 6, 8). Normally, fracture mechanics includes an additional correction based on the size of the plastic zone adjacent to the crack tip. The plastic zone correction is not used in this report. However, the wide use of the plastic zone correction, makes it desirable to discuss the reasons for not including it in the computations of stress intensity.

The plastic zone correction to the stress intensity parameter requires that the radius of the plastic zone be added to each end of the crack tip and that the resulting increased length be used in stress intensity calculations as an "effective crack length."

The Irwin model for computation of the plastic zone size can be expressed as

$$r_p = \frac{1}{2}\left(\frac{k}{\sigma_y}\right)^2 \qquad (10)$$

where $k = \sigma_o\sqrt{\pi \frac{\ell}{2}}$

r_p = radius of the plastic zone

An improved form[14] based on the Dugdale model for a crack[15] shows the size of the plastic zone to be dependent on the crack length in the form

$$r_p = \frac{\ell}{2}\left[\sec\left(\frac{\pi}{2}\frac{\sigma_o}{\sigma_y}\right) - 1\right] \qquad (11)$$

The dependence of r_p on crack length, as proposed in Equation (11) can be seen in its series expansion[15].

$$r_p = \frac{Q^2}{4}\left[1 + \frac{5}{12}\left(\frac{Q^2}{\ell}\right) + \frac{61}{360}\left(\frac{Q^2}{\ell}\right)^2 + \frac{277}{4032}\left(\frac{Q^2}{\ell}\right)^3 + \cdots\right] \qquad (12)$$

where

$$Q = \frac{\pi}{2} \frac{k}{\sigma y}$$

It would appear that use of a correction to crack length based on a plastic zone predicted by equations (10) or (12) would considerably improve the lower limit to the range of widths for which strength could be predicted by use of stress intensity parameter k. Hence width influences shown in Figures 3, 4, and 5 might be greatly reduced.

An attempt to apply this correction to data obtained during the test program for 2024-T3 aluminum showed an interesting fact. With reduced width for panels of 20 inches, 12 inches, and 9 inches, unstable tear (k_2) occurred at reduced stress levels. Gross stress at unstable tear plotted against crack length to panel width ratio at instability, showed all three widths to have nearly equal failure stresses at the same ℓ/w ratio (Figure 6). To illustrate the influence of this relationship between ℓ/w and gross stress on the computed plastic zone sizes, equation 10 may be used to write the ratio of plastic zone sizes for a 9-inch and 12-inch panel of 2024-T3 aluminum.

$$\frac{r_{p9}}{r_{p12}} = \frac{\frac{1}{2}\left(\frac{k_9}{\sigma_y}\right)^2}{\frac{1}{2}\left(\frac{k_{12}}{\sigma_y}\right)^2} = \left(\frac{k_9}{k_{12}}\right)^2 \qquad (13)$$

From Figure 6, a crack of ℓ/w ratio of .3 will fail at the same gross stress σ_0 in panels of 9-inch and 12-inch widths. Since the relationship between gross stress and width corrected stress, $\bar{\sigma}$, is dependent on the ℓ/w ratio (equation 6), the values of $\bar{\sigma}$ will also be the same at failure. For this example, equation (13) can be written.

$$\frac{r_{p9}}{r_{p12}} = \frac{\left[\bar{\sigma}\,(.3 \times 9)^{\frac{1}{2}}\right]^2}{\left[\bar{\sigma}\,(.3 \times 12)^{\frac{1}{2}}\right]^2} = \frac{9}{12} \quad \text{or } .75 \qquad (14)$$

Equation (12), while giving slightly different results, still has the same trend as shown in equation (14). Computed plastic zone corrections are thus proportional to both panel width and crack lengths and revised values of the stress intensity parameter k_2 showed the same relative influence of width. To verify that this phenomenon does occur in 2024-T3 aluminum, data from Reference 3 were also analyzed (Figure 7). No particular fundamental significance is attached to this phenomenon as it does not occur for wider widths. The 20-inch wide and 30-inch wide panels of the test program showed no difference in strengths when compared on the basis of computed stress intensity at instability. Also, this ℓ/w vs. stress relationship would not hold for panels of lesser ductility than 2024-T3 aluminum shown on Figure 3. Figures 6 and 7, and equation (14) do point out, however, that the practice of adding a plastic zone correction to crack length is less effective than the influence of width on stress intensity for the aluminum alloy 2024-T3. Due to the above reasoning, plastic zone corrections were not considered in the presentation of data of this report.

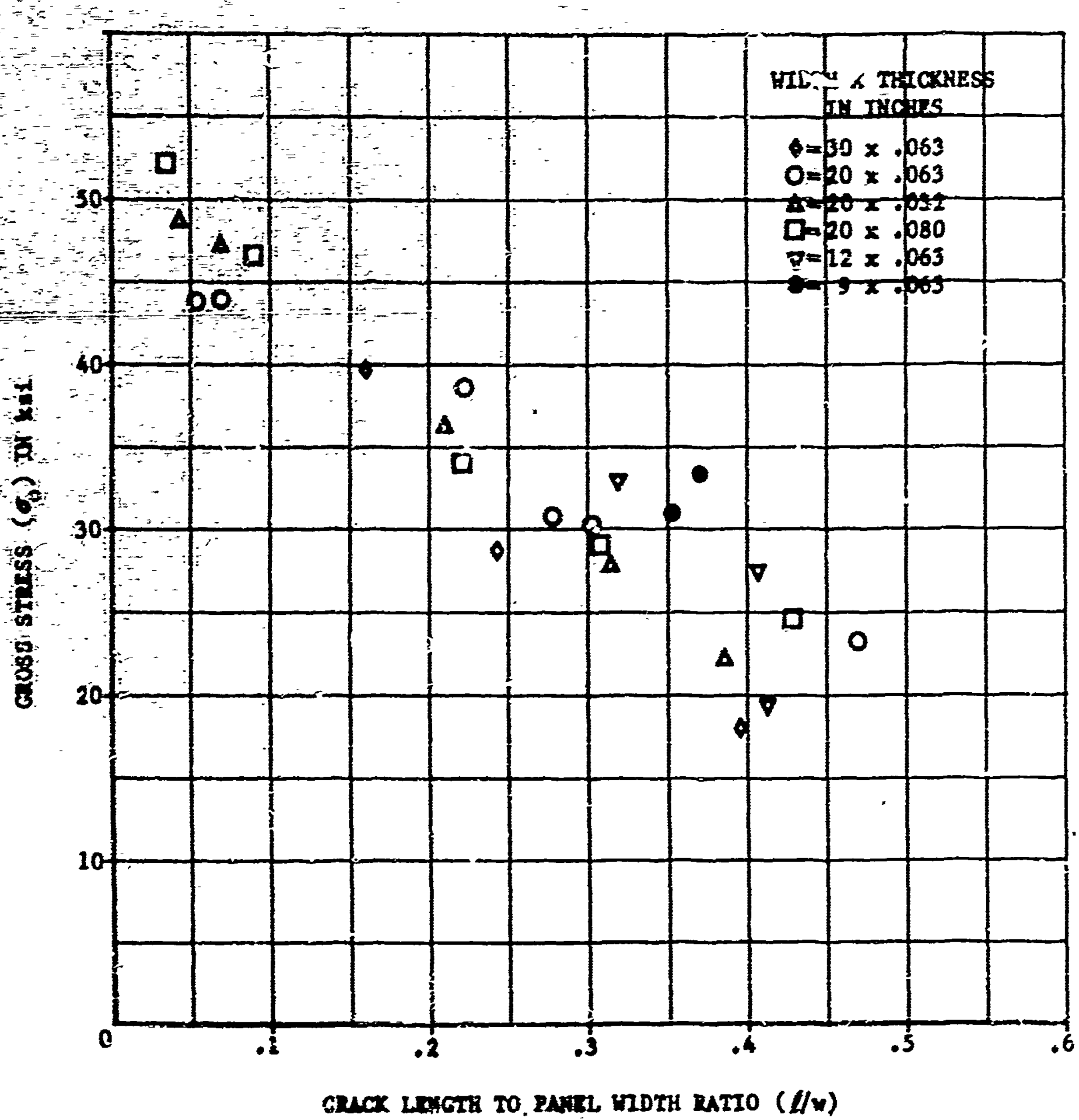

FIGURE 6 GROSS STRESS AT UNSTABLE TEAR VS. CRACK LENGTH TO PANEL WIDTH RATIO AT INSTABILITY FOR GUIDED 2024-T3 ALUMINUM PANELS

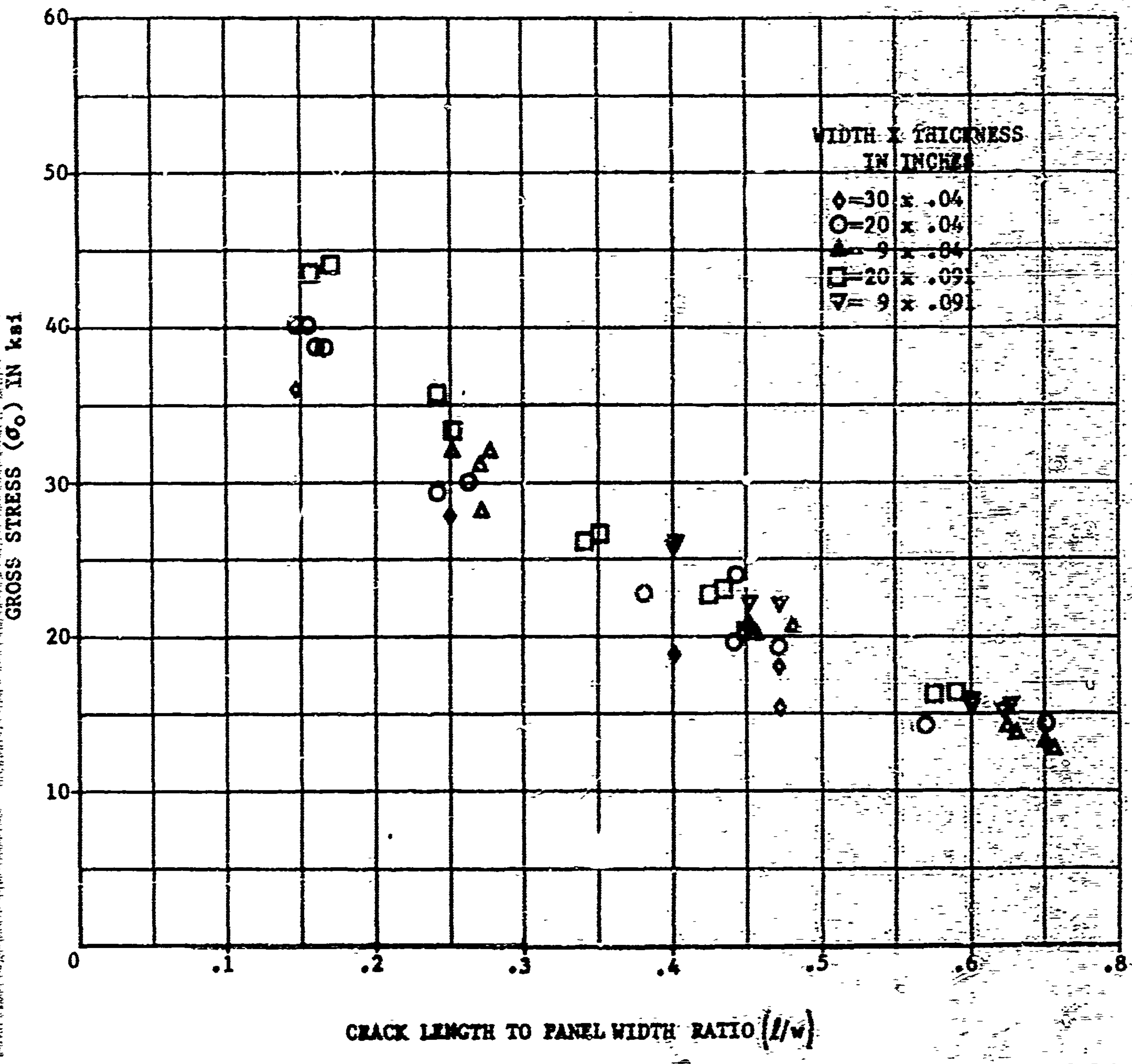

FIGURE 7 GROSS STRESS AT UNSTABLE TEAR VS. CRACK LENGTH TO PANEL WIDTH RATIO AT INSTABILITY FOR 2024-T3 ALUMINUM PANELS (DATA FROM REF. 3)

INFLUENCE OF PANEL THICKNESS

In general, the thickness of a panel can have significant influence on the stress intensity at which slow tear and crack instability will occur. However, the range of thickness for the materials studied in this report caused both the beginning of slow tear and the beginning of unstable tear to occur in the shear mode (plane stress). While minor differences in tear behavior are bound to be present, they are considered subordinate to the more gross phenomena of geometric influences. For this reason, thickness differences have for the most part been ignored, and average values of stress intensity have been used.

SUMMARY OF THEORY FOR GUIDED PANELS WITH ELASTIC BEHAVIOR AWAY FROM CRACK

1. For wide panels, the range of crack behavior between the onset of stable tear and crack instability can be correlated and predicted in terms of stress intensity. This stress intensity parameter can be expressed in the form

$$k = \bar{\sigma} \ell^{\frac{1}{2}} \tag{15}$$

2. For wide panels, influence of width on the elastic stress intensity parameter can generally be adequately handled by use of a stress correction derived from elastic theory. Of those available, the Dixon correction has been selected

$$\bar{\sigma} = \sigma_o \left[\frac{1}{1 - \left(\frac{\ell}{w}\right)^2} \right]^{\frac{1}{2}} \tag{16}$$

3. Crack instability can be considered to be sensitive to the rate of change of stress intensity with length. This can be qualitatively illustrated by the relationship

$$\frac{d\left[\sigma_o \ell^{\frac{1}{2}} \left(\frac{1}{1 - \left(\frac{\ell}{w}\right)^2}\right)^{\frac{1}{2}}\right]}{d\ell} = \frac{\sigma_{critical}}{\sqrt{2}} \frac{d\sqrt{\rho'}}{d\ell} \tag{17}$$

For values of ℓ/w less than 0.5, this width influence is small for 2024-T3 aluminum.

4. For panels having widths less than some minimum (Figure 3), the proximity of a free boundary can significantly influence the local plastic behavior adjacent to the crack tip and thus cause considerable reduction in strength from that predicted by elastic assumptions and wide panel behavior. In this report, panels in this category are referred to as narrow panels. The strength reduction in narrow panels generally increases as ductility increases and as panel width decreases (Figures 3, 4, and 5).

5. Plastic zone corrections to crack length are less effective as ductility increases. In 2024-T3 aluminum, a near constant relationship between ℓ/w and gross stress at the beginning of unstable tear was found to exist. This relationship caused computed plastic zone corrections also to be proportional to width resulting in no improvement in the observed differences

in the stress intensity parameter for widths of 9, 12, and 20 inches. No difference in the stress intensity for unstable tear was found for 20 and 30 inch wide panels.

6. During the stable tear, the crack tip stress and strain can be considered to remain constant at a value critical for tear while compensating influences of local plasticity permit equilibrium to be sustained at increasing values of the elastic stress intensity parameter. This can be qualitatively explained in terms of an effective radius ρ' by the relationship:

$$\frac{dk}{d\ell} = \frac{e_u E}{\sqrt{2}} \frac{d\sqrt{\rho'}}{d\ell}$$

7. The crack will continue to tear without further increase in load when

$$\frac{dk}{d\ell} > \frac{e_u E}{\sqrt{2}} \frac{d\sqrt{\rho'}}{d\ell}$$

8. All observed failures in 2024-T3 and titanium 8Al-1Mo-1V were in the shear mode. Variation in critical stress intensities with thickness in guided panels is not a major consideration in 2024-T3 aluminum for thicknesses of .032, .063, and .080 inch. For the purpose of correlating large differences in the stress intensity at unstable tear resulting from geometric influences, average values of stress intensity can be used for the range of thicknesses in this report.

V GUIDED PANELS WITH INELASTIC BEHAVIOR AWAY FROM CRACK

APPLICATIONS

For relatively ductile materials such as 2024-T3 aluminum at room temperature and titanium 8Al-1Mo-1V at 650 degrees (compare Figures 3 and 5), the behavior of fatigue cracks is such that the lower limit of the crack lengths that could reasonably be found in a structure are those that would only fail under stress conditions high enough to cause general yielding away from the crack. While this condition in itself implies a structure safe from catastrophic crack propagation at normal stress levels, it is desirable to be able to predict the ultimate strength of structure containing fatigue cracks in this range for the purpose of predicting probability of vehicle survival under severe conditions of environment. Additionally, for elevated temperatures, it would be extremely desirable to be able to interpret correctly strength studies made using short cracks in small coupons[16].

INTERACTION DIAGRAM

While there are many ways to approach the problem of fracture accompanied by yielding, the method selected herein uses the interaction diagram[17]. An interaction diagram can be constructed for any two (or more) failure mechanisms by the following steps:

1. The strength under each simple-loading condition (tension, bending, fracture, etc.) is first determined by analysis or test.

2. The combined-loading condition is represented by load (or stress) ratios R in which

$$R_i = \frac{\text{applied loading of type i}}{\text{critical loading of type i}} \tag{18}$$

   the word "critical" can be interpreted generally to mean the loading at failure under conditions represented by the ratio R_i alone, whether it occurs by buckling, rupture, or any other form. For example, for the case of simple tension stress in an uncracked panel

$$R_1 = \frac{\sigma_o}{\sigma_u} \tag{19}$$

   Thus, at failure under a simple tension loading

$$R_1 = \frac{\sigma_o}{\sigma_u} = 1 \tag{20}$$

3. The effect of one loading (represented by R_1 in Figure 8) on the allowable or critical value of another simultaneous loading (R_2) is represented by an equation or chart involving R_1 and R_2. (More than two loadings can also be handled in this way).

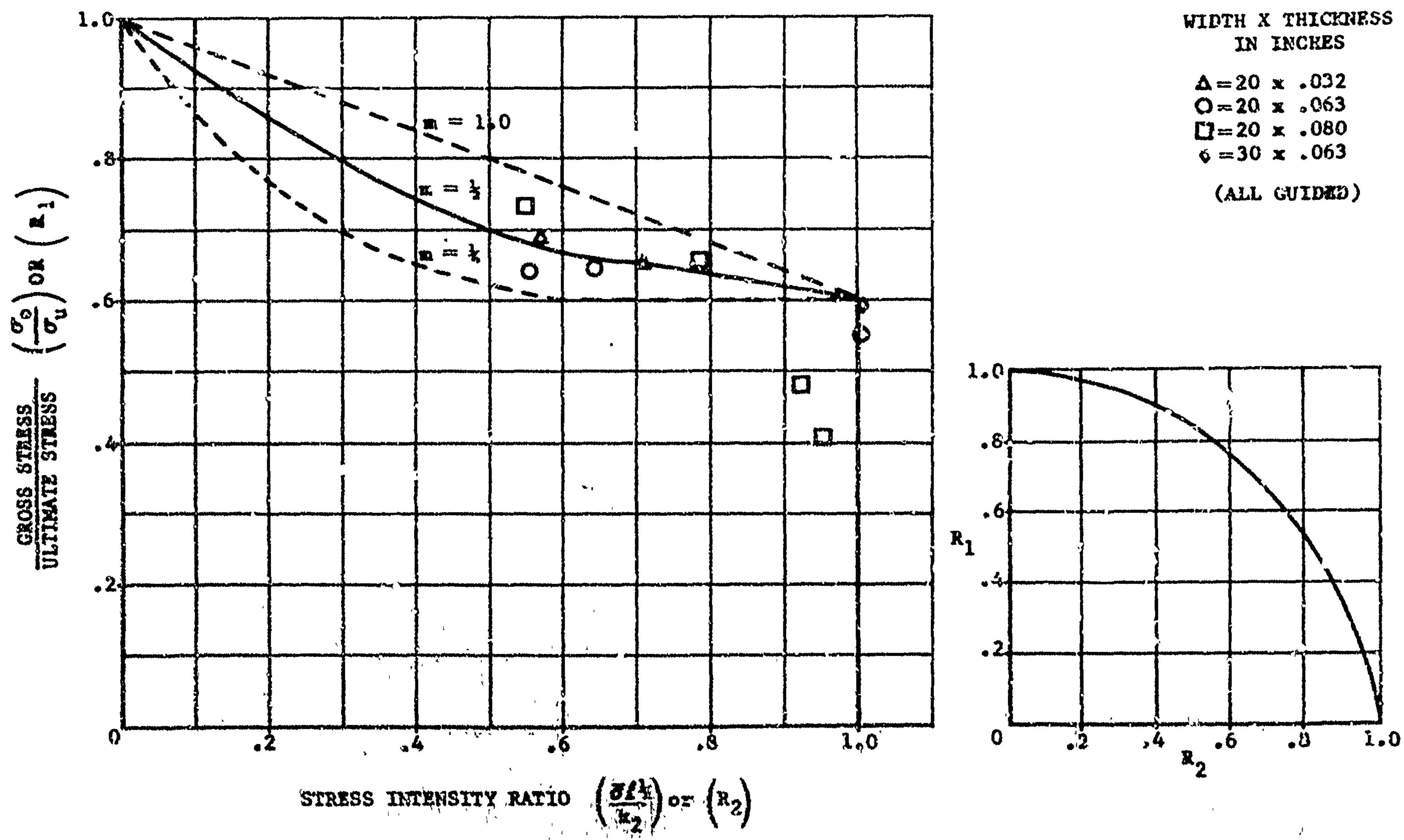

FIGURE 8 INTERACTION DIAGRAM FOR YIELDING SIMULTANEOUS WITH FRACTURE, GUIDED PANELS 2024-T3 ALUMINUM

INTERACTION EQUATION FOR YIELDING SIMULTANEOUS WITH FRACTURE

Figure 8 shows an interaction diagram developed along lines illustrated above for the interaction between the tensile mode of failure and the fracture mode of failure. Data obtained during the experimental program are shown and several interaction curves have been drawn based on the equation

$$\left\langle \frac{\sigma_o - 0.8\,\sigma_y}{\sigma_u - 0.8\,\sigma_y} \right\rangle^m + \frac{\bar{\sigma}\,\ell^{\frac{1}{2}}}{k_2} = 1 \tag{21}$$

Equation (21) is an interaction equation for the simultaneous yielding and fracture of a panel containing a fatigue crack where

σ_o = gross stress away from the crack

σ_y = the yield stress of the material

$.8\sigma_y$ = an approximation of the proportional limit stress

σ_u = ultimate stress for uniaxial tension loading

$\bar{\sigma}$ = width adjusted stress for crack tip stress intensity

ℓ = crack length

k_2 = the value of stress intensity ($\bar{\sigma}\ell^{\frac{1}{2}}$) for unstable tear without yielding

m = an interaction exponent to be determined experimentally

The bracket notation $\langle\ \rangle$ is reasonably standard [18] and indicates that the negative values of the bracketed quantity are treated as zero, i.e.

$$\langle -x \rangle^m = 0$$

where $x > 0$

$$\langle x \rangle^m = x^m$$

In the form presented, equation (21) has a discontinuity at the proportional limit and reduces to a single parameter stress intensity equation for fracture when the gross cross section is elastic ($\sigma_o < .8\sigma_y$).

THE INTERACTION EXPONENT m

The interaction exponent, m, is a strain hardening sensitive exponent and can be qualitatively explained as two limits of material behavior are approached.

These limits are:

1. The elastic limit - A material having the characteristic of a high degree of strain hardening will approach this limit as shown by curve 1 of Figure 9a.

2. The elasto-plastic limit - A material having the characteristic of low strain hardening will approach this limit as shown by curve 2 of Figure 9a.

Interaction curves predicting characteristic failure trends for materials approaching the two above limits are shown on Figure 9b. From Figures 9a and 9b, it can be seen that the strain hardening characteristics of a material and the interaction exponent m are related. A typical stress strain curve for 2024-T3 aluminum is generally of the type illustrated by curve 2 of Figure 9a. Thus, agreement of experimental data for 2024-T3 aluminum shown on Figure 8 with a curve using equation (21) and an interaction exponent $m = \frac{1}{2}$ can be seen to be qualitatively correct. In appraising the usefulness of equation (21) and the qualitative curves drawn on Figure 9, it must be remembered that the proportional limit is also a problem variable and shifts the region of the interaction diagram influenced by the exponent m. Thus, for a truly brittle material, the proportional limit approaches the ultimate strength and the region of diagram 9b influenced by the coefficient m is non-existent.

It is believed that further study of the relationship between strain hardening variables and the interaction coefficient m will result in a more quantitative definition. Until that time, some useful qualitative estimates of interaction exponents can be obtained directly from examination of the shape of uniaxial tension stress strain curves.

STRAIN INTERPRETATION OF THE INTERACTION EQUATION

The quantity $\left\langle \frac{\sigma_0 - 0.8\,\sigma_y}{\sigma_u - 0.8\,\sigma_y} \right\rangle$ can be interpreted in terms of gross strain away from the crack as shown on Figure 10. Figure 10 shows that the quantity $\left\langle \frac{\sigma_0 - 0.8\,\sigma_y}{\sigma_u - 0.8\,\sigma_y} \right\rangle$ represents a straight line approximation of the fraction of critical strain in the gross cross section if elastic strains are considered to be small and ignored.

In a similar sense, the fraction $\frac{\bar{\sigma}\,\ell^{\frac{1}{2}}}{k_2}$ can be considered to be an approximation of the fraction of critical strain in the form of a concentration at the crack tip. This requires the assumption that the elastic stress intensity factor can still give approximations of crack tip strain concentration in the presence of general yielding. This of course, is not true. The error assumed in making this assumption is accounted for in the experimental determination of the interaction exponent which implies a nonlinear interaction between an elastic crack tip strain concentration parameter and gross plastic strain. This approach, while arbitrary, does allow the elastic stress intensity factor to remain intact and, in turn, makes association with linear elastic fracture mechanics somewhat easier.

FIGURE 9a LIMITS OF STRAIN HARDENING BEHAVIOR

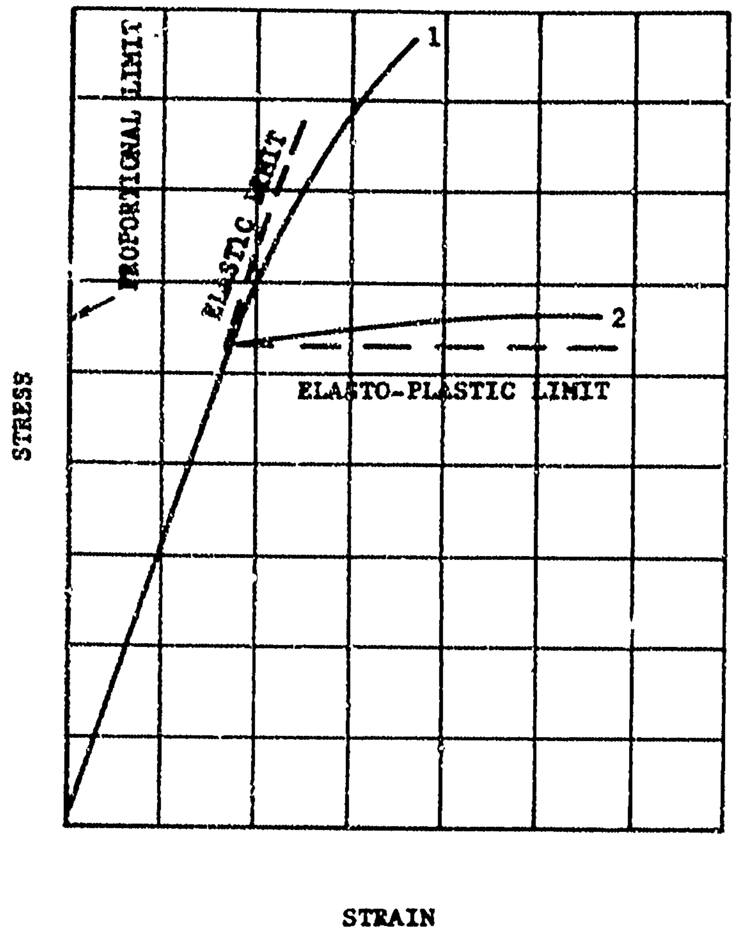

FIGURE 9b LIMITS OF YIELD-FRACTURE INTERACTION BEHAVIOR

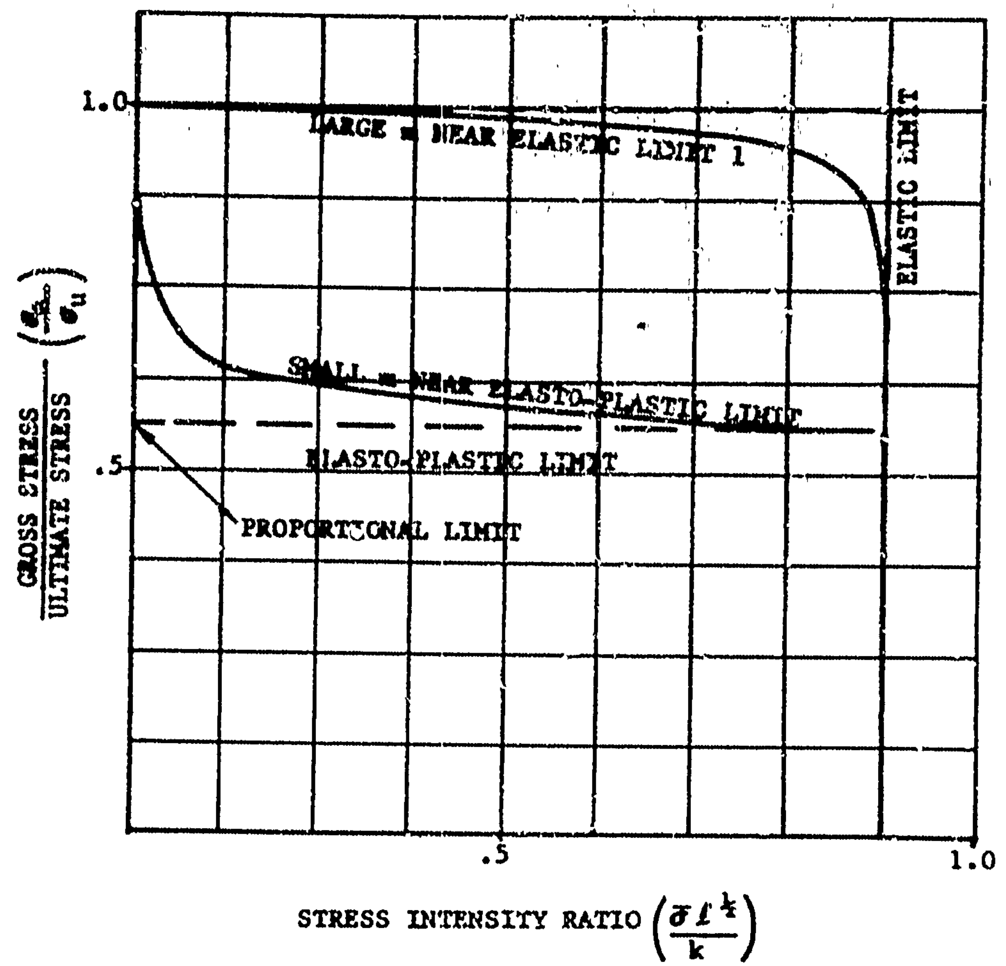

FIGURE 9 RELATIONSHIP BETWEEN STRAIN HARDENING AND YIELD-FRACTURE INTERACTION

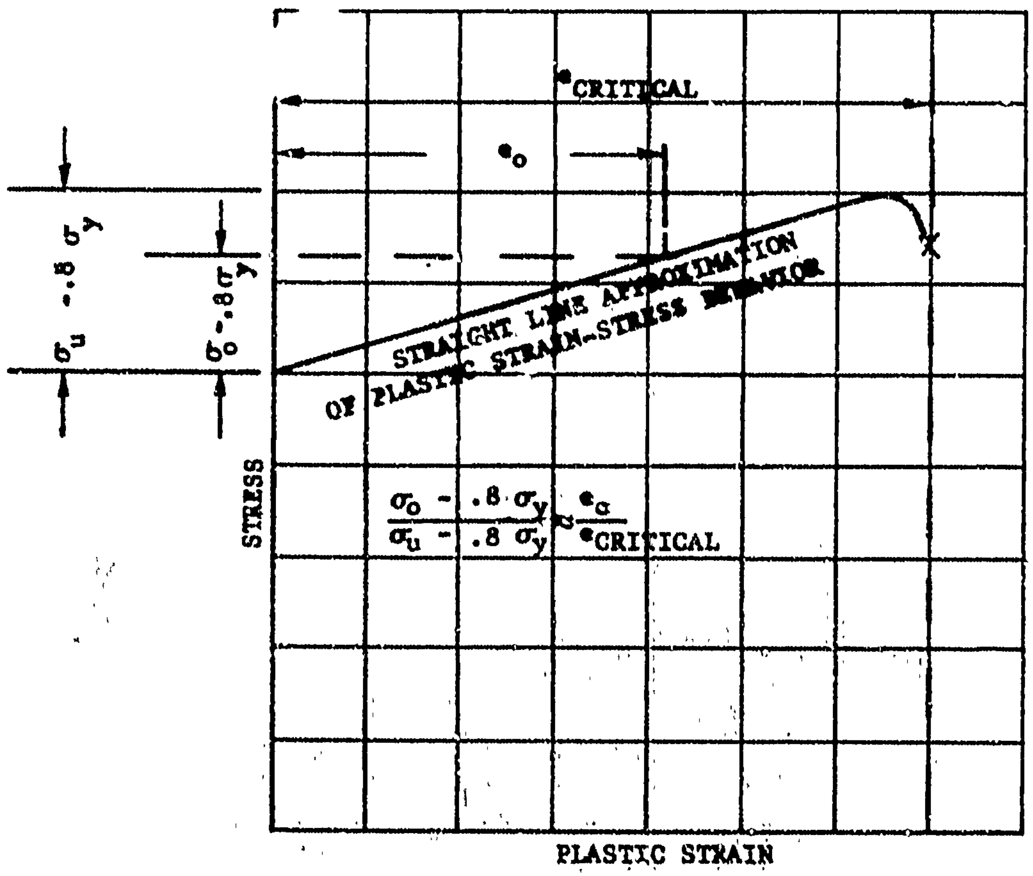

σ_y = YIELD STRESS

σ_u = ULTIMATE STRESS

σ_o = GROSS STRESS IN PANEL

$e_{critical}$ = CRACK TIP STRAIN

e_o = GROSS STRAIN IN PANEL

FIGURE 10. APPROXIMATION OF GROSS SECTION STRAIN IN TERMS OF STRESS VARIABLES

Using the above strain interpretation of equation (21), the equation may be restated:

(Gross section strain)^m + elastic crack tip strain concentration = Critical crack tip strain.

COMPARISON OF INTERACTION EQUATION AND NASA NOTCH ANALYSIS EQUATION

The NASA Notch Analysis equation (Reference 5) has a form similar to equation (21). The interpretation is, however, in terms of stress rather than strain. This equation can be written

$$\sigma_{critical} = \sigma_n + \sigma_n \sqrt{\frac{2\ell}{\rho'}} \frac{E_{sec}}{E} \qquad (22)$$

where $\sigma_{critical}$ = critical crack tip stress (Figure 11)

E_{sec} = secant modulus at the critical stress

ρ' = effective notch radius

σ_n = net cross section stress

An approximate solution for the critical strain (e_u) should be obtainable by dividing both sides of equation (22) by E_{sec} (see Figure 11) so that

$$e_u = \frac{\sigma_n}{E_{sec}} + \frac{\sigma_n}{E}\sqrt{\frac{2\ell}{\rho'}} \qquad (23)$$

For a wide panel in which the differences between net and gross stresses are small, equation (23) can be stated as

critical strain = $\dfrac{\sigma_o}{E_{sec}}$ + elastic crack tip strain concentration.

The term $\dfrac{\sigma_o}{E_{sec}}$ cannot be directly interpreted in terms of strain. Further, this term is continuous and significant for all values of σ_o at failure above and below the proportional limit. For this reason, equations (22) and (23) cannot be reduced to the fracture mechanics equation when the gross cross section stress is elastic. This lack of a discontinuity at the yield stress or proportional limit stress is regarded to be the most significant limitation of equation (22). The fact that equation (22) cannot be interpreted in terms of strain parameters is viewed as a related limitation.

Equation (21) does exhibit the required discontinuity in behavior at the proportional limit and does have a strain interpretation. Additionally, equation (21) incorporates the elastic stress intensity parameter and reduces to linear elastic fracture mechanics form in the elastic range. The interaction exponent m which is required in the inelastic range of behavior is related to

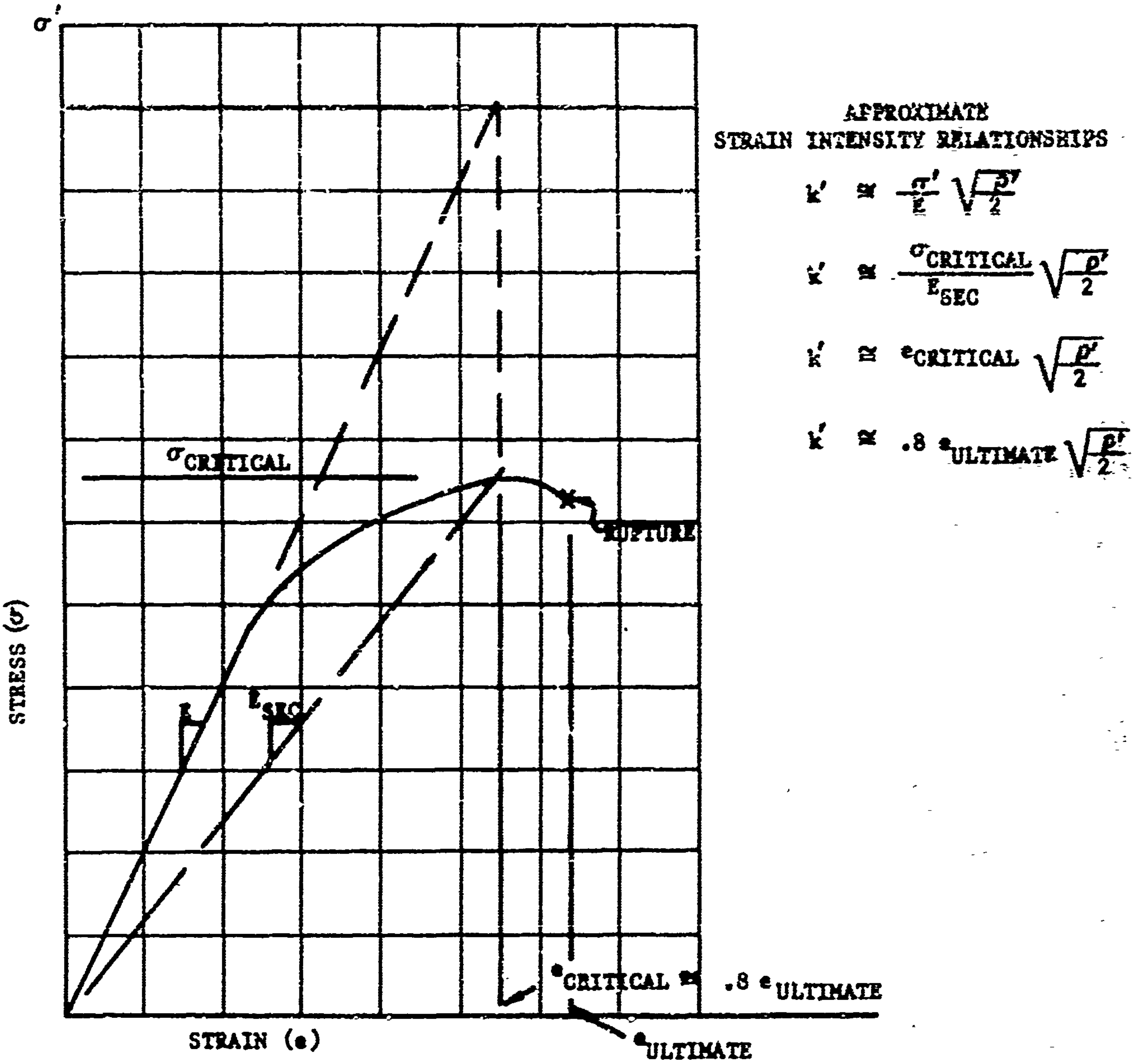

FIGURE 11 RELATIONSHIP BETWEEN STRAIN AND STRESS VARIABLES

strain hardening characteristics. For these reasons, equation (21), while still empirical in nature, is believed to have greater potential as a basis for future development. The emphasis on strain variables rather than stress should lead to further clarification and unification of theories.

SUMMARY OF THEORY FOR INELASTIC BEHAVIOR AWAY FROM THE CRACK IN WIDE GUIDED PANELS

1. The influence of gross panel yielding can be correlated in terms of an interaction equation of the form

$$\left(\frac{\sigma_o - 0.8\sigma_y}{\sigma_u - 0.8\sigma_y} \right)^m + \frac{\bar{\sigma}\ell^{1/2}}{k} = 1$$

   This equation can be restated

   (gross section strain)^m + elastic crack tip strain concentration

   = critical crack tip strain

2. The interaction equation is discontinuous at the yield point and reduces to the elastic stress intensity equation when $\sigma_o < 0.8\ \sigma_y$.

3. The exponent m varies with material strain hardening characteristics with high values of m corresponding to a high degree of strain hardening, and low values of m corresponding to low strain hardening.

VI THE INFLUENCE OF PANEL BUCKLING

IMPORTANCE

Considerations of fracture to this point have assumed that the test panel remains flat until failure. Normal fracture mechanics procedures used in material evaluation studies use restraining guides to hold the panel in this configuration. The natural tendency of the panel, however, is to buckle in the region of the crack (See Figures 12, 13, and 14). Typical dimensions of this buckled segment as obtained during the experimental portion of the program are shown in Figure 15. The strength reduction caused by buckling in 2024-T3 aluminum panels can be seen by comparing Figures 16 and 17. The problem of estimating the buckled strength of fatigue cracked panels cannot generally be resolved by testing of unguided simple tension panels. Unguided test panels with relatively large ℓ/w ratios show reduction in strength due to buckling that may not occur. Additionally, engineering structures are often subject to biaxial stresses. This stress condition is not obtained in test panels except through complex loading procedures. Therefore, an attempt at indirectly estimating the buckling influence through biaxial strain considerations is warranted.

GENERAL CONSIDERATIONS

The phenomenon of panel buckling adjacent to a crack (Figure 15) can be easily explained in a qualitative sense. Quantitative definition of this buckling and its influence on fracture strength is extremely difficult. In order to obtain a qualitative understanding of these phenomena, consider a fatigue crack in a panel loaded as shown in Figure 18. The overall width of the panel can be considered to decrease by the relationship

$$\frac{\mu \sigma_{oy} w}{E} = e_x w \tag{24}$$

where μ = Poisson's ratio

e_x = strain normal to the load direction and parallel to the crack

σ_{oy} = gross panel stress away from and normal to the crack

If the panel is to remain flat, the portion of the width directly above the crack must decrease by the amount $e_x \ell$. Since no load can be transmitted in the y direction across the crack, the transverse shortening due to the Poisson effect is not present. There are, however, compressive components of stress acting toward the center of the crack and parallel to the crack (Figure 18) which tend to force the panel segments above and below the crack to shorten by

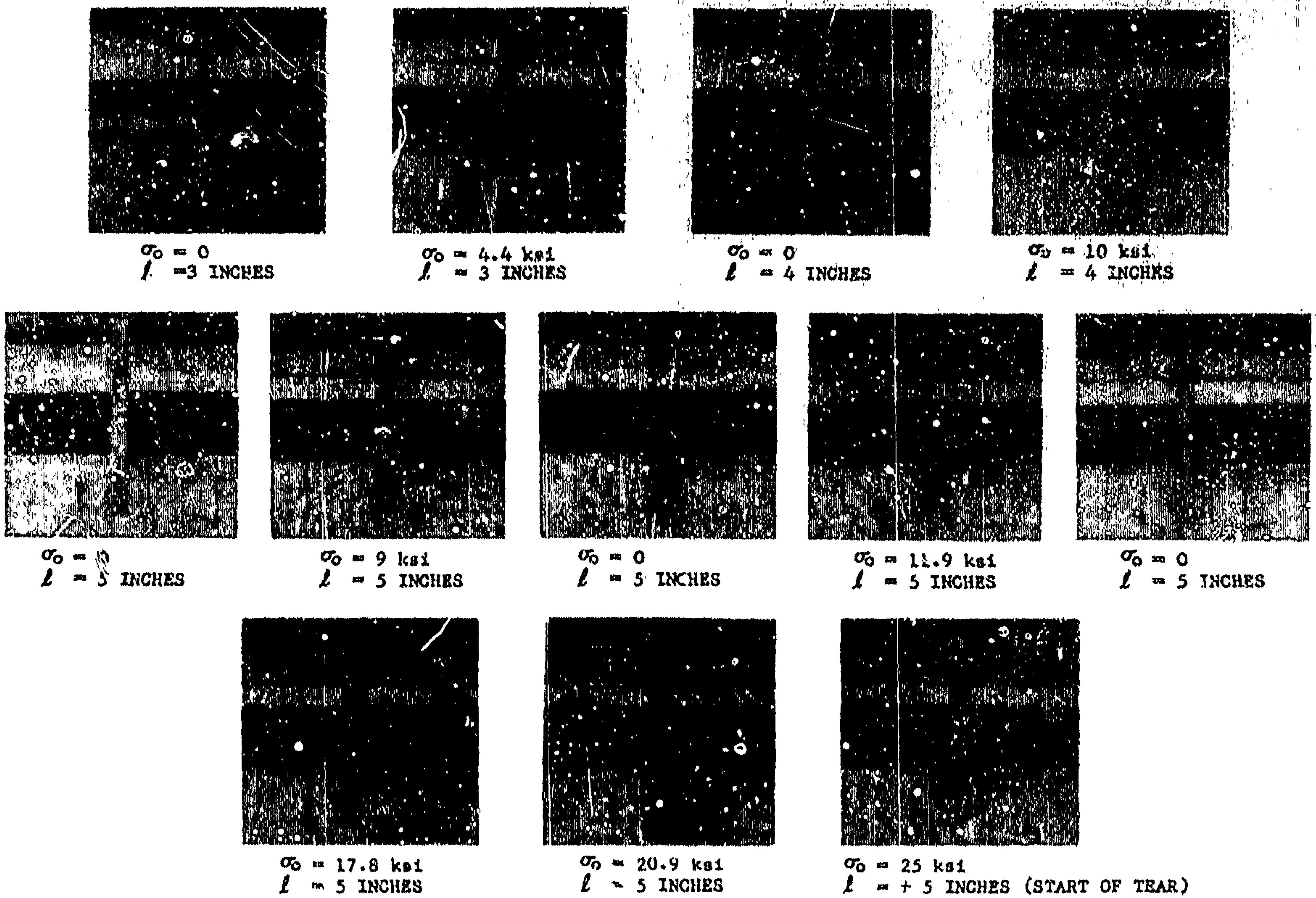

FIGURE 12 BUCKLING PATTERN SEQUENCE (NORMAL TO PANEL FACE) FOR 30 INCH WIDE X .032 INCH THICK 2024-T3 ALUMINUM PANELS

σ_o = 23.5 ksi
ℓ° = 3 INCHES

σ_o = 18.6 ksi
ℓ° = 4 INCHES

σ_o = 10.3 ksi
ℓ° = 5 INCHES

σ_o = 20.6 ksi
ℓ° = + 5 INCHES (START OF TEAR)

FIGURE 13 BUCKLING PATTERN SEQUENCE (NORMAL TO PANEL FACE) FOR 30 INCH WIDE X .063 INCH THICK 2024-T3 ALUMINUM PANELS

σ_0 = 10.9 ksi
ℓ = 5 INCHES

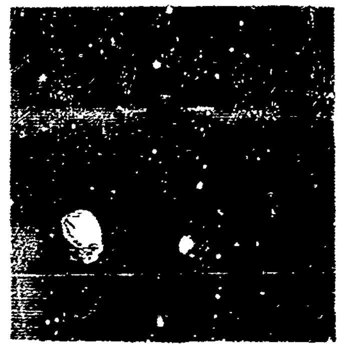

σ_0 = 17.7 ksi
ℓ = + 5 INCHES (START OF TEAR)

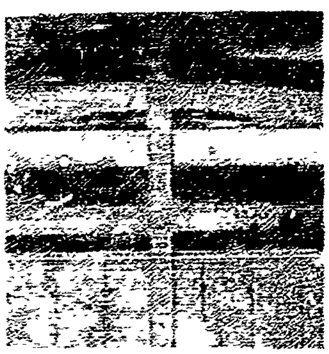

σ_0 = 21 ksi
ℓ = + 5 INCHES (START OF TEAR)

σ_0 = 26.5 ksi
ℓ = + 5 INCHES (START OF TEAR)

FIGURE 14 BUCKLING PATTERN SEQUENCE (NORMAL TO PANEL FACE) FOR 30 INCH WIDE X .08 INCH THICK 2024-T3 ALUMINUM PANELS

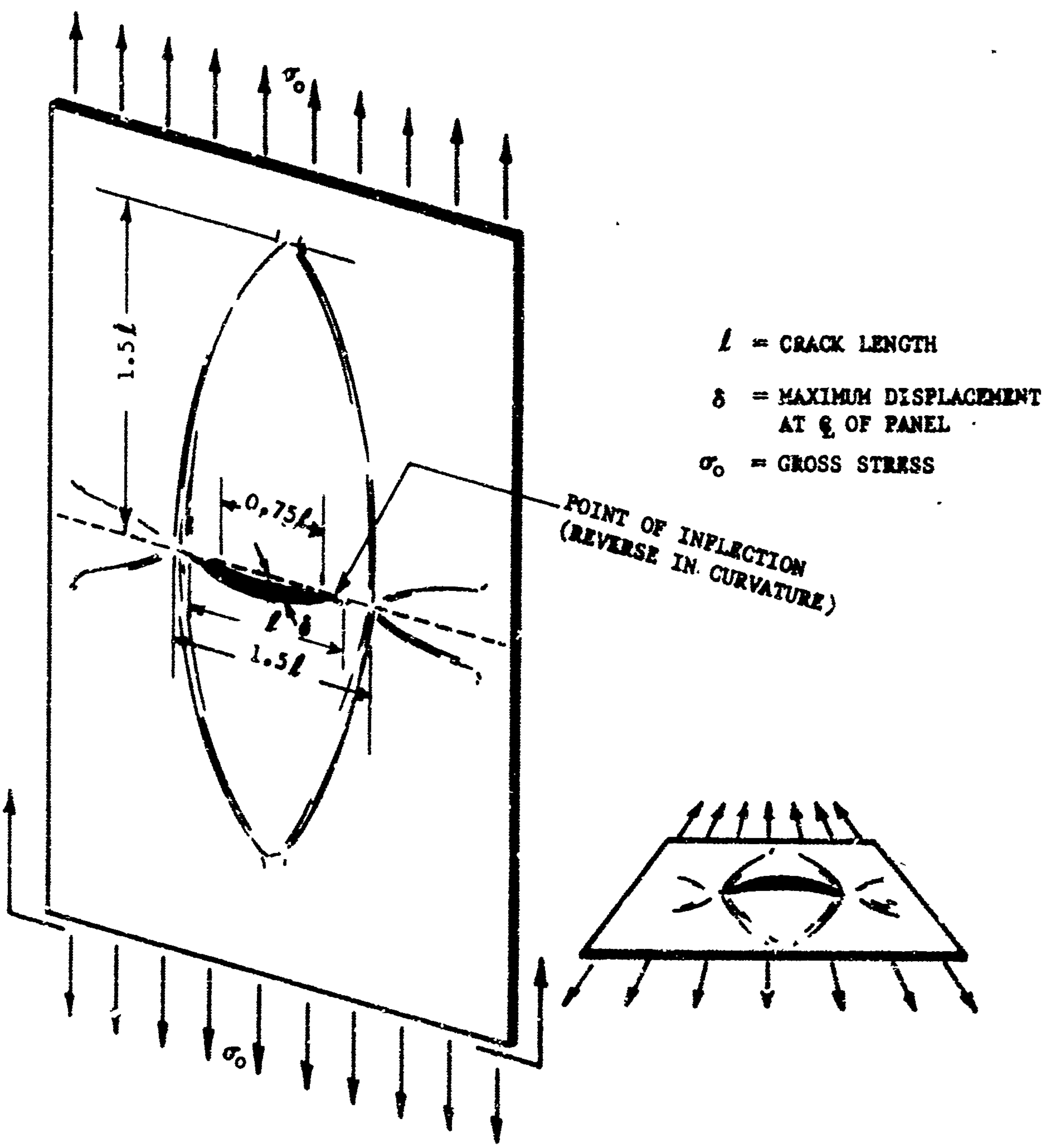

FIGURE 15 TYPICAL DIMENSIONS OF PANEL BUCKLE NEAR A CRACK IN A TENSION PANEL

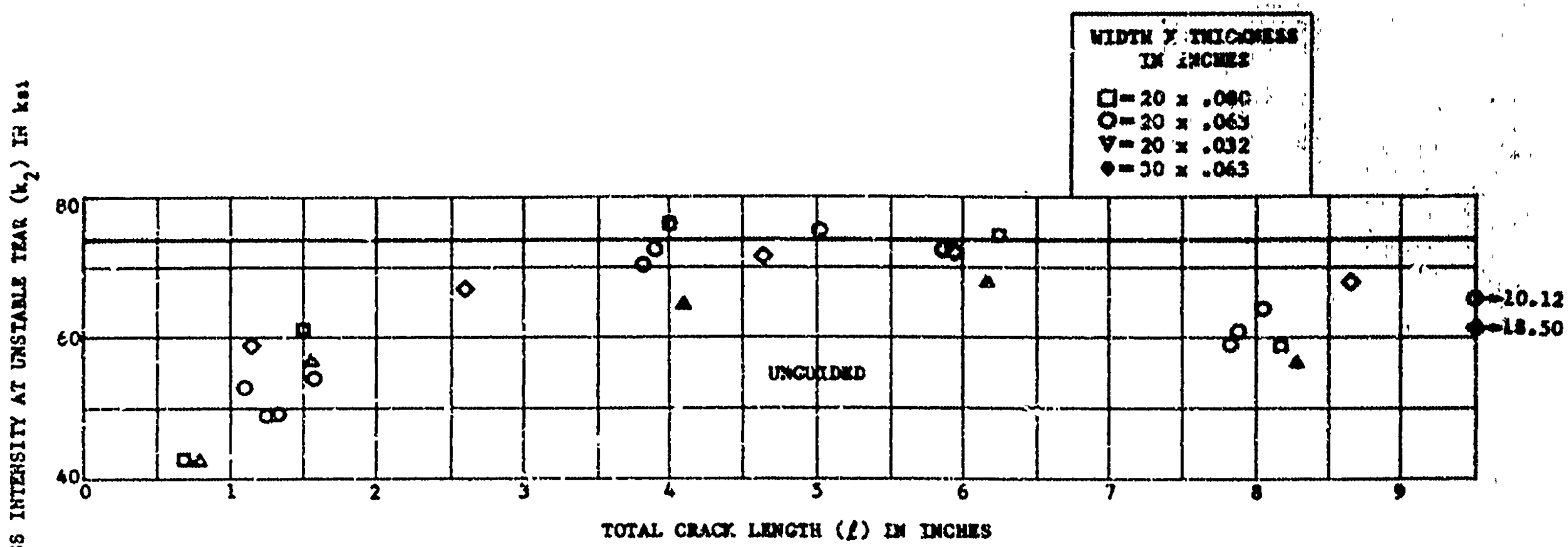

FIGURE 17 STRESS INTENSITY VS. CRACK LENGTH FOR CONSTANT LOAD IN UNGUIDED PANELS

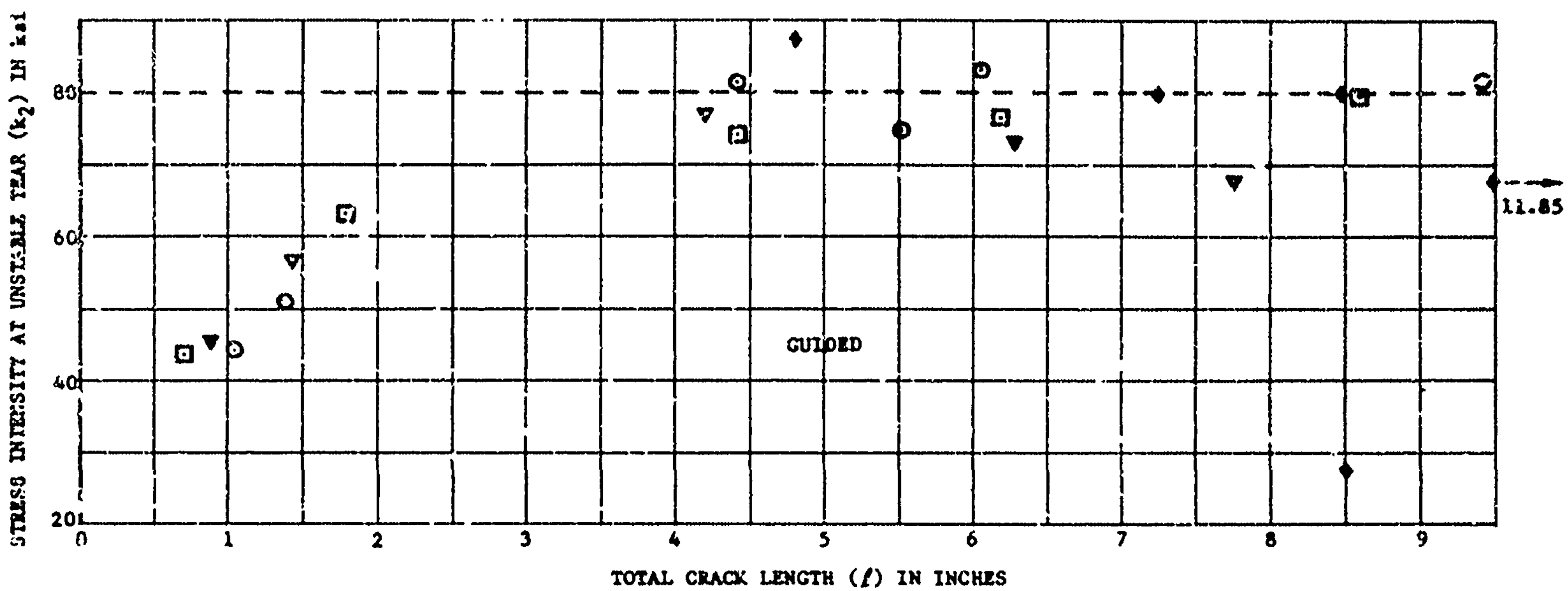

FIGURE 16 STRESS INTENSITY VS. CRACK LENGTH FOR CONSTANT LOAD IN GUIDED PANELS

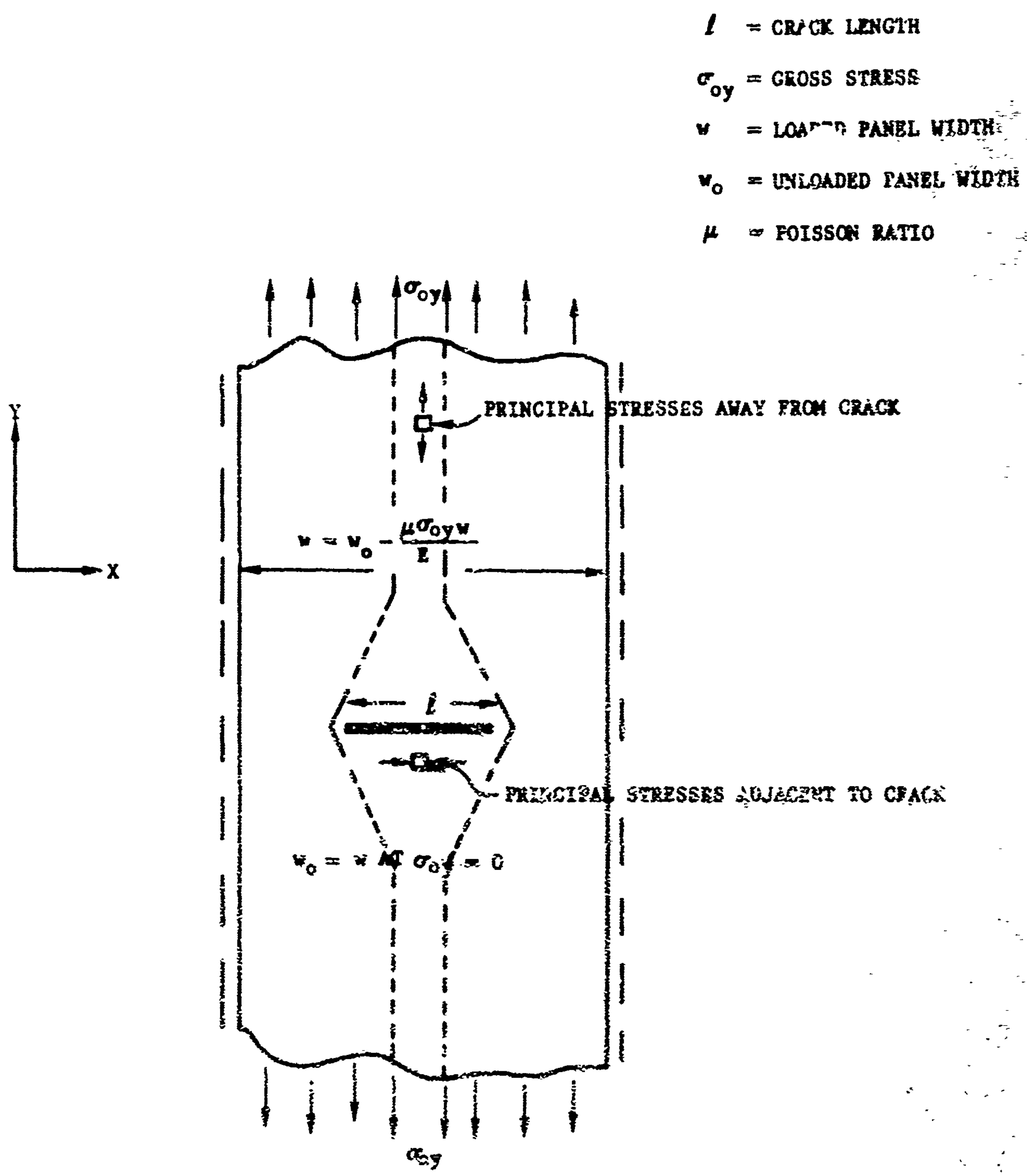

FIGURE 18 ILLUSTRATION OF STRESS AND STRAIN IN A FATIGUE CRACKED PANEL

the amount e_x. The distribution of strain parallel to the crack in these segments will, however, not be uniform and, in general, not equal to the Poisson induced strain remote from the crack. The resulting stresses and strains in the segment of the panel above and below the crack can be considered as those in a plate segment restrained on the boundaries except for one straight and free edge which corresponds to the crack. Because the load is being applied parallel to this free edge, the amount of compression that can be induced is limited by the stiffness of the panel segment. Thus, when the change in dimension away from the crack $e_x \ell$ is equal to some limiting value which corresponds to the critical buckling displacement of the panel segment, the free edge of the crack will start to buckle from the flat plane. For values of $e_x \ell$ in excess of this critical value, the corresponding change in length measured along the edge of the crack should be equal to the critical displacement for buckling plus a component of displacement resulting from the buckling of the panel segment.

The above relationship between buckling displacement adjacent to a crack and the corresponding displacement away from the crack should also be generally applicable to conditions of biaxial stress. For biaxial stress, the strain away from and parallel to the crack can be determined by considerations of plane stress and strain

$$e_x = \frac{\sigma_{ox}}{E} - \mu \frac{\sigma_{oy}}{E}$$

For the case of uniaxial tension discussed above, $\sigma_{ox} = 0$.

COLUMN ANALOGY FOR CRACK BUCKLING

Correlations of the observed beginning of buckling in 2024-T3 aluminum were made based on the assumption that the critical buckling strain adjacent and parallel to the crack will be equal to the corresponding strain away from the crack. An expression for the critical buckling strain was derived from the equation of a column on an elastic foundation[19].

$$P_B = c\left(\frac{\ell}{\pi}\right)^2 + EI\left(\frac{\pi}{\ell}\right)^2 \qquad (25)$$

where P_B = critical column load

c = spring constant for elastic restraint

When $c = 0$, equation (25) reduces to the familiar Euler buckling equation as suggested by Reference 20. Equation (25) can be presented in terms of critical buckling strain e_B by dividing both sides of the equation by the product of Young's modulus (E) and the area (A)

$$e_B = \frac{c}{AE}\left(\frac{\ell}{\pi}\right)^2 + \frac{EI}{AE}\left(\frac{\pi}{\ell}\right)^2 \qquad (26)$$

For the case of uniaxial tension where e_B is equal to the corresponding strain away from the crack, equation (26) can be written

$$\sigma_o = \frac{c}{A\mu}\left(\frac{\ell}{\pi}\right)^2 + \frac{EI}{A\mu}\left(\frac{\pi}{\ell}\right)^2 \qquad (27)$$

COMPARISON BETWEEN TEST DATA AND A SIMPLE EULER COLUMN

Considering the elastic support parameter (c) to be negligible, equation (27) can be expressed for a unit width of a wide column as

$$\sigma_c = \frac{EI}{A\mu}\left(\frac{\pi}{\ell}\right)^2 = \gamma \frac{Et^2}{\ell^2} \qquad (28)$$

where γ(gamma) = a lumped multiplying parameter to be determined experimentally

Using equation (28), values of gamma can be selected to correspond to the observed buckling instability at longer crack lengths in .032, .063, and .080 inch thick 2024-T3 aluminum. The results are shown on Figure 19. The agreement between equation (28) and the observed buckling in .032 inch thick aluminum can be seen. The lack of agreement for .063 and .080 inch thick material can also be seen. Since it is possible to shift the divergence to long crack lengths rather than short crack lengths by changing the value of gamma selected, no particular significance is attached to the crack lengths at which the divergence occurs on Figure 19. Further attempts to modify the single parameter approach of equation (28) by modifying the exponent of ℓ will not significantly improve the overall correlation.

If it is assumed that the reasons for divergence from equation (28) result from the fact that the elastic restraint provided the assumed column segment is not negligible, then a limit can be established for the use of equation (28) provided the nature of the elastic restraint can be defined. Because of the complex nature of the stress distributions, the extent of the buckled region, and boundary restraints, a direct assessment of c is difficult. It can be expected that c will, in fact, not be a constant as suggested in equation (27), but it will vary directly as EI and inversely as some function of ℓ. Examination of the data trends as shown in Figure 19 would seem to confirm this conclusion. It would appear that an empirical criterion limiting the use of equation (28) to values of $\frac{Et^2}{\ell^2} < 11$ ksi is justified until more can be learned about the problem. The curve $\frac{Et^2}{\ell^2} = 11$ ksi is also shown on Figure 19.

PARAMETRIC STUDY OF BUCKLING BEHAVIOR

Because of the above difficulties associated with definition of c and also in associated difficulties with defining variable behavior in the second "Euler" term, an attempt at a direct solution of equation (25) or a more complex plate model does not appear justified provided a parametric means of data reduction can be found. Applicable parameters can be found by reducing Equation (25) to dimensionless form[19],

$$\frac{P_B}{\sqrt{cEI}} = \left(\frac{\sqrt{2}\,\beta\ell}{\pi}\right)^2 + \left(\frac{\pi}{\sqrt{2}\,\beta\ell}\right)^2 \qquad (29)$$

where $\beta = \sqrt[4]{\frac{c}{4EI}}$

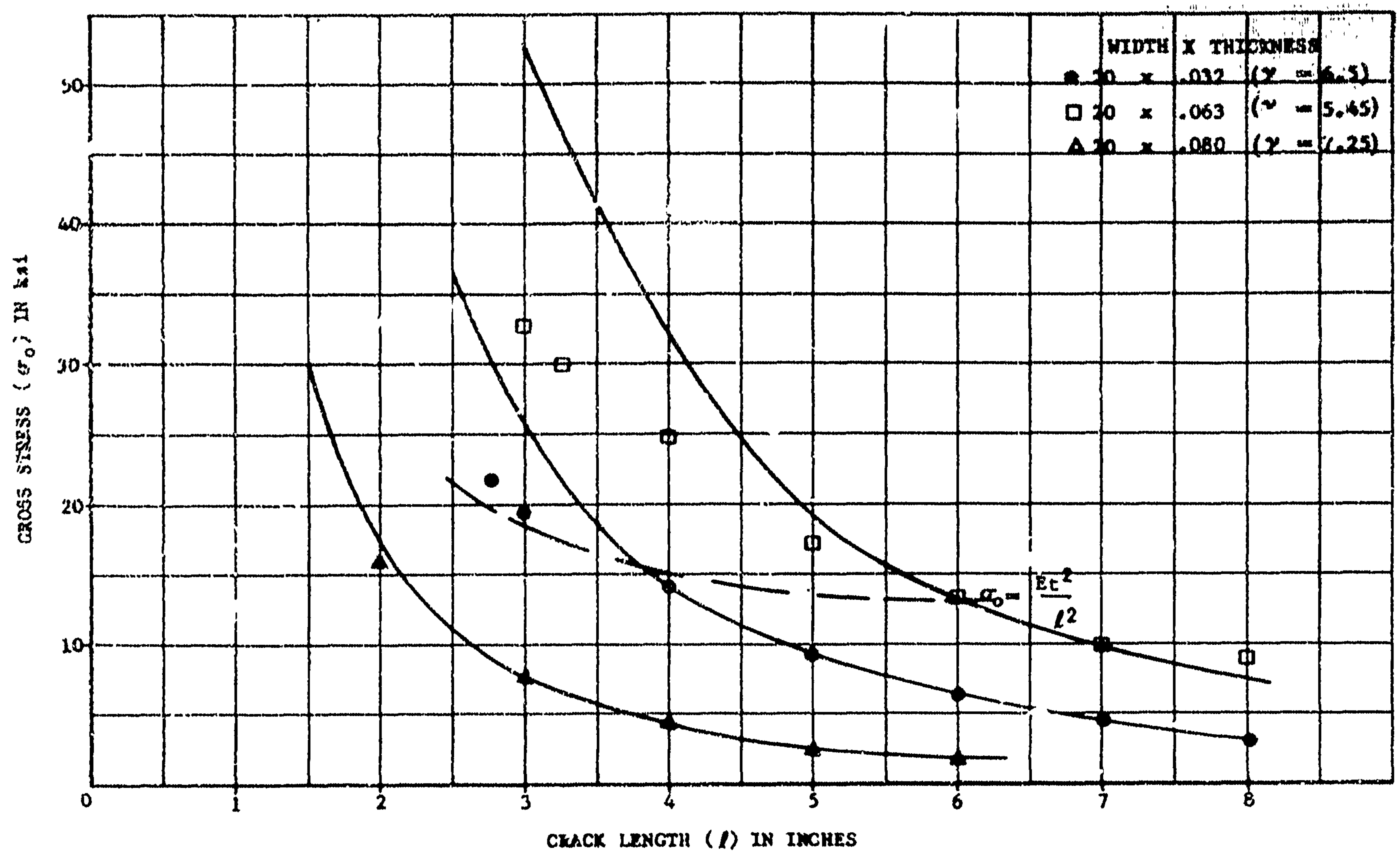

FIGURE 19 COMPARISON OF THE ONSET OF BUCKLING IN 2024-T3 ALUMINUM PANELS WITH EULER BUCKLING CURVES

From equation (27), two dimensionless parameters are available: $P_B/\sqrt{cEI}$, and $\frac{\sqrt{2}}{\pi}\beta \ell$. If constants that are not significant dimensionally are ignored in equation (27), a similar set of parameters could be defined as

$$\frac{A\,\sigma_0}{\sqrt{cEI}} \qquad\qquad (30)$$

$$\ell\sqrt[4]{\frac{c}{EI}}$$

In equation (30), neither c nor A can be adequately defined. By multiplying the two quantities of (30) by $\frac{\sqrt{A}}{\sqrt{c}}$ and $\frac{\sqrt[4]{c}}{\sqrt[4]{A}}$ respectively, and assuming that the ratio $\frac{A}{c} \approx 1$, the parameters of (30) are reduced to

$$\frac{\sigma_0}{\sqrt{EI/A}} \cdot \sqrt{\frac{A}{c}} \approx \frac{\sigma_0}{\sqrt{Et^2}} \qquad\qquad (31)$$

$$\frac{\ell}{\sqrt[4]{EI/A}} \cdot \sqrt[4]{\frac{c}{A}} \approx \frac{\ell}{\sqrt[4]{Et^2}}$$

Figure 20 shows the collapse of data from Figure 19 along with data obtained during the study of titanium panels. Good correlation can be seen. The two empirical parameters of equation (31) eliminate the need to define separate multiplying parameters for each material as was seen necessary in the use of equation (28) (Figure 19). Since the data correlated represent 5 thicknesses and two values of Young's modulus, general applicability of the correlating parameters can be assumed for values of Et^2 between 7.2 ksi (in.^{2}) and 55.9 ksi (in.^{2}). Figure 21 shows the correlation of the data of Figure 19 with curves obtained by use of the average buckling curve of Figure 20. Some divergence in behavior can be seen in the .080 inch thick aluminum. Until further evaluation of possible relationships for the elastic support of the crack can be studied, the curve shown on Figure 20 can provide a means of estimating the onset of buckling for variables of the range represented.

THE RELATIONSHIP BETWEEN GROSS STRAIN AND BUCKLING DISPLACEMENT

Panel buckling can be assumed to occur when the strain away from and parallel to a fatigue crack exceeds the critical buckling strain of the panel segments above and below the crack. This critical strain level can be computed using the stress levels obtained from Figure 20 if the crack length and panel geometry are known. After panel buckling occurs, the total required shortening of the panel segments above and below the crack is made up of two parts: the critical buckling displacement and a component of displacement resulting from the deflection of the panel segment from a flat plane.

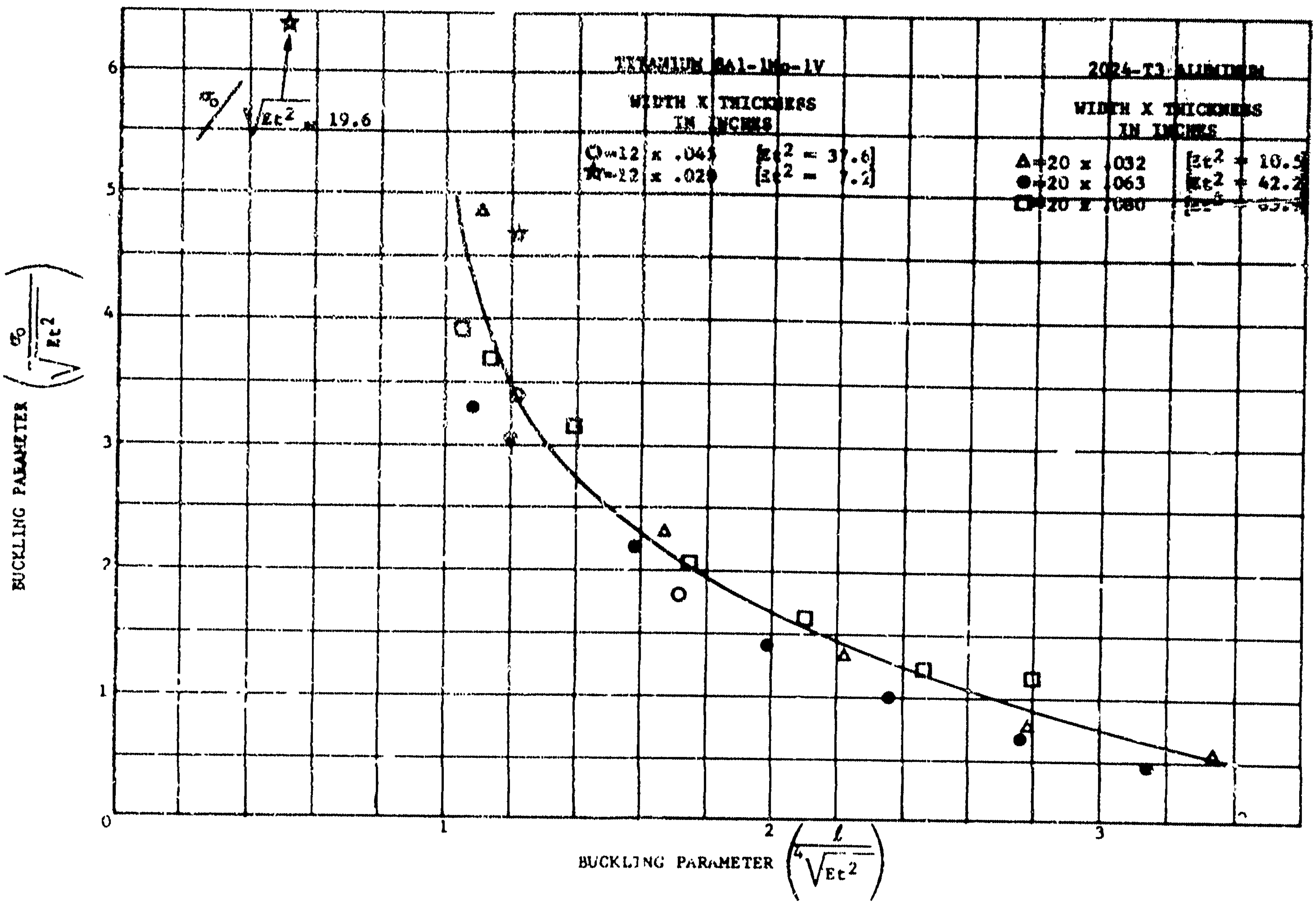

FIGURE 20 CORRELATION OF CROSS PANEL STRESS AND BUCKLING FOR Et^2 BETWEEN 7.2 ksi (IN.^{2}) AND 65.9 ksi (IN.^{2})

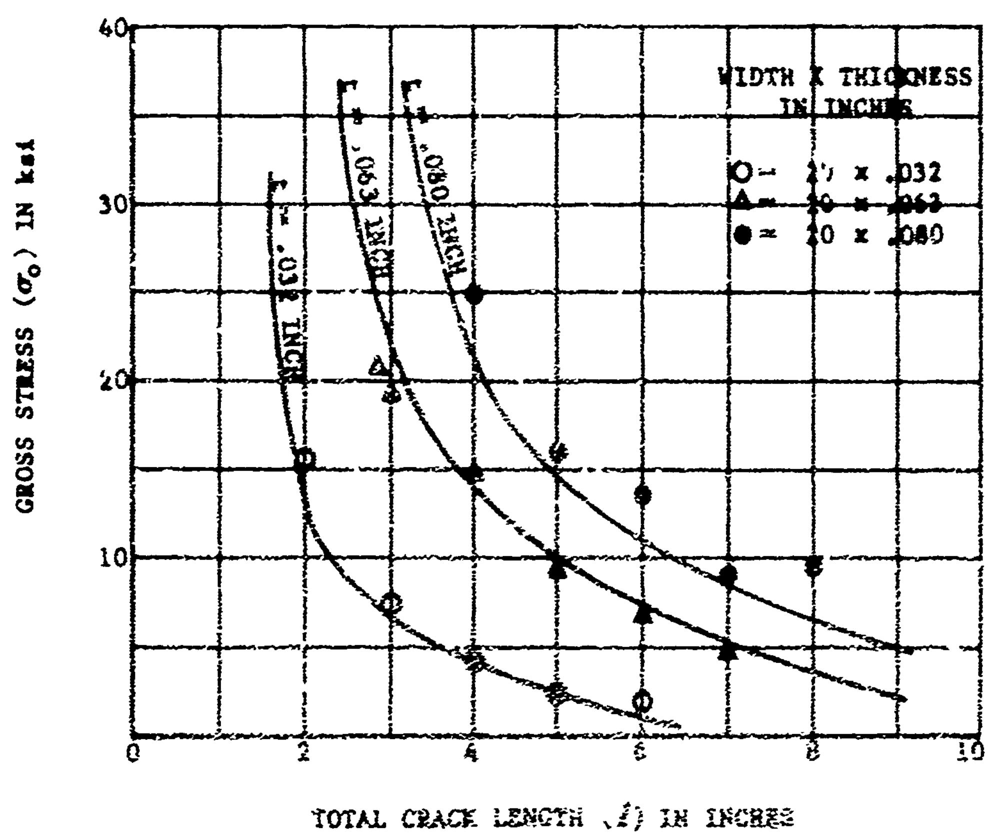

FIGURE 21 COMPARISON OF THE BEGINNING OF BUCKLING IN 20 INCH WIDE 2024-T3 ALUMINUM PANELS WITH CURVES DEFINED BY FIGURE 19

Results obtained during the experimental portion of the program (Table 19 and Figures 12, 13, and 14) showed that the characteristics of the buckle measured in the plane of the unloaded panel did not appreciably change from that shown on Figure 15 as the load was increased. Thus, it can be reasonably assumed that the characteristics of the buckled crack will show parallel trends to some easily measured quantity such as the center line displacement of the crack from a flat plane. In this manner, strain parallel to and away from the crack, the critical buckling strain, centerline deflection of the crack, and strength reduction can be interrelated.

$$\frac{\mu}{E} (\sigma_o - \sigma_B) \ell = \delta B_1 = \frac{(\sigma_2) B_2}{E} \qquad (32)$$

where σ_B = Gross panel stress corresponding to the critical buckling strain

σ_o = Gross panel stress

δ = Deflection from a flat plane measured at the center of the crack

σ_2 = Stress at the beginning of unstable tear

B_1 and B_2 = Constants to be determined experimentally

From equation (32) dimensionless parameters for data correlation can be defined:

$$\frac{\mu}{E} (\sigma_o - \sigma_B) \quad \text{and} \quad \frac{\delta}{\ell} \qquad (33)$$

Figure 22 shows a correlation of measured centerline displacements for cracked panels in terms of the above parameters. Scatter in data at the lower range of values of μ/E $(\sigma_o - \sigma_B)$ can be contributed in part to the increased influence of error in computed values of σ_B. From Figure 22, qualitative agreement between the correlating parameters(33)and equation (32) indicate that it should be possible to correlate strength reduction trends observed to occur as a result of buckling with the parameter μ/E $(\sigma_o - \sigma_B)$. This correlating parameter can also be interpreted for conditions of biaxial stress for structural applications.

THE INFLUENCE OF PANEL WIDTH ON BUCKLING DISPLACEMENTS

Before proceeding to the correlation of strength reduction resulting from buckling, a qualitative understanding of the influence of panel width on buckling of a crack must be obtained. Referring to equation (26), and Figure 15, buckling of panel segments above and below the crack result in a corresponding damped buckling pattern beyond the ends of the crack. This buckling pattern is analogous to the damped displacements of a continuous column (or beam) on an elastic foundation as implied by equation (27). If this damped buckling pattern is terminated at a free edge before the pattern has progressed far enough away from the crack, a significant reduction in the buckling restraint of the segment of panel above and below the crack could result.

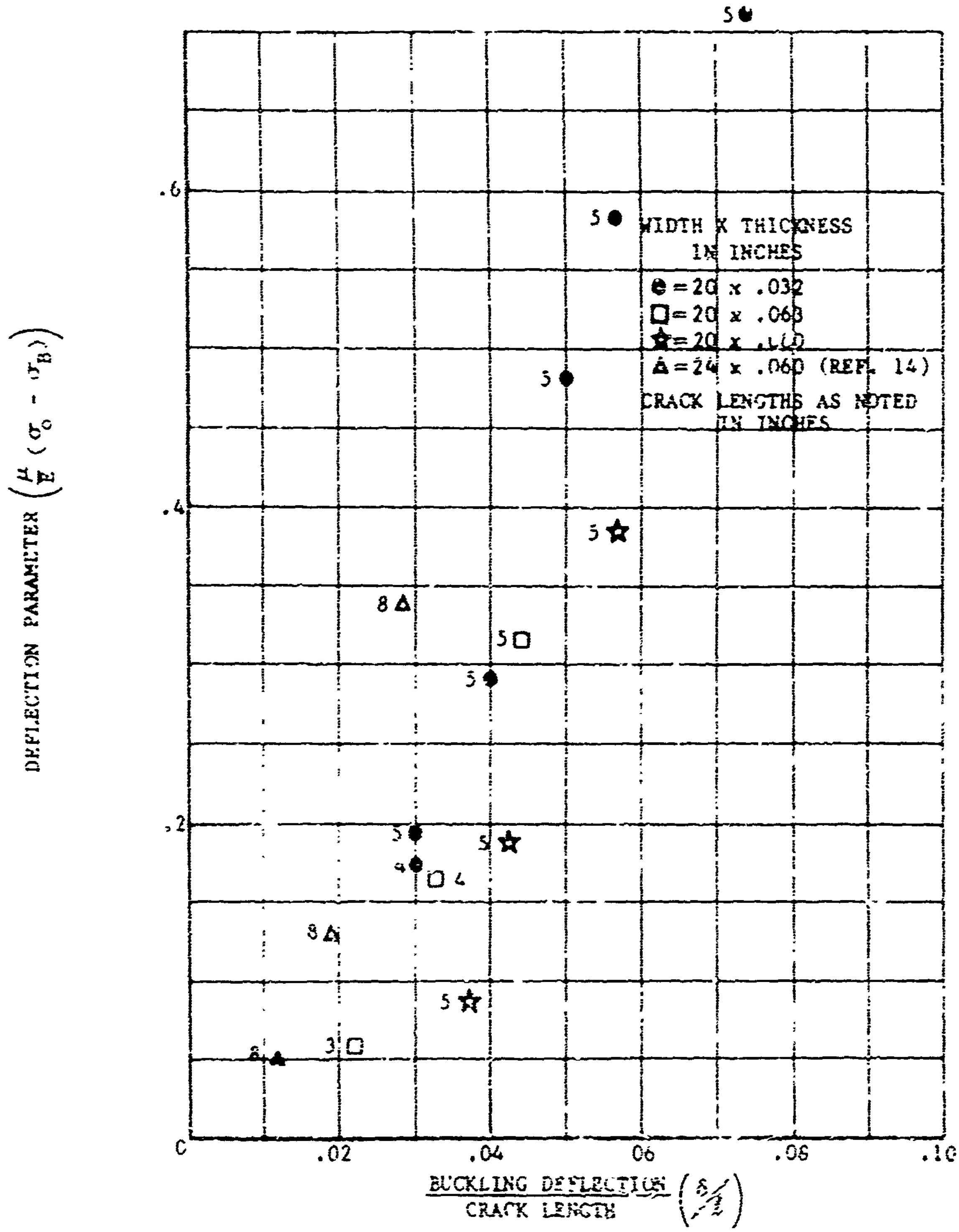

FIGURE 22 BUCKLING DEFLECTION CORRELATION FOR FATIGUE CRACKED PANELS OF 2024-T3 ALUMINUM

In Figure 23, the relationship between the beginning of buckling and the stress away from the crack for 12-inch wide 2024-T3 aluminum is compared to curves representing behavior of 20-inch wide panels taken from Figure 21. The beginning of buckling can be seen to occur at lower stress levels in the .080 inch thick, 12-inch wide panels than would be expected from measurements made on the same crack lengths in 20-inch panels. The stress at which buckling occurs in .032 and .063 inch thick, 12-inch wide panels is the same as that obtained in the 20-inch wide panels. This would indicate that the length of the buckle pattern (wave length) can be expected to increase with increased Et^2.

In order to demonstrate this interpretation of the buckling pattern in the laboratory, the buckle in 12-inch wide panels was forced from side to side. A visible corresponding change in the displacement of the free edges of the panel was seen.

Since the manner in which the panel width influences buckling is different from the manner in which width influences the strength of guided panels, the two width influences should be considered separately. Thus, there may still be buckling width influences on strength in panels whose width is sufficient to allow elastic stress intensity parameter correlations when the panel is guided.

THE INFLUENCE OF BUCKLING ON THE STRESS INTENSITY FOR UNSTABLE TEAR (k_2) IN WIDE PANELS

From Figure 17, the strength reduction in unguided panels from that in guided panels (Figure 16) can be seen. In wide panels the range of crack lengths between 3 and 6 inches show a strength reduction due to buckling from an average stress intensity of 80 ksi $\sqrt{in.}$ in guided panels to an average stress intensity of 74 ksi $\sqrt{in.}$ in unguided panels. For longer crack lengths, the stress intensity at the beginning of unstable tear is further reduced to an average value of about 62 ksi $\sqrt{in.}$ A trend of increasing stress intensity with increasing thickness is noticeable in unguided panels, Figure 17. This trend was not apparent in guided panel data (Figure 16). Representative stress intensities for crack lengths between 3 and 6 inches (Figure 17) were found to be

$t = .032$ inches $\quad k = 68.5$ ksi $\sqrt{in}$
$t = .063$ inches $\quad k = 73.5$ ksi $\sqrt{in}$
$t = .080$ inches $\quad k = 76.0$ ksi $\sqrt{in}$

These trends could be the result of buckling and the differences of the quantity $\frac{\mu}{E}(\sigma_o - \sigma_B)$ where σ_B increases with the square of the thickness.

A study of the quantity $\frac{\mu}{E}(\sigma_o - \sigma_B)$ for the assumption that the beginning of unstable tear would occur at constant stress intensity in 2024-T3 aluminum

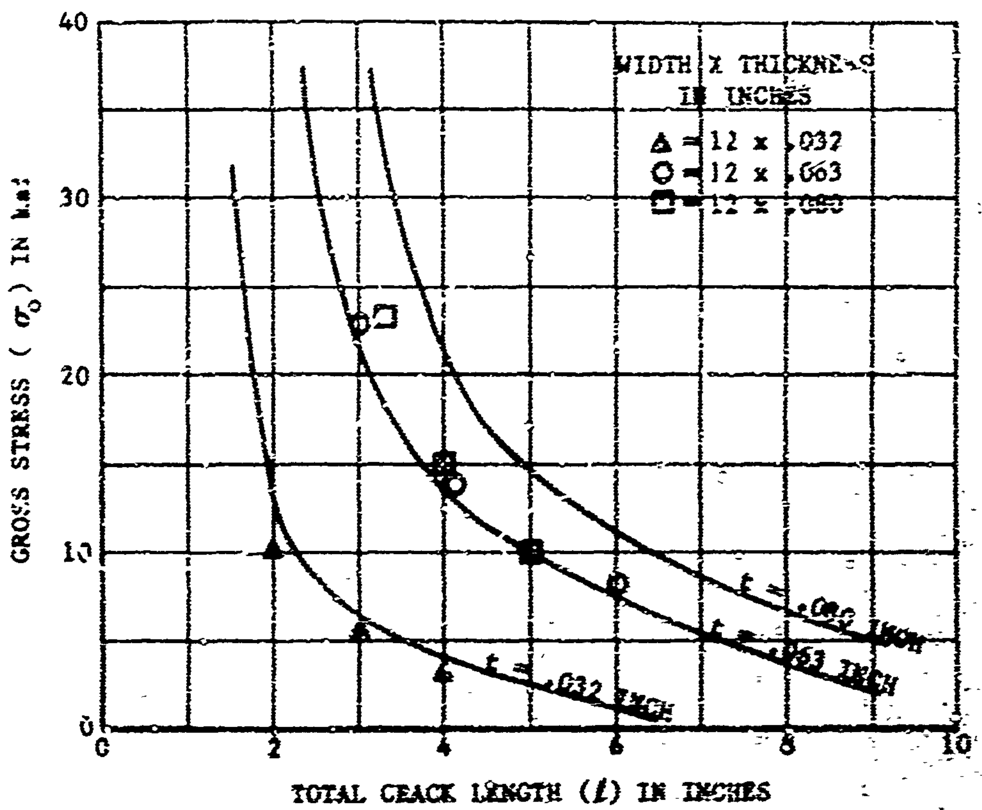

FIGURE 23 COMPARISON OF THE BEGINNING OF BUCKLING IN 12 INCH WIDE 2024-T3 ALUMINUM PANELS WITH CURVES DEFINED BY FIGURE 20

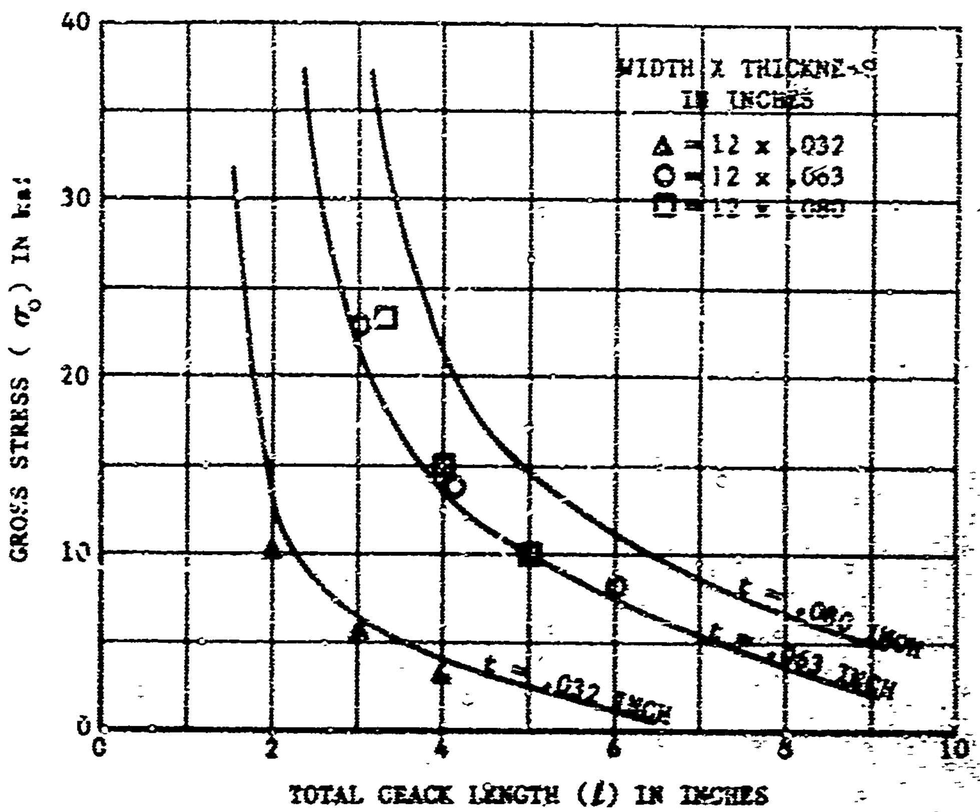

FIGURE 23 COMPARISON OF THE BEGINNING OF BUCKLING IN 12 INCH WIDE 2024-T3 ALUMINUM PANELS WITH CURVES DEFINED BY FIGURE 20

shows that ($\sigma_o - \sigma_B$) would be a near constant for a given thickness over the entire range of crack lengths from 3 inches to 10 inches (the curves of critical buckling stress and the curves of constant stress intensity are very close to parallel in this range). From the observed critical stress intensities, a similar study shows a near constant ($\sigma_o - \sigma_B$) between crack lengths of 3 and 6 inches and lower values for crack lengths greater than 6 inches. These observations are in line with assumed constant relationship between $\frac{\mu}{E}$ ($\sigma_o - \sigma_B$) and the reduction of the stress intensity at the beginning of unstable tear. The reduced stress intensity for unstable tear at longer crack lengths can most probably be accounted for in terms of a width influence on buckling behavior. However, the possibility of a discontinuity in behavior from some other cause cannot be entirely ruled out.

Until such time as further investigations are made, it can be assumed that the additional strength reduction seen at long crack lengths in wide buckled panels is a width sensitive phenomenon. The portion of Figure 17, which has meaning in terms of application to reinforced structure is, therefore, the crack length range between 3 inches and 6 inches. A crack length of 6 inches roughly corresponds to a l/w of 1/3 in 20-inch wide panels.

It is interesting to note that in the 20-inch wide panels, the buckling width influence seems to become effective over a narrow range of crack lengths for all thicknesses, Figure 17. This would indicate that the relatively large differences noted in the beginning of buckling (Figure 23) as a function of width and thickness is not carried over into the width influence on k_2. Physically, this probably means that the total shortening parallel to the crack at k_2 is large and differences in the critical buckling displacement are thus not a major consideration in determining the buckling wave length. Based on observations of 2024-T3 aluminum a limiting value of $l/w = 1/3$ can be assumed for the buckling influence on strength for the thickness range considered. This corresponds roughly to one buckling wave on each side of the crack within the boundaries of the panel.

THE INFLUENCE OF BUCKLING ON THE STRESS INTENSITY FOR UNSTABLE TEAR IN NARROW PANELS

The influence of buckling on the stress intensity at the beginning of unstable tear in narrow panels can be assessed by assuming that the total width influence is separated into a two-dimensional stress and strain influence which should be close to that seen in guided panels (Figures 3, 4, and 5) and a buckling width influence similar to that seen in Figure 17.

In 12-inch wide panels (Figure 24) the buckling width influence on the stress intensity at the beginning of unstable tear starts near a crack length of 4 inches. This is approximately the same l/w ratio ($l/w \approx 1/3$) as that observed in 20-inch wide panels. A comparison of the stress intensity in guided and unguided 12-inch wide panels shows a change in average stress intensity from 67 ksi $\sqrt{in.}$ to 57 ksi $\sqrt{in.}$ for crack lengths unaffected by either gross section yielding or a buckling width influence.

Data from the 9-inch panel tests showed no distinct range of crack lengths for strength reduction due to buckling without a buckling width influence. This is due to the fact that the minimum crack lengths which result in fracture without general yielding is nearly 1/3 of the panel width.

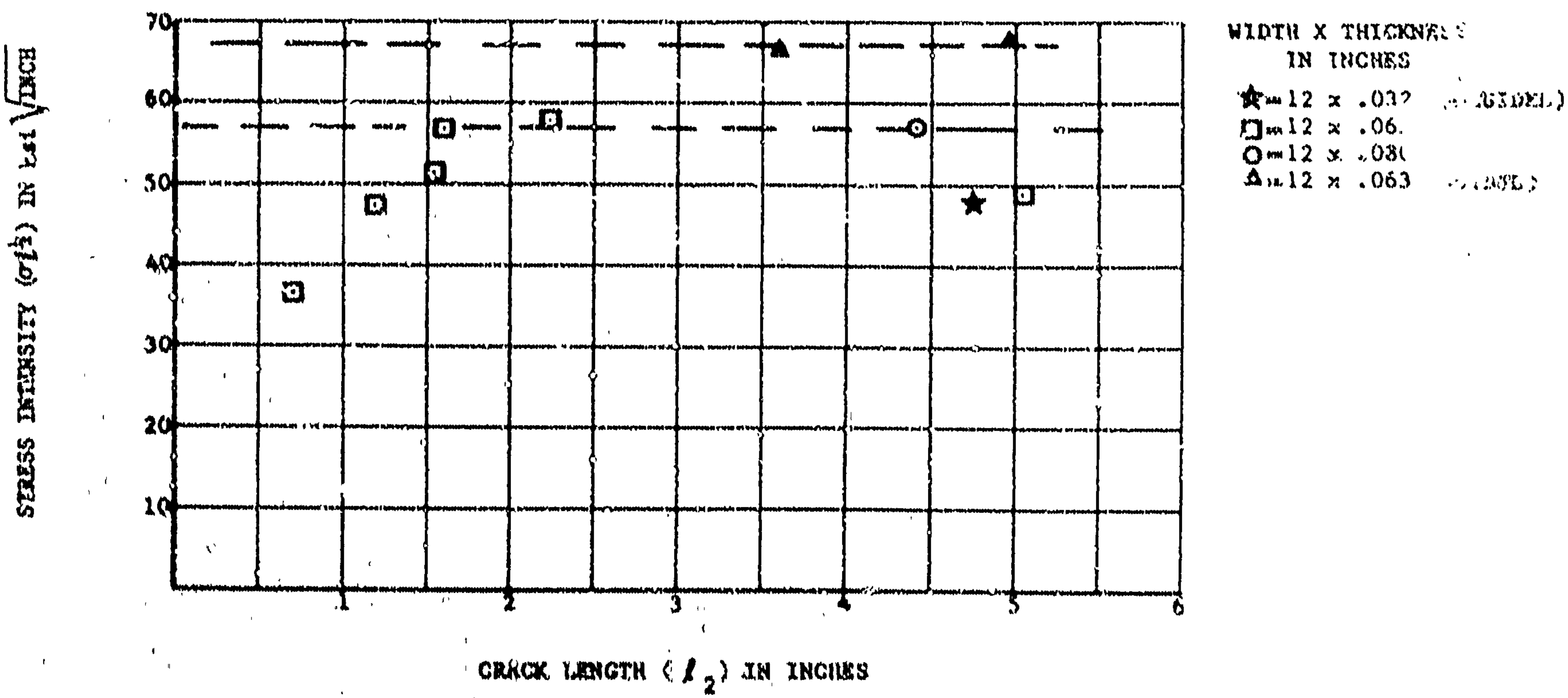

FIGURE 24 CRITICAL STRESS INTENSITY FOR FRACTURE VS. CRACK LENGTH IN 12 INCH WIDE UNGUIDED AND GUIDED 2024-T3 ALUMINUM PANELS

... ne abo... , ... ould appear that the stress intensity at the beginning of unstable tear will show a buckling width influence whenever $l/w \approx 1/3$. Considerably more work must be done, however, before any general quantitative estimates can be made regarding the variance of panel strength as a function of buckling in either wide or narrow panels.

THE INFLUENCE OF BUCKLING ON THE STRESS INTENSITY FOR UNSTABLE TEAR (k_2) WITH GROSS SECTION STRAIN ABOVE THE PROPORTIONAL LIMIT

It is difficult to see any influence of buckling on the strength of cracks less than 3 inches in length in 2024-T3 aluminum of the thickness range shown in Figures 16 and 17. It can be expected that the strains away from and parallel to the crack will increase more rapidly with gross stress when the gross section is stressed above the proportional limit. This is due to the fact that the strain parallel to and away from the crack will be:

$$e_x = \mu \frac{\sigma_c}{E} + \mu_p \, e_{py} \qquad (34)$$

where

- e_x = total strain in the x direction (parallel to the crack)
- μ = Poisson's ratio (approximately 1/3)
- σ_g = gross stress away from crack
- E = Young's modulus
- μ_p = Poisson's ratio for plastic strain (approximately 1/2)
- e_{py} = plastic strain in the direction normal to the crack

Assuming the strength reduction for a given crack length varies as e_x, reduction in strength due to buckling might be expected to exceed that of the elastic range. This influence is assumed in the construction of Figure 25 which shows an interaction diagram of the type shown in Figure 8. Figure 25 is identical to Figure 8 with the exception that for the purpose of developing the interaction curves, the stress intensity for the beginning of unstable tear with elastic behavior away from the crack has been assumed at an average value for all thicknesses as .93 times the stress intensity for the beginning of unstable tear in guided panels. Data whose crack length to panel width ratio is greater than 1/3 has not been shown on Figure 25.

SUMMARY OF THE INFLUENCES OF PANEL BUCKLING

1. The phenomena of buckling of panel segments above and below a crack which is normal to an applied uniaxial tension loading can be qualitatively explained by considering the Poisson effect and the resulting strains parallel to and remote from the crack.

2. The buckling of the panel segments above and below the crack can be predicted by a single curve for values of Et^2 between approximately 7 and 70.

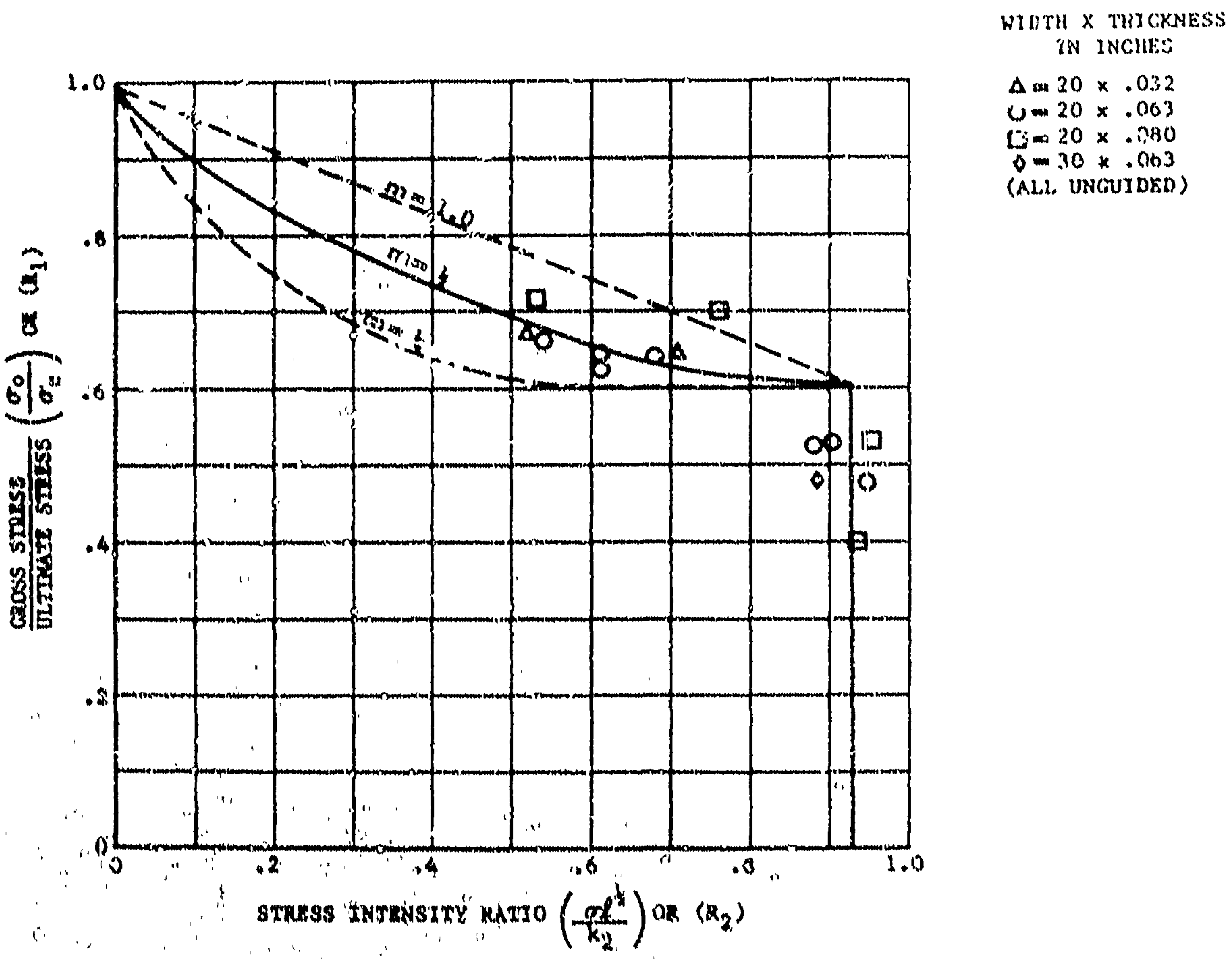

FIGURE 25 INTERACTION DIAGRAM FOR YIELDING SIMULTANEOUS WITH FRACTURE AND BUCKLING, UNGUIDED PANELS 2024-T3 ALUMINUM

This curve is based on the empirical correlating parameters as follows:

$$\frac{\sigma_0}{\sqrt{Et^2}}$$

$$\frac{\ell}{\sqrt[4]{Et^2}}$$

3. Buckling deflections and reduction of the stress intensity at the beginning of unstable tear will vary as the difference between the strain away from and parallel to the crack and the critical buckling strain of the panel segment adjacent to the crack.

4. The influence of panel buckling on the stress intensity at the beginning of unstable tear is nearly constant for the elastic range of behavior for values of $\ell/w < 1/3$ in 2024-T3 aluminum. For values of $\ell/w > 1/3$ further reduction in stress intensity occurs.

5. The influence of buckling varies with panel width in narrow panels.

6. In 2024-T3 aluminum, the reduction in stress intensity at the beginning of unstable tear resulting from buckling is not measurable in the range of crack lengths where unstable tear occurs with gross panel stresses above the proportional limit of the material. A small increase in buckling influence is probable, however, as the strain parallel to the crack should increase more than in elastic behavior.

7. Because of the observed constant influence of buckling on the stress intensity for unstable tear in 2024-T3 aluminum, the interaction between gross section yielding, panel buckling and fracture may be handled in the same way as the interaction between gross section yielding and fracture in guided panels with the exception that a reduced value of the constant stress intensity for unstable tear must be used.

VII STABLE TEAR

IMPORTANCE

In relatively ductile materials such as 2024-T3 aluminum and titanium 8Al-1Mo-1V, appreciable amounts of stable tear precede unstable tear. If the condition of first unstable tear is used as a criterion for the ultimate strength of a fatigue cracked panel, then an estimate of the amount of stable tear preceding the unstable crack length is needed. Without an estimate of the amount of stable tear, it is not possible to determine the stress at which failure will occur for a given initial crack length.

GENERAL CONSIDERATIONS

Previous discussion of variance in stress intensity cannot be easily interpreted to yield changes in slow tear characteristics. A change in stress intensity can take place through either changes in stress or crack length, or a combination of the two. Thus, differences in the stress intensity at the beginning of unstable tear for guided and unguided panels does not indicate whether these changes are predominately the result of changes in stress or crack length. Figure 26 shows typical tear behavior of guided and unguided 2024-T3 panels. Similar slow tear behavior was found in titanium 8Al-1Mo-1V. Tear behavior of this type was also shown to occur in 2024-T81 aluminum and AM 350 CRT and AM 355 CRT steel[15].

Stable tear was explained in Section IV in terms of an effective notch radius ρ' that increased as plastic deformation adjacent to the crack tip increased (equation (3)).

$$k = \bar{\sigma}\ell^{\frac{1}{2}} = \frac{e_u E}{\sqrt{2}} \sqrt{\rho'}$$

During stable tear, the crack tip strain was assumed to be at some ultimate value e_u. Additional increases in stress intensity accompanied by stable tear was considered possible only with corresponding increases in ρ' (equation (4))

$$\frac{dk}{d\ell} = \frac{d(\bar{\sigma}\ell^{\frac{1}{2}})}{d\ell} = \frac{e_u E}{\sqrt{2}} \frac{d\sqrt{\rho'}}{d\ell}$$

From a study of the stable tear behavior under incremental loading, the general nature of the dependence of ρ' on changes in stress and crack length can be deduced. If an additional increment of loading is applied to a panel containing a stable crack whose crack tip strain is e_u, tear will start and continue with some increase in length to a new stable configuration. It can thus be seen that increase in ρ' is predominately dependent upon changes in length.

$$\frac{dk}{d\ell} = \frac{e_u E}{\sqrt{2}} \frac{d\sqrt{f(\ell)}}{d\ell} \qquad (35)$$

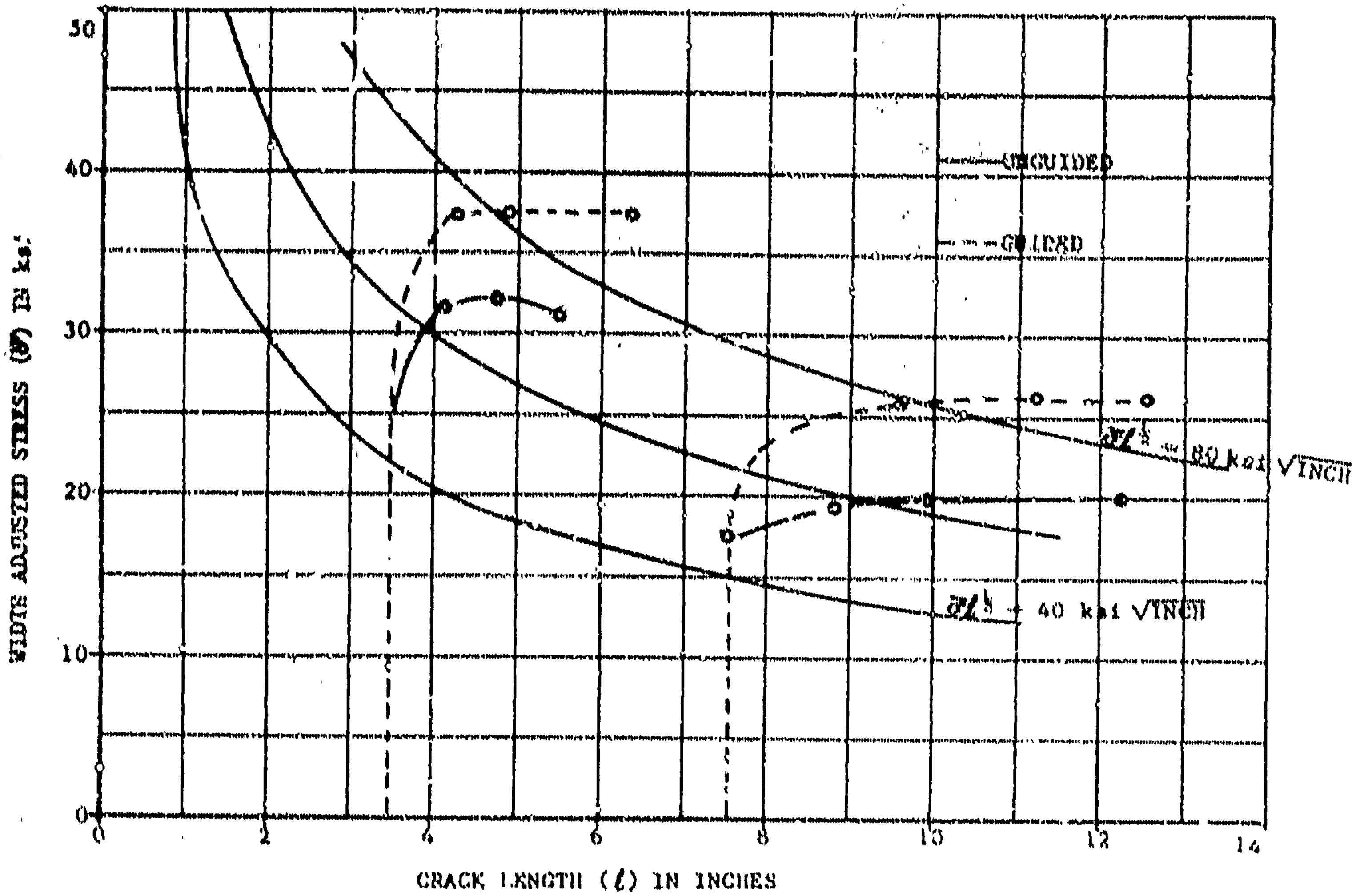

FIGURE 26 TYPICAL TEAR BEHAVIOR IN 2024-T3 ALUMINUM SHEET

THE RELATIONSHIP BETWEEN THE AMOUNT OF STABLE TEAR AND THE INIT. L CRACK LENGTH IN WIDE PANELS

In wide panels of 2024-T3 aluminum, there is a trend of increasing amounts of stable tear with increasing initial crack length (Figure 27). No corresponding increase in stress intensity (k_2) occurs (Figures 16 and 17). Similar behavior was observed in titanium 8Al-1Mo-1V (Figure 28). Figure 28 represents two heats of titanium; thus, no significance can be attached to differences occurring as a function of thickness. From the trends observed (Figures 27 and 28) it is suggested that the amount of stable tear in wide unreinforced panels be estimated as a fraction of the initial crack length (ℓ_1)[1]. For example, the critical unstable crack length (ℓ) could be written for guided panels of 2024-T3 aluminum (Figure 29) as

$$\ell = \ell_1 + (\Delta \ell / \ell_1)\, \ell_1$$

$$\ell = \ell_1 + 0.33\ \ell_1 = 1.33\ \ell_1$$

and the critical stress intensity could be written

$$k_2 = \bar{\sigma}\,(1.33\ \ell_1)^{\frac{1}{2}} = \bar{\sigma}\,(1.33\ )^{\frac{1}{2}} \ell_1^{\frac{1}{2}}$$

$$k_2 = \bar{\sigma} s \ell_1^{\frac{1}{2}} = \bar{\sigma} \ell^{\frac{1}{2}} \qquad (36)$$

where

ℓ_1 = initial crack length

$s = \sqrt{1 + \Delta\ell/\ell_1}$ = constant for a given material and condition of lateral buckling restraint.

Equation (36) can provide a direct means of estimating the ultimate strength of fatigue cracked panels from a given initial crack length ℓ_1 in a wide panel. This procedure appears equally applicable to guided and unguided panels [1].

THE RELATIONSHIP BETWEEN THE AMOUNT OF UNSTABLE TEAR AND INITIAL CRACK LENGTH IN NARROW PANELS

The stable tear of cracks in narrow panels was found to be significantly less than that of wide panels. This could be accounted for in part by the width dependence of the rate of change of stress intensity (equation 8). However, in an attempt to construct curves of the type shown in Figure 2a, it was apparent that the differences in unstable crack length could not be entirely accounted for by tangency considerations. Each width appeared to have its own set of tear versus crack length curves. Because of this observed decrease in stable tear with width, in both 2024-T3 aluminum and titanium 8Al-1Mo-1V, it was concluded that tear studies applicable to reinforced panels could only be obtained from relatively wide panels. Additionally, and what might prove to be of utmost importance in considerations of delayed fracture in titanium, it is possible that delayed fracture studies in narrow panels could lead to false conclusions as to the severity of the problem as it pertains to wide and reinforced panels.

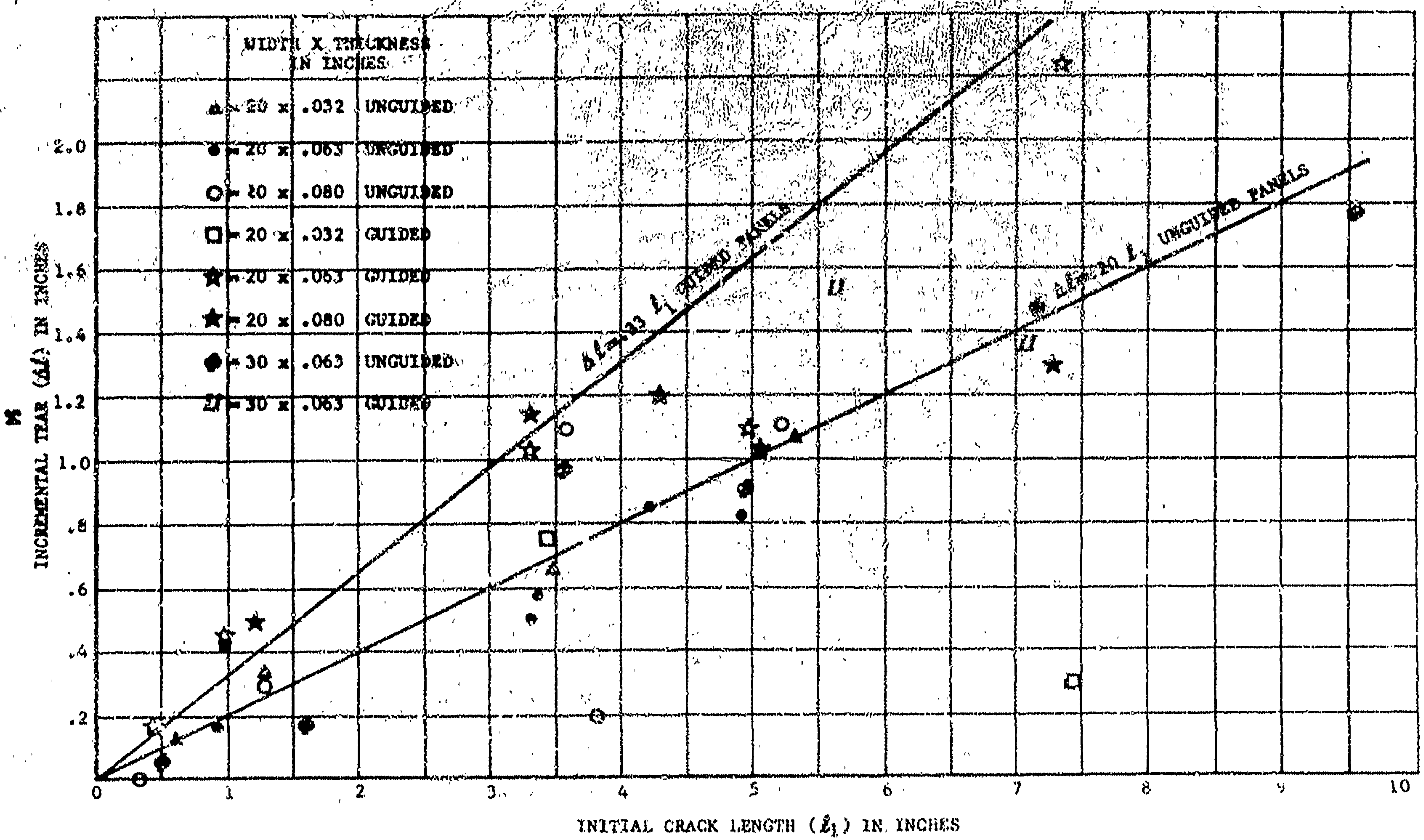

FIGURE 27 INCREMENT OF STABLE TEAR ($\Delta \ell$) VS. INITIAL CRACK LENGTH (ℓ_1) FOR 20 INCH WIDE PANELS OF 2024-T3 ALUMINUM

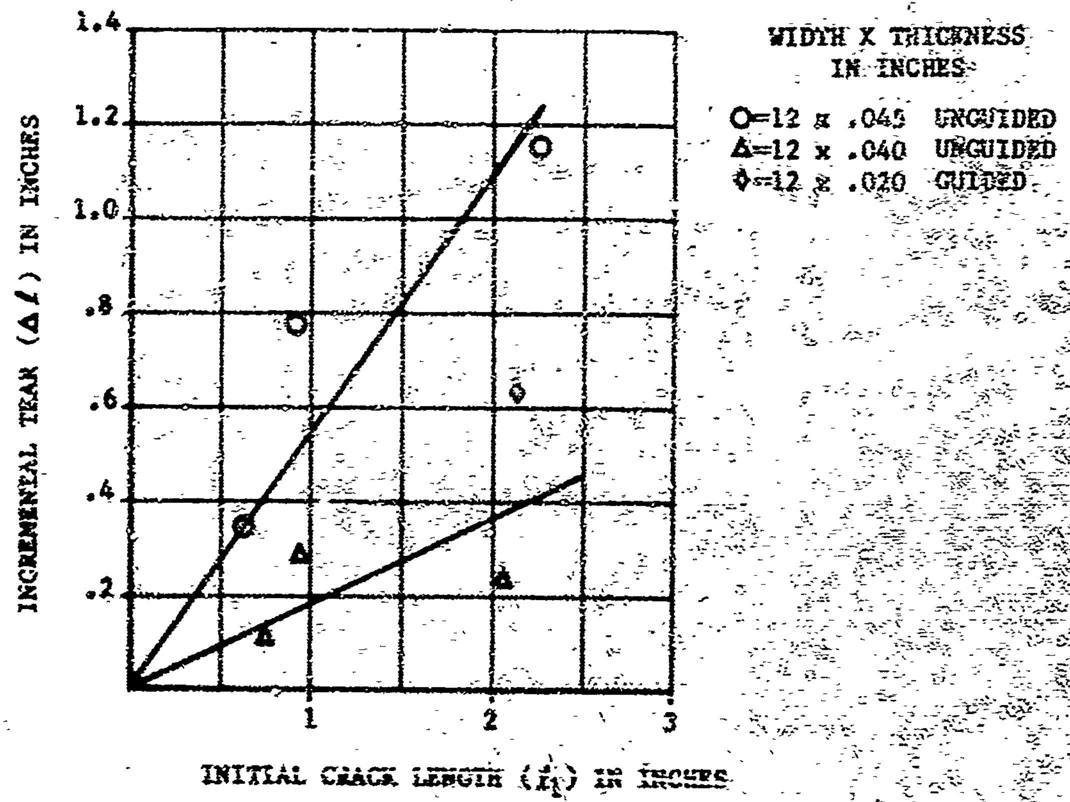

FIGURE 28 INCREMENT OF STABLE TEAR ($\Delta \ell$) VS. INITIAL CRACK LENGTH (ℓ_1) FOR 12 INCH WIDE PANELS OF TITANIUM 8Al-1Mo-1V

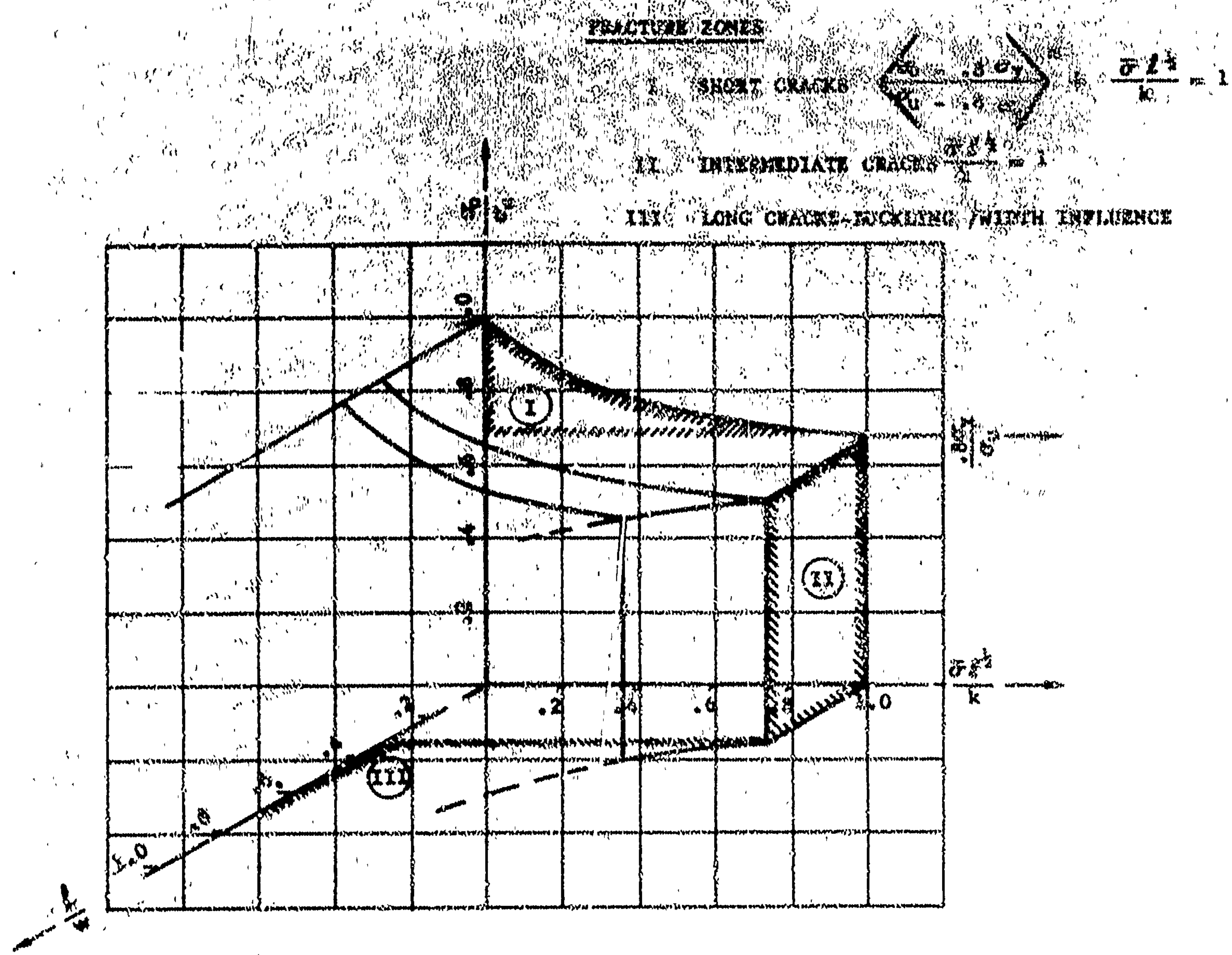

FIGURE 29 INTERACTION DIAGRAM AND FRACTURE ZONES FOR UNREINFORCED AXIALLY LOADED PANELS

VIII SYNTHESIS OF STRENGTH INFLUENCING PARAMETERS FOR WIDE PANELS

The influences of gross section yielding and panel buckling on the stress intensity for the beginning of stable tear in wide unreinforced panels can be collected and presented in a single diagram. This diagram can aid in the overall understanding of the relationship between strength influencing variables. The diagram is a three-dimensional representation with two of the axes representing an interaction diagram of the type shown in Figures 8 and 25. The third axis is the panel ℓ/w ratio which denotes the limit of crack lengths for buckling width influence as $\ell/w = 1/3$. This diagram is shown in general form in Figure 29. For convenience of discussion, zones of behavior are designated on this diagram as follows:

Zone I Short Cracks - The beginning of unstable tear $(\bar{\sigma}\ell^{\frac{1}{2}})$ occurring due to a combination of fracture and gross section yielding. The suggested equation for predicting the stress intensity at the beginning of unstable tear is

$$\left\langle \frac{\sigma_G - 0.8\,\sigma_y}{\sigma_u - 0.8\,\sigma_y} \right\rangle^m + \frac{\bar{\sigma}\ell^{\frac{1}{2}}}{k_2} = 1$$

Zone II Intermediate Cracks - The beginning of unstable tear occurs with gross panel stress in the elastic range. The influence of panel buckling can be assumed constant with the stress intensity k_2 at the onset of unstable tear correspondingly less than in guided panels. The quantity $\left\langle \frac{\sigma_G - 0.8\,\sigma_y}{\sigma_u - 0.8\,\sigma_y} \right\rangle^m$ is negative and, thus, assumed as zero so that the equation for predicting unstable tear is

$$\frac{\bar{\sigma}\ell^{\frac{1}{2}}}{k_2} = 1$$

Zone III Long Cracks - Cracks with length to panel width ratio exceeding 1/3 can be expected to show further reduction in the stress intensity k_2 resulting from the influence of panel width on buckling. This fracture zone is to be expected only in unreinforced panels and, thus, not of interest to the majority of structural problems dealing with reinforced panels.

The test data for 2024-T3 aluminum from Figures 17 and 25 is shown in Figure 30. Figure 30 along with curves of the type shown on Figures 3, 4, and 5 can provide the required understanding of the interaction between strength influencing variables. In plotting Figure 30, small variances in the stress intensity at the unstable crack length with thickness were included by using separate k_2 values for each thickness. Also, the small variance in yield stress and ultimate stress were incorporated. These refinements were not considered in construction of previous figures.

VIII SYNTHESIS OF STRENGTH INFLUENCING PARAMETERS FOR WIDE PANELS

The influences of gross section yielding and panel buckling on the stress intensity for the beginning of stable tear in wide unreinforced panels can be collected and presented in a single diagram. This diagram can aid in the overall understanding of the relationship between strength influencing variables. The diagram is a three-dimensional representation with two of the axes representing an interaction diagram of the type shown in Figures 8 and 25. The third axis is the panel ℓ/w ratio which denotes the limit of crack lengths for buckling width influence as $\ell/w = 1/3$. This diagram is shown in general form in Figure 29. For convenience of discussion, zones of behavior are designated on this diagram as follows:

Zone I Short Cracks - The beginning of unstable tear $(\bar{\sigma}\ell^{\frac{1}{2}})$ occurring due to a combination of fracture and gross section yielding. The suggested equation for predicting the stress intensity at the beginning of unstable tear is

$$\left\langle \frac{\sigma_G - 0.8\,\sigma_y}{\sigma_u - 0.8\,\sigma_y} \right\rangle^m + \frac{\bar{\sigma}\ell^{\frac{1}{2}}}{k_2} = 1$$

Zone II Intermediate Cracks - The beginning of unstable tear occurs with gross panel stress in the elastic range. The influence of panel buckling can be assumed constant with the stress intensity k_2 at the onset of unstable tear correspondingly less than in guided panels. The quantity $\left\langle \frac{\sigma_G - 0.8\,\sigma_y}{\sigma_u - 0.8\,\sigma_y} \right\rangle^m$ is negative and, thus, assumed as zero so that the equation for predicting unstable tear is

$$\frac{\bar{\sigma}\ell^{\frac{1}{2}}}{k_2} = 1$$

Zone III Long Cracks - Cracks with length to panel width ratio exceeding 1/3 can be expected to show further reduction in the stress intensity k_2 resulting from the influence of panel width on buckling. This fracture zone is to be expected only in unreinforced panels and, thus, not of interest to the majority of structural problems dealing with reinforced panels.

The test data for 2024-T3 aluminum from Figures 17 and 25 is shown in Figure 30. Figure 30 along with curves of the type shown on Figures 3, 4, and 5 can provide the required understanding of the interaction between strength influencing variables. In plotting Figure 30, small variances in the stress intensity at the unstable crack length with thickness were included by using separate k_2 values for each thickness. Also, the small variance in yield stress and ultimate stress were incorporated. These refinements were not considered in construction of previous figures.

WIDTH X THICKNESS IN INCHES	σ_u (ksi)	σ_Y (ksi)	k (ksi $\sqrt{\text{INCH}}$)
◇=20 x .032	71.0	52.0	68.5
●=20 x .063	68.2	51.9	73.5
▼=20 x .080	71.1	53.3	76.0

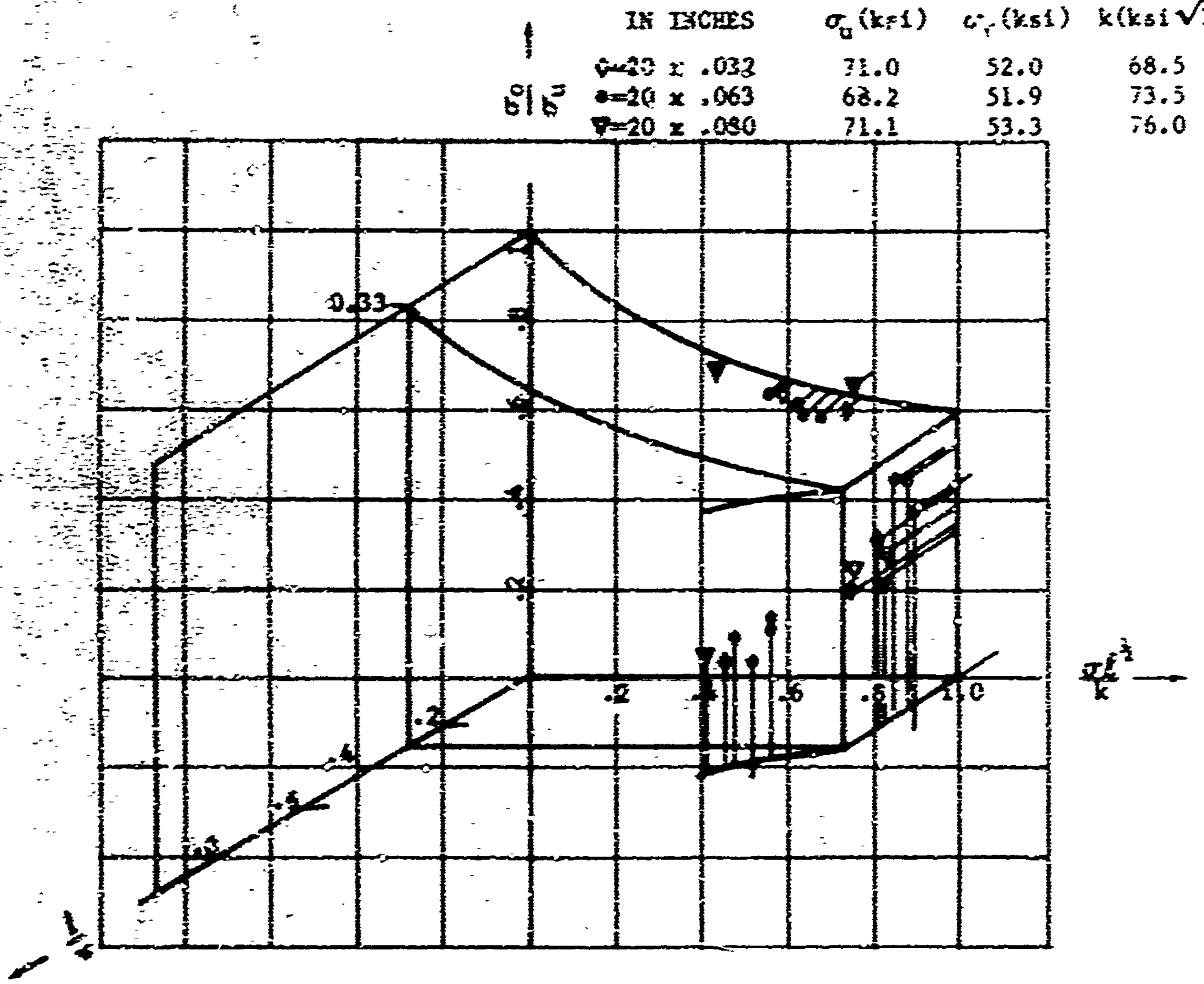

FIGURE 30 SUMMARY OF THE STRENGTH INFLUENCING PARAMETERS FOR WIDE 2024-T3 ALUMINUM PANELS

Figure 30 shows the agreement between actual panel data and the division of the overall problem into zones are suggested by Figure 29. It is believed that Figures 29 and 30 can provide investigators with a data evaluation technique that will clarify many confusing geometric interrelationships influencing the strength of fatigue cracked panels. For application to design problems requiring the determination of the ultimate strength associated with an initial crack length ℓ_1, it is suggested that the quantity $s\ell_1^{\frac{1}{2}}$ (equation 36) be substituted for $\ell^{\frac{1}{2}}$ in the interaction equation.

The data correlation shown in Figures 26 and 27 works equally well for narrow panels. The 12-inch wide panel data for 2024-T3 aluminum will plot in with the data for 20-inch wide panels shown if an appropriate value of k_2 is assumed. Figures 29 and 30 thus represent nondimensional properties of the behavior of 2024-T3 aluminum over a reasonable range of geometries. Two specific additional parameters to adjust k_2 are required, however, before a general solution to the problem is at hand.

1. A guided panel width correction (illustrated in curve form in Figures 3, 4, and 5).

2. An unguided panel width adjustment for the influence of buckling.

IX CONCLUSIONS

Based on the analysis of test data for 2024-T3 aluminum and supported in part by data from titanium 8Al-1Mo-1V and data from other investigations, it is concluded that in narrow panels, width has a significant influence on crack extension that cannot be adequately accounted for by current fracture mechanics theory. Much of the available test data is from panels of this width range. Thus, use of data from these panels for the evaluation of the strength of reinforced panels is extremely difficult. Additional studies directed towards a more complete understanding of interaction between local yielding at the crack tip and the panel boundaries are needed. Direct correlation of width influences with material properties should also prove fruitful. In this respect, a correlating parameter is needed which includes total elongation and strain hardening characteristics as well as the yield and ultimate stresses used in Figure 3.

The correlation and prediction of the beginning of unstable tear with gross stress above the yield stress can be accomplished by an interaction equation (equation 21). While actual data correlations were limited to 2024-T3 aluminum, it is believed that the equation is sufficiently general for application to other relatively ductile materials including materials at elevated temperatures. It is therefore recommended that additional studies be undertaken using materials at room temperature and elevated temperatures. These studies should provide more information on the variation of the interaction exponent "m" with strain hardening characteristics and prove the general usefulness of the interaction approach to fracture problems involving gross section strains above the proportional limit.

The results obtained during this program showed the influence of panel width on the reduction in strength due to buckling. For 2024-T3 aluminum, it was shown that the buckling influence was nearly constant when gross section yielding or buckling width influences were not involved. Studies should be undertaken to determine whether a similar range of constant buckling influence exists in other materials so long as the quantity $(\sigma_o - \sigma_B)$ remains nearly constant. In these studies, thicknesses and fracture characteristics should be selected to test the influence of buckling under conditions where $(\sigma_o - \sigma_B)$ varies appreciably within the elastic range with $\frac{\ell}{w} < \frac{1}{3}$. Studies of the influence of buckling under conditions of biaxial stress should also be undertaken.

The problem of stable tear requires considerably more investigation. This important aspect of the engineering problem of strength prediction has not had adequate study. From the results of this study, prediction of stable tear in wide panels can be accomplished by considering stable tear as a constant fraction of the initial crack length. This is undoubtedly an over simplification of the problem, but one that may prove useful.

Further studies of stable tear in wide panels should be undertaken. These studies should include delayed tear and fracture such as has been observed in titanium 8Al-1Mo-1V. The results of this study could prove that the phenomenon of delayed unstable tear will not be as significant in wide panels.

REFERENCES

1. Srawley, J. E. & Brown, Jr., W. F., Fracture Toughness Testing, NASA TN D-2599, January 1965.

2. Tiffany, C. F. & Lorenz, P. M., An Investigation of Low-Cycle Fatigue Failures Using Applied Fracture Mechanics, ML-TDR-64-53, May 1964.

3. Crichlow, W. J., The Ultimate Strength of Damaged Structure, ICAF, AGARD Symposium on Full-Scale Aircraft Testing, Amsterdam, Netherlands, 9-11 June 1959.

4. Douglas Aircraft Company, Crack Propagation Prediction and Crack-Stopper Techniques for Stiffened and Unstiffened Flat Sheet in a Supersonic Transport Environment, ASD-TDR-63-773, September 1963.

5. Kuhn, P. & Figge, I.E., Unified Notch-Strength Analysis for Wrought Aluminum Alloys, NASA TN D-1259, May 1962.

6. Fuselage Fail-Safe Design Data and Bomb-Resistant Analysis for the Supersonic Transport, FDL-TDR-64-80, June 1964.

7. Neuber, H., Theory of Notch Stresses, Springer Publishers, 1958.

8. Boeing, North American, Fracture Toughness and Tear Tests, ML-TDR-64-238, October 1964.

9. Griffith, A. A., The Phenomena of Rupture and Flow in Solids, Transactions of the Royal Society, Section A., Vol. CCXXI, October 1920.

10. Welborne, E. R., The Correlation of Unstable Crack Length Data for Sheet Materials, The Aeronautical Quarterly, November 1961.

11. Dixon, J. R., Stress Distribution Around Edge Slits in a Plate Loaded in Tension - The Effect of Finite Width of Plate, Journal of the Royal Aeronautical Society (T.N.), Vol. 66, No. 617, May 1962.

12. Barrois, W., Critical Study on Fatigue Crack Propagation, Advisory Group for Aeronautical Research & Development, Report No. 412, June 1962.

13. Krafft, J.M., Sullivan, A.M. & Boyle, R.W., Effect of Dimensions on Fast Fracture Instability of Notched Sheets, Proceedings of the Crack Propagation Symposium, Cranfield, Vol. 1, September 1961.

14. Forman, R. G., Experimental Program to Determine Effect of Crack Buckling and Specimen Dimensions on Fracture Toughness of Thin Sheet Materials, AFFDL-TR-65-146, 1965.

15. Dugdale, D. S., Yielding of Steel Sheets Containing Slits, J. Mech. Phys. Solids, Vol. 8, May 1960.

REFERENCES (Cont.)

16. Healy, M.S., Marschall, C.W., Holden, F.C., and Hyler, W.S., The Fatigue Behavior of Materials for the Supersonic Transport, NASA CR-215, April 1965.

17. Shanley F.R., Strength of Materials, McGraw-Hill Book Company, Inc., New York, 1957.

18. Crandall, S.H., and Dahl, N.C., An Introduction to the Mechanics of Solids, McGraw-Hill Book Company, Inc., New York, 1957.

19. Den Hartog, J.P., Advanced Strength of Materials, McGraw-Hill Book Company, Inc., New York, 1952.

20. Liu, H.W., Discussion - - Proceedings of the Crack Propagation Symposium, Cranfield, Vol. II, 1961.

APPENDIX

TEST PROGRAM

SCOPE

The test program consisted of an in-depth study of the tear and failure characteristics of bare 2024-T3 aluminum and a limited supporting study of duplex annealed titanium 8Al-1Mo-1V. The test program was conducted for the purpose of providing a consistent set of data which extends beyond the limits of normal fracture mechanics measurements to include the influence of panel buckling and yielding on the strength of fatigue cracked panels. Panel widths tested were 30 inch, 20 inch, 12 inch and 9 inch for the bare 2024-T3 aluminum. Nominal thicknesses were .080 inch, .063 inch and .032 inch. For the duplex annealed titanium 8Al-1Mo-1V the widths were 12 inch and 9 inch. Nominal thicknesses were .045 inch and .020 inch.

MATERIALS

The bare 2024-T3 aluminum was selected from available stock of the three thicknesses, .032, .063, and .080 inch. At least one tensile coupon was taken from each sheet. In some instances where failure stresses were relatively low, coupons were obtained directly from the test panels after failure. Strain rates were varied from .002 in/in/min. to .004 in/in/min. which approximately coincided with the strain rates of the 12 inch and 20 inch wide, .063 inch thick panels. No significant trends were noted. A summary of the average engineering properties of the aluminum panels is given in Table 1. Coupon data and panel and sheet designations are given in Table 3.

Table 1

Average Properties of Bare 2024-T3 Aluminum

Nominal Thickness (Inches)	Yield Strength σ_y (ksi)	Ultimate Strength σ_u (ksi)	Elongation (2" Gage Length)
0.032	52.0	71.1	18.0
0.063	51.9	68.2	19.2
0.080	53.3	71.1	19.6

$E = 10.3 \times 10^3$ ksi

The duplex annealed titanium 8Al-1Mo-1V was obtained from the Titanium Metals Corporation of America. The two thicknesses were of one different heats. Their yield and ultimate strengths were nearly identical. However, the elongations were less for the .020 inch thick material. Significantly the resistance to tear and fracture was subsequently found to be less in the .020 inch thick material. Two coupons were taken from each heat. The engineering properties are given in Table 2 as follows:

Table 2

Properties of Duplex Annealed Titanium 8Al-1Mo-1V

Heat No.	Nominal Thickness (Inches)	Yield Strength σ_y(ksi)	Ultimate Strength σ_u(ksi)	Elongation (2" Gage Length)
D-9226	.045	133.8	145.0	14.0
D-9226	.045	131.4	142.9	14.5
G-699	.020	135.9	146.6	13.0
G-699	.020	135.0	145.0	11.6

$t = .045;\quad E = 18.0 \times 10^3$ ksi
$t = .020;\quad E = 16.0 \times 10^3$ ksi

TEST PROCEDURES

The test panels were unreinforced initially flat panels containing centrally located saw slots perpendicular to the load axis. All panels were cut with the slot perpendicular to the rolling direction. The length of all panels measured between the grips was 2.5 times the panel width.

The initial saw slots were extended by jewelers saw cuts from which fatigue cracks were grown for a distance necessary to obtain a crack extension at least three times the thickness of the panel and parallel to the axis of the saw slot. All cracks in the 2024-T3 aluminum panels were grown at a single value of stress intensity of $\bar{\sigma}\ell^{\frac{1}{2}} = 30$ ksi $\sqrt{\text{in.}}$ where $\bar{\sigma}$ is the width adjusted stress and ℓ is the crack length. This value was approximately 75 percent of the lower limit of stress intensity at which slow tear was observed to start. A value of $\bar{\sigma}\ell^{\frac{1}{2}} = 40$ ksi was selected for fatigue cracking in the titanium panels. All fatigue cracks quickly developed into a shear mode of cracking once out of the influence of the notch. Thus all specimens were fatigued and failed in the through-the-thickness 45 degree shear mode.

After the fatigue cracks were developed so as to simulate fatigue cracks of the required length, initial crack lengths were observed through a transit. The load was then slowly increased until slow tear was observed to start. In an attempt to gain consistency in the recording of slow tear the vertical cross hair of the transit was placed at the end of the visible crack and slow tear was recorded when the crack was visible beyond the cross hair.

After the start of slow tear was observed, the panels were loaded at a rate of 30,000 pounds per minute and the remainder of the panel behavior was recorded on film. The film record was reduced to give the following information:

1. The crack length vs. load.
2. The beginning of maximum load.
3. A crack velocity of one inch per second.
4. The last recorded crack length prior to rupture.

TABLE 3
MATERIAL PROPERTIES OF BARE 2024-T3 ALUMINUM
FROM 1 INCH WIDE TENSILE COUPONS

COUPON	PANEL NO.	COUPON THICKNESS	STRAIN RATE in/in/min.	σ_y ksi	σ_u ksi	PERCENT ELONGATION IN 2 INCH GAGE
S-1	-	.062	.004	50.6	65.2	20.0
S-2	-	.062	.004	50.6	65.7	21.5
S-3	-	.062	.004	53.2	68.8	21.5
S-4	-	.062	.0035	52.7	66.7	18.5
S-5	-	.0625	.0033	50.2	68.3	17.0
S-6	-	.062	.0025	53.4	69.4	18.5
S-7	-	.0625	.0025	51.4	68.3	20.0
S-8	-	.062	.0025	51.6	66.1	18.0
S-9	-	.061	.0025	53.5	69.3	19.0
S-10	-	.062	.0025	52.4	69.8	22.0
S-11	-	.061	.004	53.1	69.2	17.5
S-12	-	.062	.004	52.4	68.2	17.5
S-13	-	.063	.0035	53.5	68.9	19.0
S-14	-	.063	.0025	51.3	66.4	19.0
S-14	-	.061	.0030	50.3	63.7	19.0
S-15	-	.062	.0025	51.0	66.4	19.0
S-16	-	.062	.0025	52.5	67.2	21.0
S-17	-	.079	.0035	47.6	67.4	21.5
S-17	-	.079	.0030	55.1	66.5	21.0
-	31	.079	.003	53.5	71.3	18.0
-	31	.079	.0025	53.7	71.8	18.5
-	27	.080	.003	52.6	71.4	15.0
-	27	.080	.004	55.3	76.9	20.0
-	28	.079	.004	54.8	71.5	22.0
-	29A	.079	.0035	55.3	71.2	17.5
-	33	.082	.0035	54.6	71.4	26.0
-	32	.080	.0025	54.8	71.6	20.5
S-18	25	.033	.003	50.3	69.2	18.0
S-19	26	.032	.003	52.4	73.0	16.0
S-20	22	.033	.003	52.4	71.5	18.0
S-20	21	.032	.003	52.5	70.4	17.0
S-21	-	.032	-	52.8	72.3	17.0

TEST EQUIPMENT

The testing was accomplished using a load frame and a 300,000 pound hydraulic load cylinder (Figures 31 and 32). Load control was attained by the use of an electro-hydraulic servo channel and a feedback signal provided by a strain gauge bridge with the strain gauge attached to a load link in series with the test panel and the hydraulic load cylinder. For development of fatigue cracks prior to loading the panels to failure, a combination of mean plus sinusoidal signal was used as input to the servo valve. For final loading to failure, a motor driven potentiometer calibrated to provide a nominal load rate of 30,000 pounds per minute was used. Incremental loading was applied by manually operating the mean load potentiometer. Load monitoring was obtained through two additional strain gauges on the load link. One strain gauge was used for visual monitoring on an oscilloscope using a BA-12 bridge unit. The second gauge provided a signal operating a voltmeter which was photographed simultaneously with the crack length by a 35 millimeter camera operating at 16 frames-per-second. The signal from this second strain gauge was also recorded directly as load on an x-y plotter. All load recording elements usually agreed within 3 percent.

CURVES AND TABULAR DATA

In order to provide information and discussion on the tear characteristics of the materials, it was necessary to record the entire failure sequence on film. Actual tear behavior determined from film records showed the tear to be comprised of a series of bursts of tear rather than a smooth continuous process. These bursts were sporadic in time and tended to differ slightly for the two ends of the crack. In general, however, the total tear accumulated at either end of the crack was very nearly the same, the crack thus remaining symmetrical about the panel center line until final rupture. Rupture often occurred simultaneously on both sides of the crack (particularly for higher stress levels and shorter cracks). In other instances (usually at longer crack lengths) rupture would occur on one side only, these ruptures being about equally divided between the left and right side. Failure surfaces were of the shear type in all panels with no visual distinction noted between the slow tear and rupture surfaces. The results of the interpretation of film records are shown as average tear curves on Figures 33 through 43. The ordinate ($\bar{\sigma}$) of these figures is a width corrected stress in the sense that it represents the nominal (gross) panel stress multiplied by the Dixon[1] finite panel width correction (Equation 6).

Direct visual comparison between all curves in terms of elastic stress theory is thus possible.

Four points representing significant changes in behavior are marked on the tear curve for each panel (Figures 33 through 43) unless two of the events occurred simultaneously as was occasionally the case. The crack lengths and loads corresponding to these points are given in Tables 4 through 12. The significance of these points along with remarks pertinent to their interpretation are summarized below in the sequence of their normal occurrence.

1. The beginning of slow tear: The beginning of slow tear proved difficult to record in a consistent manner. First, the slow tear did not always start simultaneously on each end of the crack. Second, the visibility and amount of initial slow tear varied with crack length and geometry.

FIGURE 31 TEST FRAME SHOWING THIRTY INCH WIDE PANEL IN PLACE

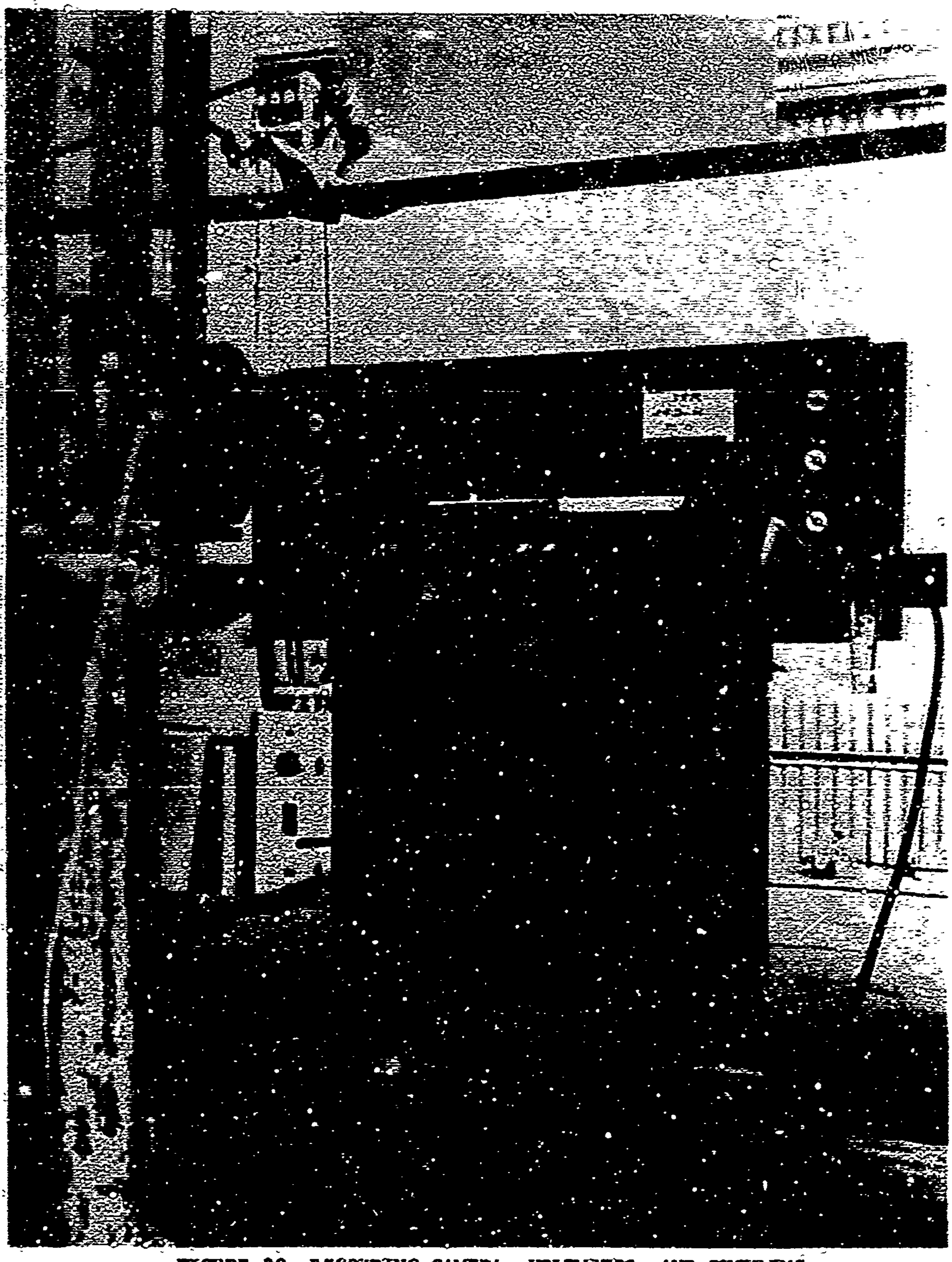

FIGURE 32 RECORDING CAMERA, VOLTMETER, AND BUCKLING GUIDES WITH THIRTY INCH WIDE PANEL

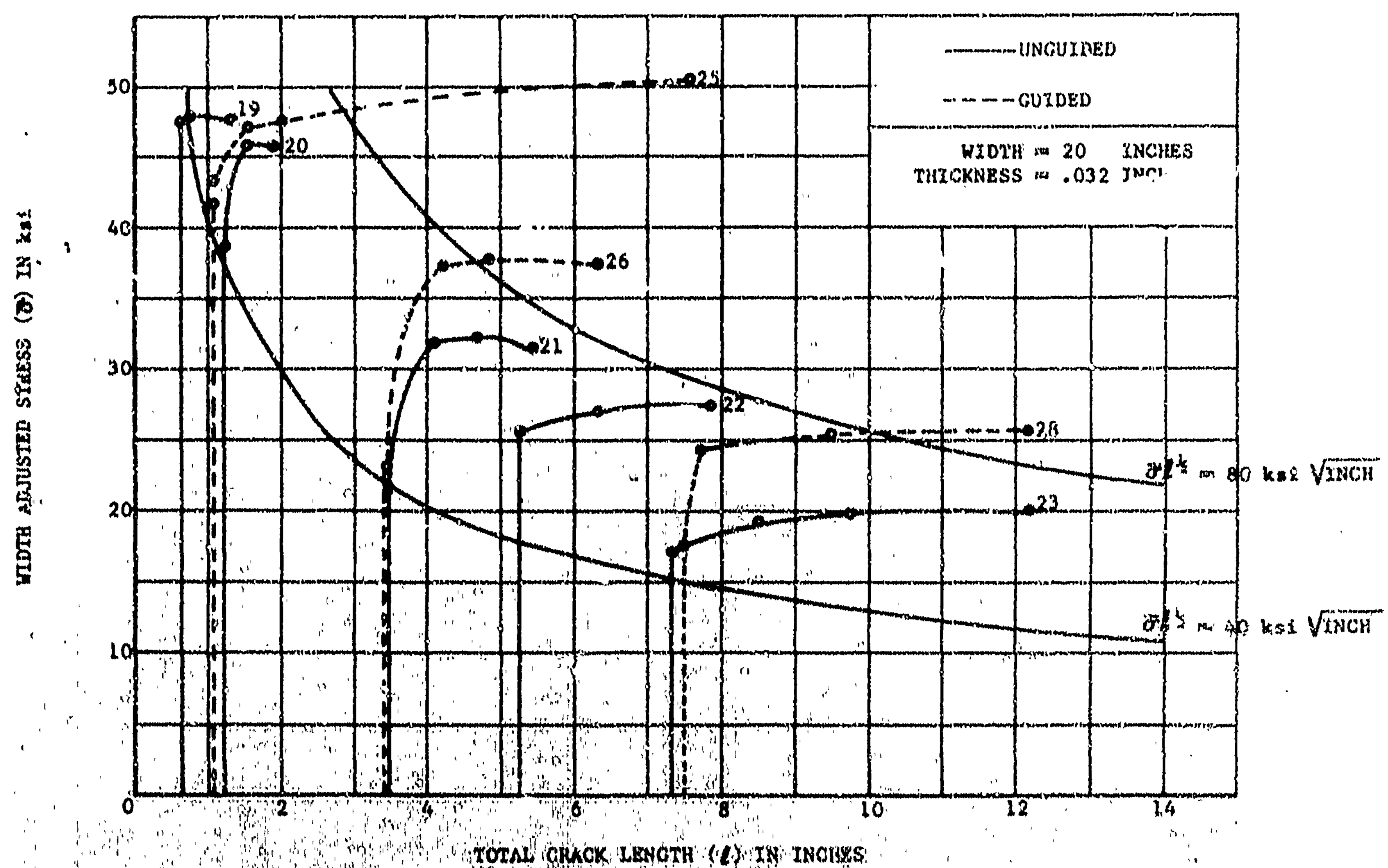

FIGURE 33 STRESS VS. CRACK LENGTH 2024-T3 ALUMINUM

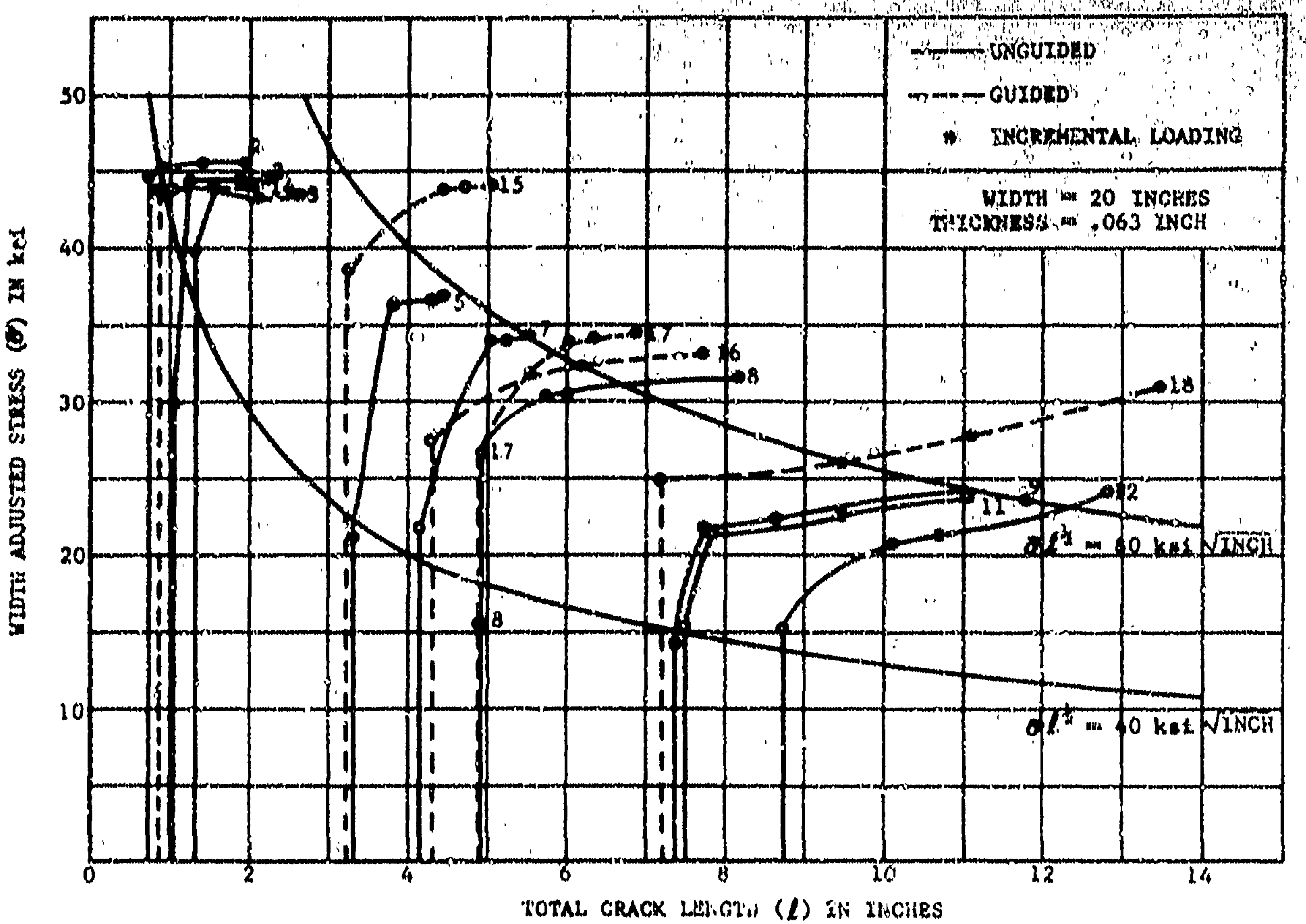

FIGURE 34 STRESS VS. CRACK LENGTH 2024-T3 ALUMINUM

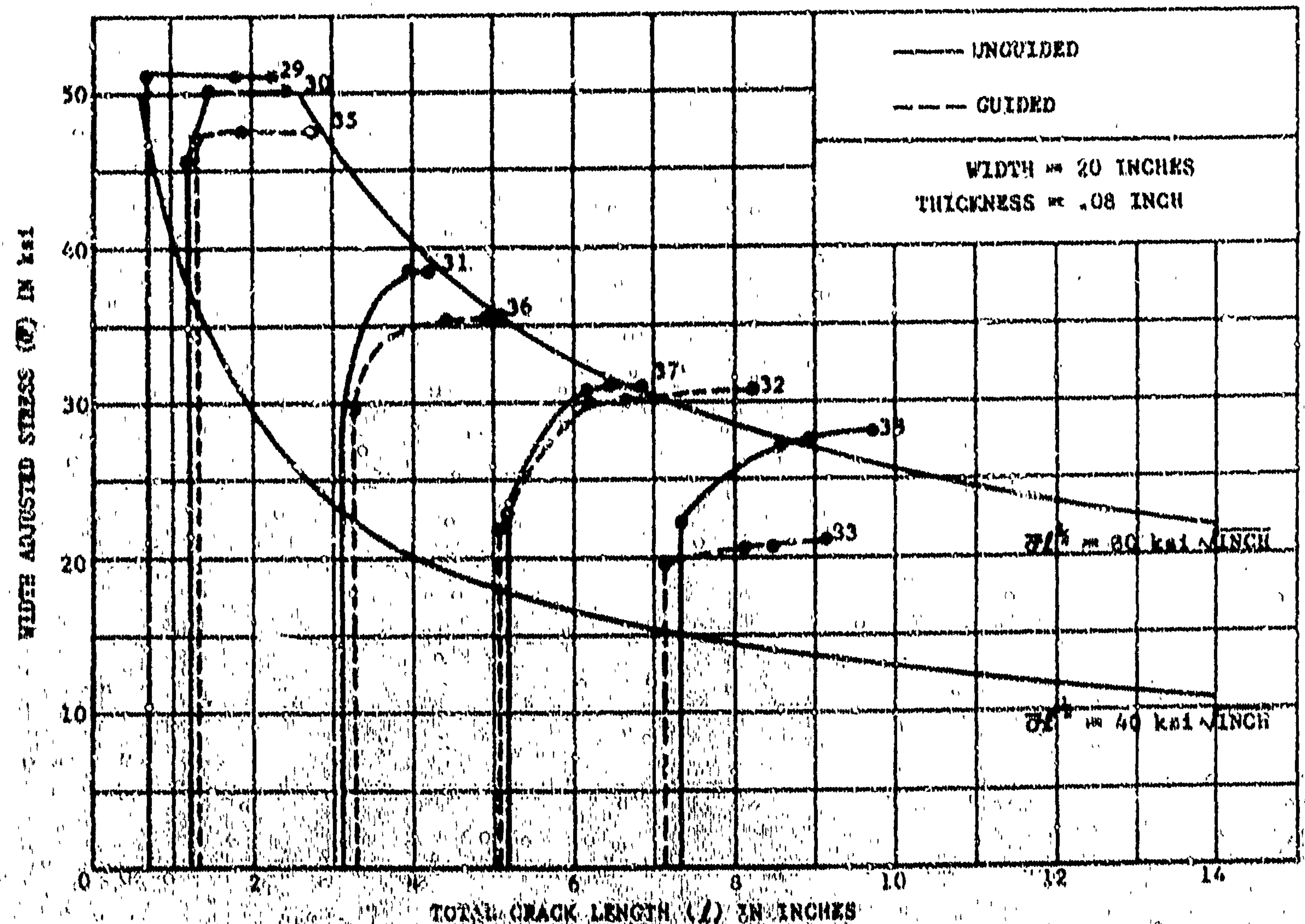

FIGURE 33 STRESS VS. CRACK LENGTH 2024-T3 ALUMINUM

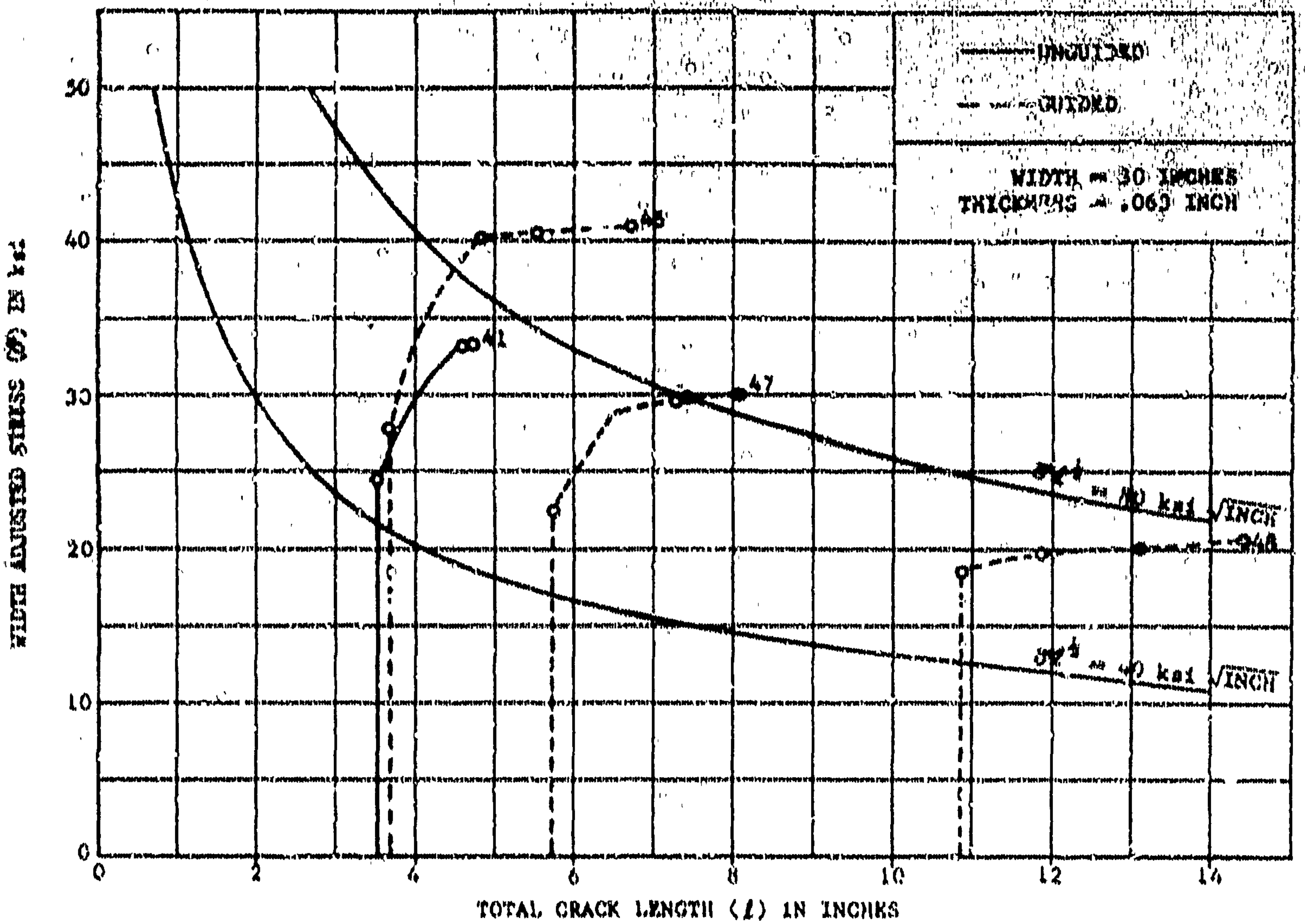

FIGURE 36 STRESS VS. CRACK LENGTH 2024-T3 ALUMINUM

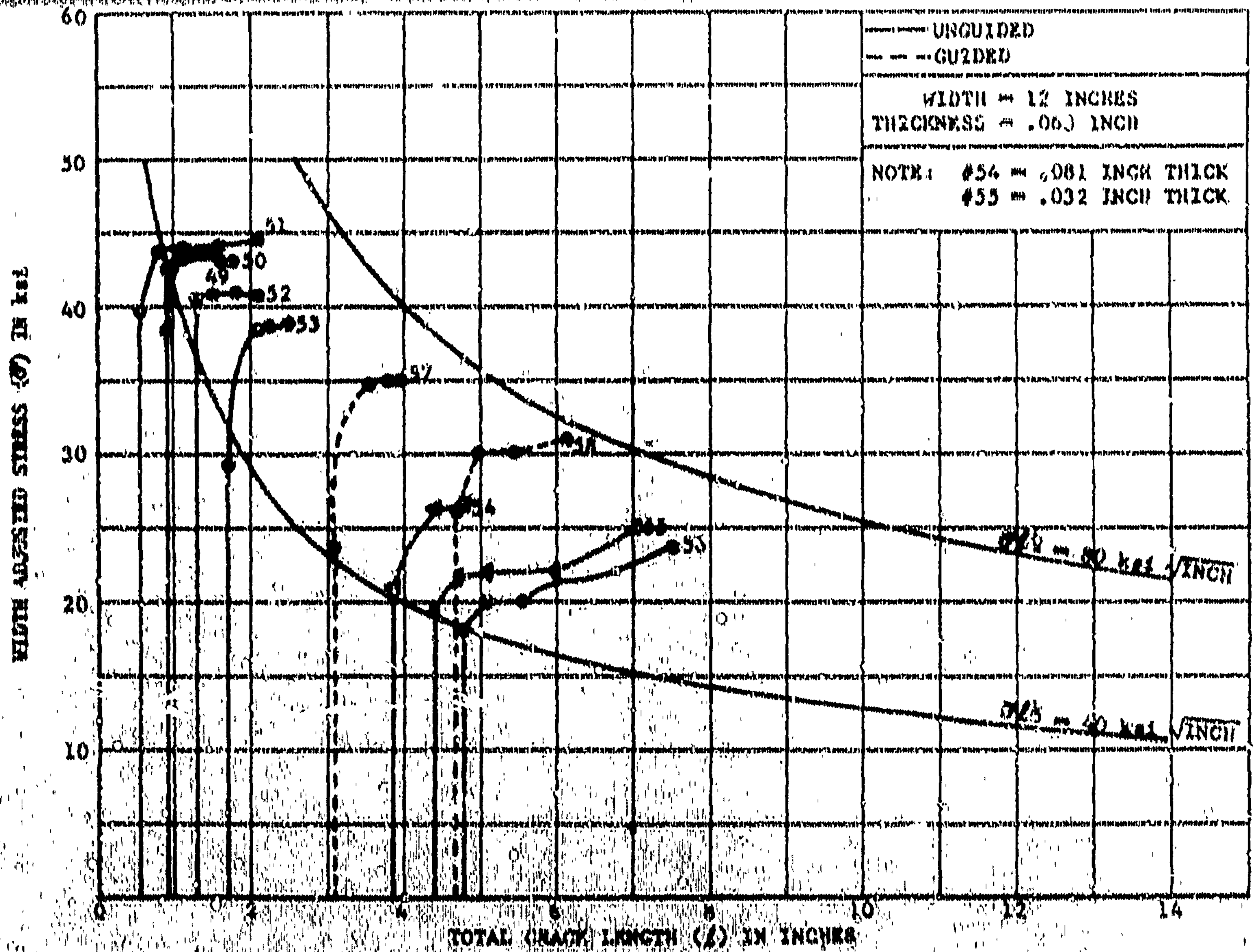

FIGURE 37 STRESS VS. CRACK LENGTH 2024-T3 ALUMINUM

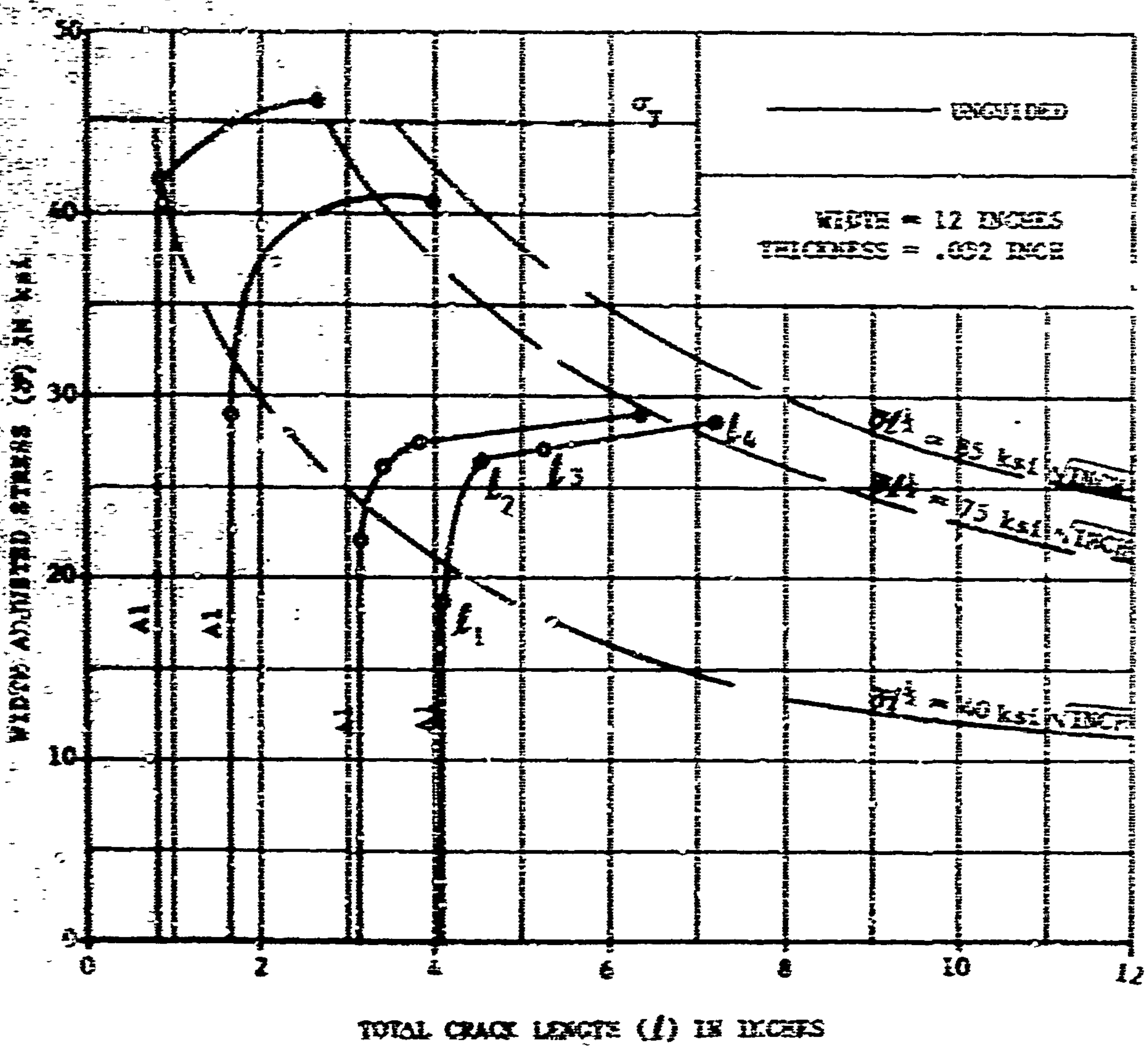

FIGURE 33 STRESS VS. CRACK LENGTH 2024-T3 ALUMINUM (Al SERIES)

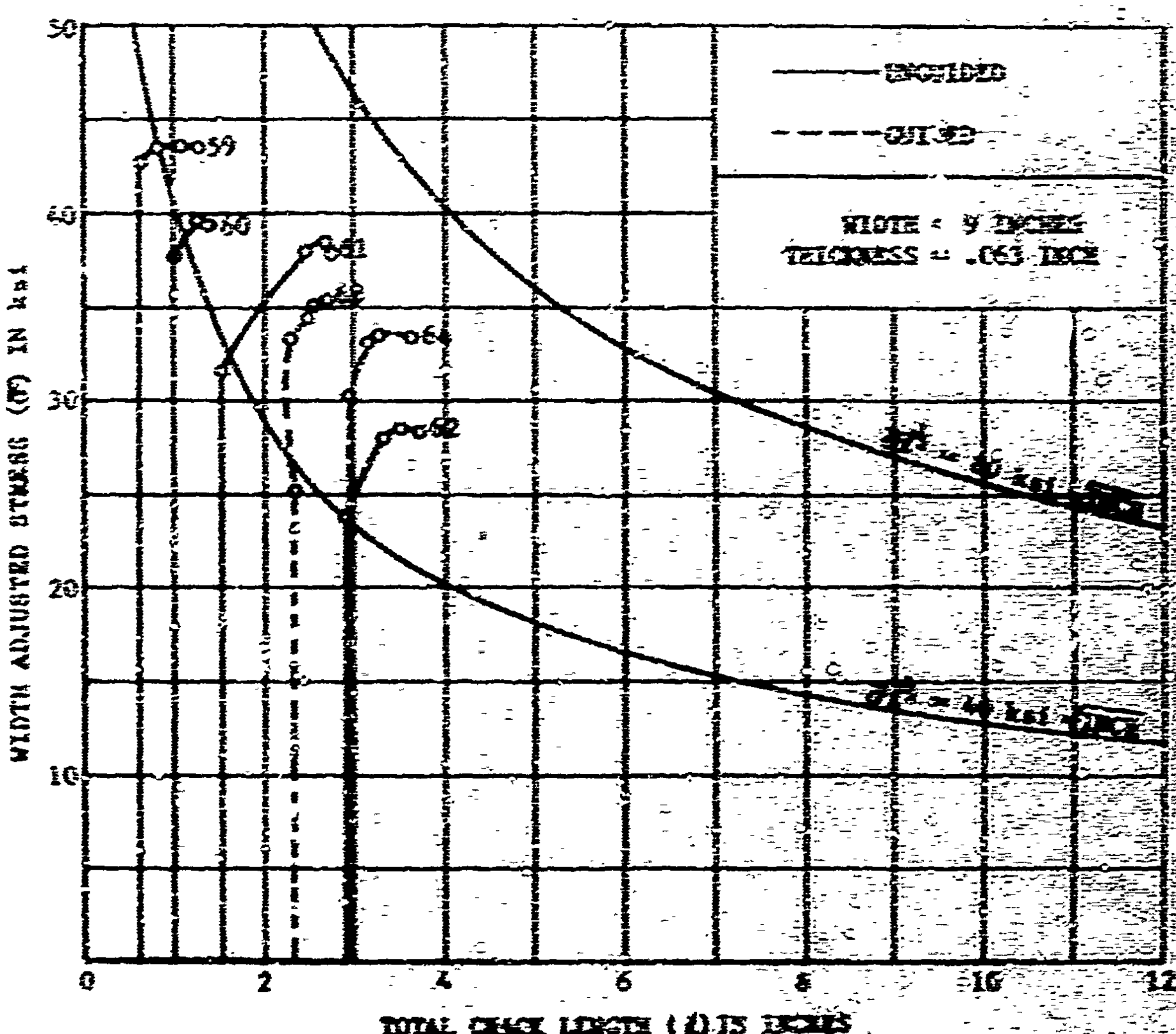

FIGURE 39 STRESS VS. CRACK LENGTH 2024-T3 ALUMINUM

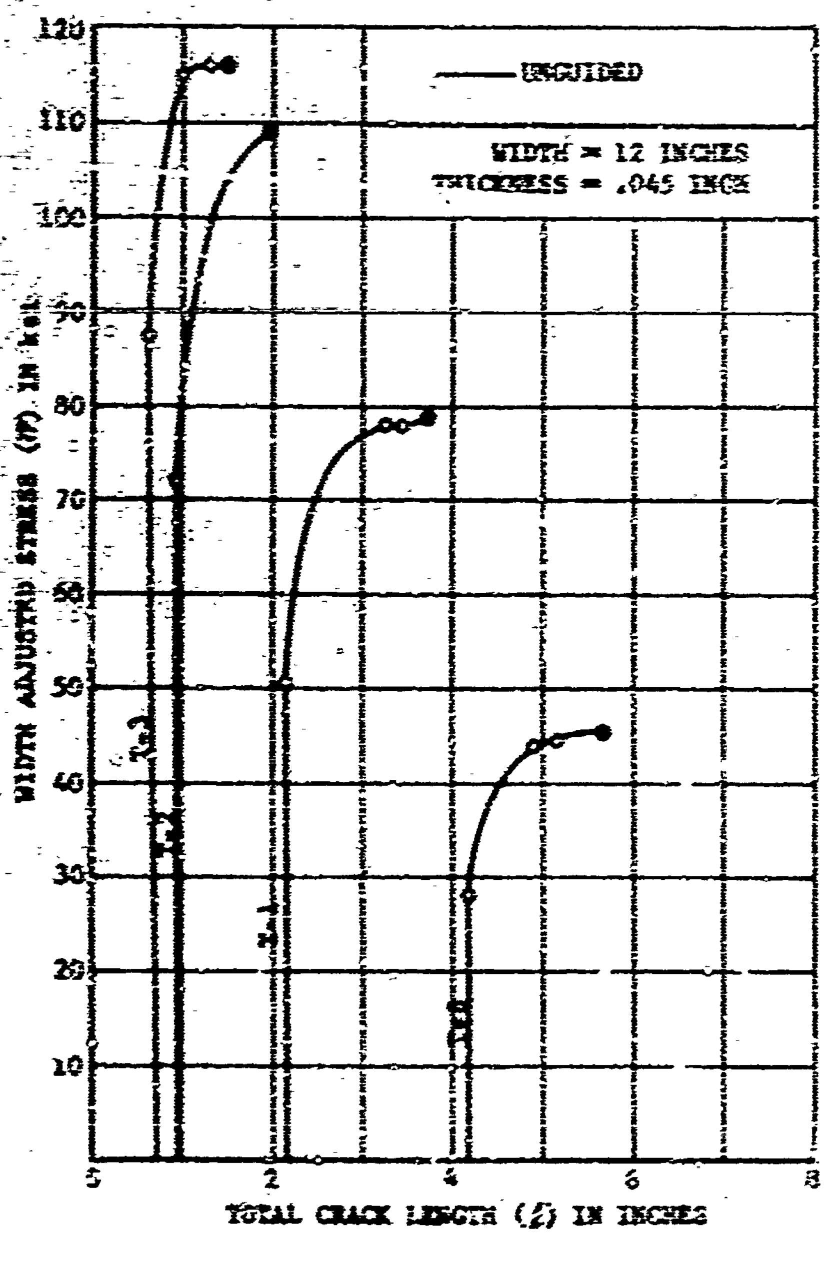

FIGURE 40 STRESS VS. CRACK LENGTH TI-8AL-1MO-1V

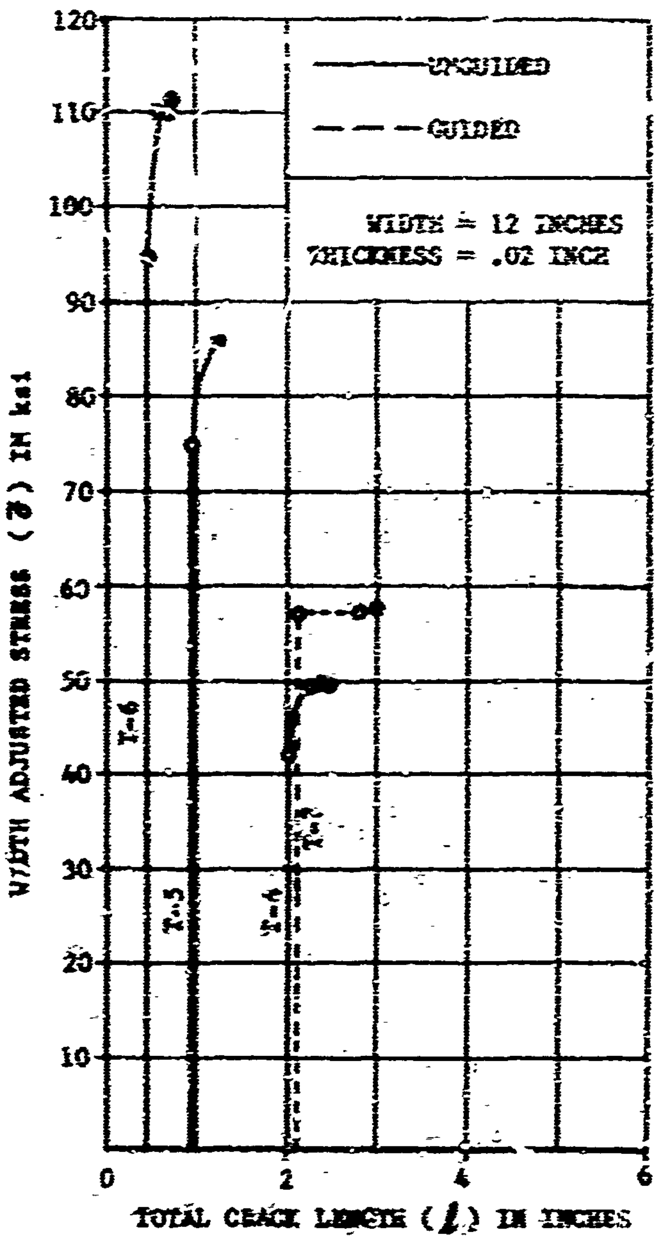

FIGURE 41 STRESS VS. CRACK LENGTH Ti-8Al-1Mo-1V

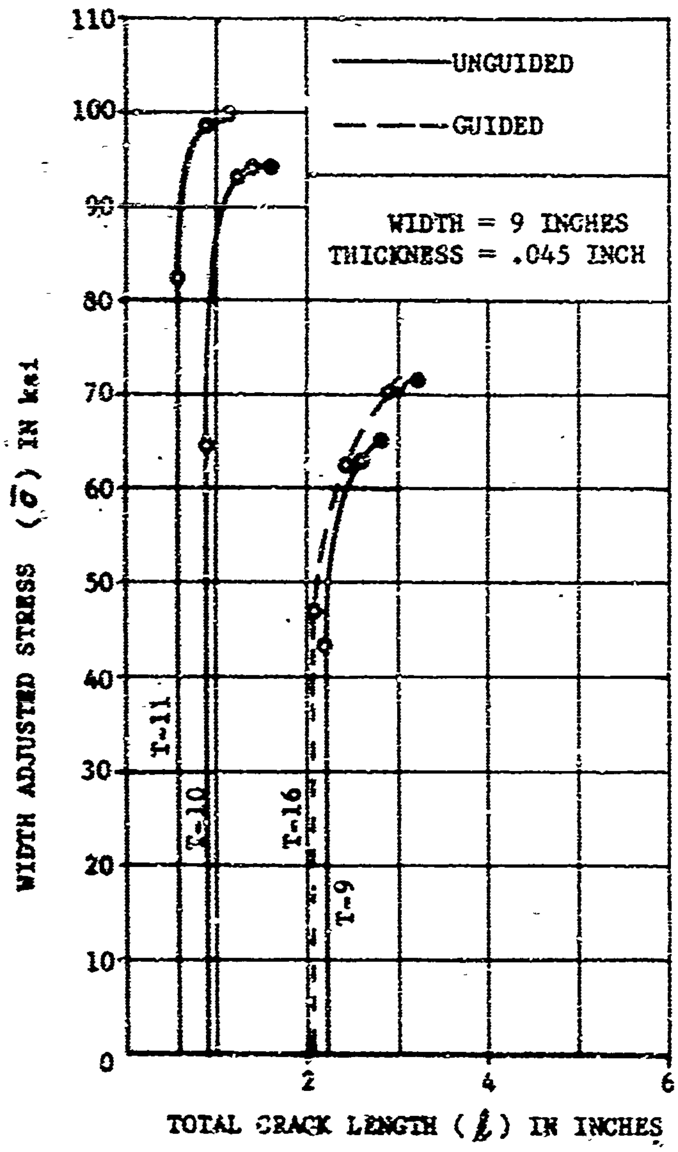

FIGURE 42 STRESS VS. CRACK LENGTH Ti-8Al-1Mo-1V

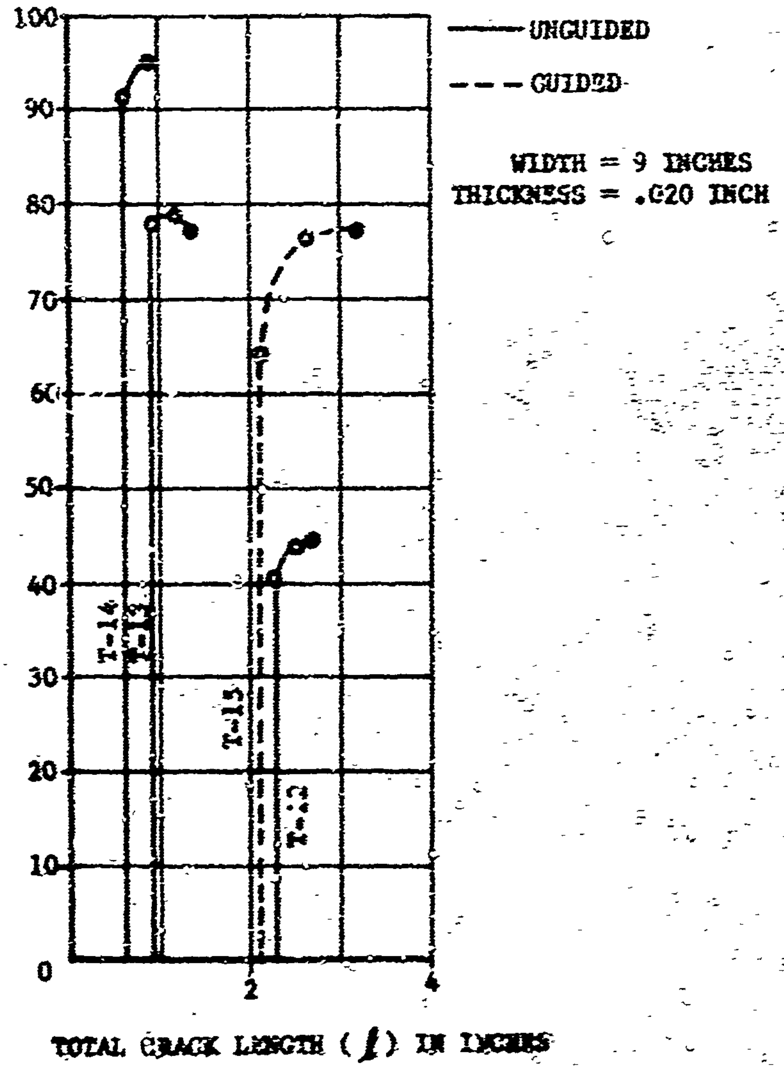

FIGURE 43 STRESS VS. CRACK LENGTH Ti-8Al-1Mo-1V

TABLE 4
2024-T3 ALUMINUM
WIDTH = 20 INCHES, THICKNESS = .032 INCH

PANEL NUMBER	SHEET NUMBER	ℓ_1 (INCHES)	ℓ_2 (INCHES)	ℓ_3 (INCHES)	ℓ_4 (INCHES)	P_1 $(lbs \times 10^{-3})$	P_2 $(lbs \times 10^{-3})$	P_3 $(lbs \times 10^{-3})$	P_4 $(lbs \times 10^{-3})$	BUCKLING RESTRAINT
19	S-19	0.65	0.79	1.37	1.37	30.3	30.5	30.3	30.3	No
20	S-20	1.23	1.55	1.91	1.91	24.6	29.2	29.0	29.0	
21	S-18	3.44	4.10	4.71	5.45	13.6	20.0	20.0	19.3	
22	S-18	5.30	6.37	6.37	7.89	15.7	16.4	16.4	16.2	
23	S-20	7.37	8.47	9.68	12.20	10.0	11.3	11.0	10.0	
24	S-19	0.64	0.87	1.20	1.45	30.5	31.0	30.8	30.7	Yes
25	S-20	1.12	1.43	2.06	7.59	27.6	30.1	30.0	30.0	
26	S-18	3.45	4.21	4.86	6.32	14.6	23.3	23.3	22.7	
27	S-19	5.26	6.27	7.07	10.77	12.8	17.7	17.7	17.0	
28	S-20	7.46	7.75	9.50	12.18	10.4	14.33	14.33	13.0	

TABLE 5
2024-T3 ALUMINUM
WIDTH = 20 INCHES, THICKNESS = .063 INCH

PANEL NUMBER	SHEET NUMBER	ℓ_1 (INCHES)	ℓ_2 (INCHES)	ℓ_3 (INCHES)	ℓ_4 (INCHES)	P_1 (lbs x 10^{-3})	P_2 (lbs x 10^{-3})	P_3 (lbs x 10^{-3})	P_4 (lbs x 10^{-3})	BUCKLING RESTRAINT
1	S-15	0.74	0.90	1.41	1.96	56.0	56.5	56.5	56.5	No
2	S-4	1.06	1.24	1.90	2.16	37.5	55.5	55.5	55.5	
3	S-14	1.28	1.55	2.10	2.65	50.0	55.0	54.0	54.0	
4	S-15	1.28	1.31	1.35	1.35	52.0	54.0	54.0	54.0	
5*	S-8	3.29	3.81	4.32	4.43	26.2	44.9	44.9	44.9	
6	S-8	3.34	3.91	4.32	4.81	36.0	45.4	45.4	45.4	
7	S-7	4.18	5.03	5.33	5.58	26.7	41.0	41.0	41.0	
8	S-6	4.93	5.74	6.06	8.19	19.0	36.4	36.4	36.4	
9*	S-5	7.39	7.78	8.63	11.80	16.7	25.6	25.6	24.3	
10	S-8	7.40	8.04	9.05	10.43	21.7	26.0	26.0	26.0	
11	S-8	7.56	7.34	9.51	11.02	17.8	23.2	24.8	24.8	
12	S-7	8.78	10.12	10.70	12.87	17.0	22.6	22.6	22.6	
13	S-15	0.87	1.03	1.57	2.20	55.0	55.0	55.0	55.0	Yes
14	S-4	0.96	1.38	1.77	2.60	48.5	55.0	53.0	55.0	
15	S-6	3.27	4.42	4.77	5.03	24.2	47.5	47.5	47.5	
16	S-4	4.31	5.51	6.23	7.72	33.6	38.6	38.6	38.6	
17	S-6	4.93	6.07	6.37	6.90	32.3	40.6	40.6	40.6	
18	S-8	7.20	9.42	11.10	13.50	29.2	29.2	29.2	27.7	

*Incremental loading to ℓ_2

TABLE 5
2024-T3 ALUMINUM
WIDTH = 20 INCHES, THICKNESS = .063 INCH

PANEL NUMBER	SHEET NUMBER	ℓ_1 (INCHES)	ℓ_2 (INCHES)	ℓ_3 (INCHES)	ℓ_4 (INCHES)	P_1 (lbs x 10^{-3})	P_2 (lbs x 10^{-3})	P_3 (lbs x 10^{-3})	P_4 (lbs x 10^{-3})	BUCKLING RESTRAINT
1	S-15	0.74	0.90	1.41	1.96	56.0	56.5	56.5	56.5	No
2	S-4	1.06	1.24	1.90	2.16	37.5	55.5	55.5	55.5	
3	S-14	1.28	1.55	2.10	2.65	50.0	55.0	54.0	54.0	
4	S-15	1.28	1.31	1.35	1.35	52.0	54.0	54.0	54.0	
5*	S-8	3.29	3.81	4.32	4.43	26.2	44.9	44.9	44.9	
6	S-8	3.34	3.91	4.32	4.81	36.0	45.4	45.4	45.4	
7	S-7	4.18	5.03	5.33	5.58	26.7	41.0	41.0	41.0	
8	S-6	4.93	5.74	6.06	8.19	19.0	36.4	36.4	36.4	
9*	S-5	7.39	7.78	8.63	11.80	16.7	25.6	25.6	24.3	
10	S-8	7.40	8.04	9.05	10.43	21.2	26.0	26.0	26.0	
11	S-8	7.56	7.34	9.51	11.02	17.8	23.2	24.8	24.8	
12	S-7	8.78	10.12	10.70	12.87	17.0	22.6	22.6	22.6	
13	S-15	0.87	1.03	1.57	2.20	55.0	55.0	55.0	55.0	Yes
14	S-4	0.96	1.38	1.77	2.60	48.5	55.0	55.0	55.0	
15	S-6	3.27	4.42	4.77	5.03	24.2	47.5	47.5	47.5	
16	S-4	4.31	5.51	6.23	7.72	33.6	38.6	38.6	38.6	
17	S-6	4.93	6.07	6.37	6.90	32.3	40.6	40.6	40.6	
18	S-8	7.20	9.42	11.10	13.50	29.2	29.2	29.2	27.7	

*Incremental loading to ℓ_2

TABLE 6
2024-T3 ALUMINUM
WIDTH = 20 INCHES, THICKNESS = .080 INCH

PANEL NUMBER	SHEET NUMBER	ℓ_1 (INCHES)	ℓ_2 (INCHES)	ℓ_3 (INCHES)	ℓ_4 (INCHES)	P_1 (lbs x 10^{-3})	P_2 (lbs x 10^{-3})	P_3 (lbs x 10^{-3})	P_4 (lbs x 10^{-3})	BUCKLING RESTRAINT
29	S-17	0.69	0.69	1.82	2.34	81.5	81.5	80.0	79.0	No
30	S-17	1.21	1.50	1.52	2.45	71.0	79.5	79.5	79.5	
31	C-28	3.81	4.00	4.25	4.25	38.4	60.0	60.0	60.0	
32	C-32	5.17	6.25	6.64	8.23	33.8	45.5	45.0	45.0	
33	C-30	7.14	8.18	8.48	9.16	29.2	30.2	30.0	30.0	
34	S-17	0.70	0.70	1.44	2.39	83.0	83.0	82.0	81.5	Yes
35	S-17	1.27	1.78	1.90	2.79	74.6	76.9	76.9	76.9	
36	C-27	3.31	4.42	4.95	5.08	46.6	54.8	54.8	54.8	
37	C-31	5.09	6.19	6.45	6.89	34.1	46.5	46.5	46.5	
38	C-29A	7.35	8.60	8.95	9.73	33.3	39.7	39.7	39.3	

TABLE 7
2024-T3 ALUMINUM
WIDTH = 30 INCHES, THICKNESS = .063 INCH

PANEL NUMBER	SHEET NUMBER	ℓ_1 (INCHES)	ℓ_2 (INCHES)	ℓ_3 (INCHES)	ℓ_4 (INCHES)	P_1 (lbs x 10^{-3})	P_2 (lbs x 10^{-3})	P_3 (lbs x 10^{-3})	P_4 (lbs x 10^{-3})	BUCKLING RESTRAINT
39	-	0.53	1.12	1.20	1.37	105.0	108.0	108.0	108.0	No
40	-	1.67	2.61	2.71	2.71	63.7	77.7	77.7	77.7	
41	-	3.57	4.63	4.65	4.65	46.4	62.0	62.0	62.0	
42	-	5.0	5.92	6.21	6.55	38.8	55.0	55.0	55.0	
43*	-	7.21	8.65	-	-	27.5	42.5	-	-	
44	-	10.80	12.66	13.25	18.65	27.2	29.6	29.6	28.4	
45	-	3.67	4.80	5.55	6.71	52.0	75.0	75.0	75.0	Yes
46	-	7.13	8.49	9.41	10.71	37.5	50.0	50.0	50.0	
47	-	5.73	7.25	7.34	8.09	41.5	54.5	54.5	54.5	
48	-	10.86	11.85	13.10	14.40	33.2	34.5	34.0	34.0	

* Incrementally loaded.

TABLE 8
2024-T3 ALUMINUM
WIDTH = 12 INCHES, THICKNESS = .063 INCH
(EXCEPT WHERE NOTED)

PANEL NUMBER	SHEET NUMBER	ℓ_1 (INCHES)	ℓ_2 (INCHES)	ℓ_3 (INCHES)	ℓ_4 (INCHES)	P_1 (lbs x 10^{-3})	P_2 (lbs x 10^{-3})	P_3 (lbs x 10^{-3})	P_4 (lbs x 10^{-3})	BUCKLING RESTRAINT
49	S-12	0.59	0.69	1.06	1.61	30.0	32.8	32.6	32.4	No
50	S-13	0.92	1.18	1.49	1.72	28.8	32.6	32.5	32.2	
51	S-5	0.97	1.60	1.05	2.11	32.0	33.5	33.0	33.5	
52	S-4	1.33	1.52	1.80	2.10	30.4	30.7	30.7	30.4	
53	S-13	1.68	2.23	2.10	2.51	21.8	28.8	28.8	28.8	
54*	-	3.90	4.40	4.76	4.81	19.2	23.6	23.6	23.6	
55**	-	4.44	4.76	5.10	7.30	7.0	7.7	7.7	6.7	
56	S-2	4.79	5.05	5.57	7.45	14.8	15.0	14.6	14.2	
57	S-13	3.08	3.58	3.81	3.96	17.6	25.1	25.0	25.0	Yes
58	S-13	4.72	4.99	5.42	6.14	18.4	20.9	20.4	20.4	

* Thickness = .081 INCHES

** Thickness = .032 INCHES

TABLE 9
2024-T3 ALUMINUM
WIDTH = 12 INCHES, THICKNESS = .032 INCH

PANEL NUMBER	SHEET NUMBER	ℓ_1 (INCHES)	ℓ_2 (INCHES)	ℓ_3 (INCHES)	ℓ_4 (INCHES)	P_1 (lbs x 10^{-3})	P_2 (lbs x 10^{-3})	P_3 (lbs x 10^{-3})	P_4 (lbs x 10^{-3})	BUCKLING RESTRAINT
A-1	-	4.10	4.54	5.20	7.20	6.8	9.0	9.0	8.8	No
A-2	-	3.14	3.66	3.85	6.34	8.2	9.8	9.8	9.5	↓
A-3	-	1.68	2.18	2.20	3.97	8.2	14.8	14.8	14.7	↓
A-4	-	0.83	2.20	2.26	2.68	16.0	17.5	17.5	17.3	↓

TABLE 10
2024-T3 ALUMINUM
WIDTH = 9 INCHES, THICKNESS = .063 INCH

PANEL NUMBER	SHEET NUMBER	l_1 (INCHES)	l_2 (INCHES)	l_3 (INCHES)	l_4 (INCHES)	F_1 (lbs $\times 10^{-3}$)	F_2 (lbs $\times 10^{-3}$)	F_3 (lbs $\times 10^{-3}$)	F_4 (lbs $\times 10^{-3}$)	BUCKLING RESTRAINT
59	8-13	0.63	0.83	1.04	1.34	24.0	24.5	24.3	24.3	No
60	8-13	1.02	1.26	1.40	1.40	21.2	22.0	22.3	22.3	
61	8-13	1.57	2.50	2.74	2.80	17.6	20.7	20.7	20.7	
62	8-13	2.95	3.28	3.55	3.68	12.8	14.8	14.8	14.8	
63	8-13	2.26	2.46	2.76	2.76	13.8	19.0	18.8	18.8	Yes
64	8-13	2.89	3.16	3.37	3.67	16.2	17.6	17.5	17.3	

TABLE 11

12 INCH WIDE TITANIUM 8Al-1Mo-1V

PANEL NUMBER	THICKNESS (INCHES)	ℓ_1 (INCHES)	ℓ_2 (INCHES)	ℓ_3 (INCHES)	ℓ_4 (INCHES)	P_1 (lbs $\times 10^{-3}$)	P_2 (lbs $\times 10^{-3}$)	P_3 (lbs $\times 10^{-3}$)	P_4 (lbs $\times 10^{-3}$)	BUCKLING RESTRAINT
T-1	.045	2.15	3.25	3.45	3.68	24.0	36.0	36.0	36.0	No
T-2	.045	0.91	-	1.70	1.95	34.4	55.4	56.4	50.4	
T-3	.045	0.64	1.00	1.30	1.50	42.0	55.0	55.0	55.0	
T-8	.045	4.18	4.89	5.15	5.64	14.2	21.7	21.7	21.7	No
T-4	.020	2.02	2.26	2.36	2.48	10.0	11.7	11.7	11.7	Yes
T-5	.020	0.95	1.24	1.24	1.24	18.0	20.4	20.4	20.4	
T-6	.020	0.58	0.63	0.70	0.75	22.8	36.5	26.5	26.7	
T-7	.020	2.12	2.80	2.80	3.00	10.2	13.4	13.4	13.4	Yes

TABLE 12

9 INCH WIDE TITANIUM 8AL-1Mo-1V

PANEL NUMBER	THICKNESS NUMBER	ℓ_1 (INCHES)	ℓ_2 (INCHES)	ℓ_3 (INCHES)	ℓ_4 (INCHES)	P_1 (lbs x 10^{-3})	P_2 (lbs x 10^{-3})	P_3 (lbs x 10^{-3})	P_4 (lbs x 10^{-3})	BUCKLING RESTRAINT
T-9	.045	2.20	2.48	2.60	2.83	17.0	25.0	25.0	25.0	No
T-10	.045	0.90	1.21	1.40	1.55	26.0	37.7	37.7	37.7	↓
T-11	.045	0.60	0.88	1.14	1.15	33.2	40.0	40.0	40.0	↓
T-16	.045	2.10	2.88	2.97	3.21	18.6	26.8	26.8	27.0	Yes
T-12	.020	2.26	2.46	2.64	2.64	7.0	7.7	7.7	7.7	No
T-13	.020	0.91	1.05	1.19	1.36	14.0	14.1	14.1	13.7	↓
T-14	.020	0.62	0.87	0.87	0.87	16.4	17.0	17.0	17.0	↓
T-15	.020	2.11	2.59	2.63	3.20	11.2	13.2	13.2	13.0	Yes

Third, the initial slow tearing was small and was accompanied by relatively large changes in load. As a result, considerable scatter in the recorded values of the onset of tear was observed.

2. The beginning of maximum load: The stable slow crack extension was obtained during a continuous loading process of approximately 30,000 pounds-per-minute after verifying the approximate equivalence of incremental slow tear and slow tear at a load rate of 30,000 pounds-per-minute (Figures 44 and 45). At a point corresponding to the maximum load obtained by incremental loading, the load, which was initially increasing at 30,000 pounds-per-minute, was observed to hold constant even though the signal to the servo value was continually increasing. (This can be attributed to the relatively large volume of oil required to displace the 300,000 pound load cylinder and to the combined characteristics of the oil supply system and pressure sensitive servo valve.) Because of this observed characteristic of the test machine and the convenience afforded in loading and in recording subsequent unstable crack behavior, the majority of maximum load points were determined during the continuous loading process.

3. A crack velocity of one inch per second: Initially, attempts were made to separate tear at constant velocity from the latter stage of acceleration as suggested by Lorenz[2]. Curves of film frames versus crack length were plotted. As it was not possible to definitely distinguish a tear of constant velocity from tear accompanied by acceleration, an alternate definition of a slope of one inch per second was chosen. This slope occurred in all instances just at or shortly before the very rapid crack growth immediately preceding rupture.

4. The crack length at rupture: The last frame of film record at 16 frames-per-second was taken for this point. Since the crack velocity near failure is high, the scatter in crack length obtained as a result of the random relationship between exposure at 1/125 second and rupture is considerable.

Figures 46 through 55 show summaries of the first three points for all widths of 2024-T3 aluminum. Because of differences in behavior, the 20 and 30 inch wide panels are shown separately from the 9 and 12 inch wide panels.

SUPPLEMENTAL STUDIES

During the course of the main test program, questions arose regarding procedures and possible influences that required clarification. When these occurred, supplemental studies were undertaken.

A study of the dependence of maximum load and critical crack length on the rate of loading was conducted at the beginning of the test program. Prior to adopting the procedure of continuous loading at a nominal rate of 30,000 pounds per minute through the slow tear phase, an evaluation of the difference between this procedure and an incremental loading procedure was made (Figures 44 and 45). Panels 5 and 9 were loaded incrementally. The load was first raised until slow tear could be seen. After the crack length and load were recorded, the load was increased until additional tearing was seen. This process was continued until at the last small increment of load, the crack continued to extend with the load held constant. At this point, the camera was turned on

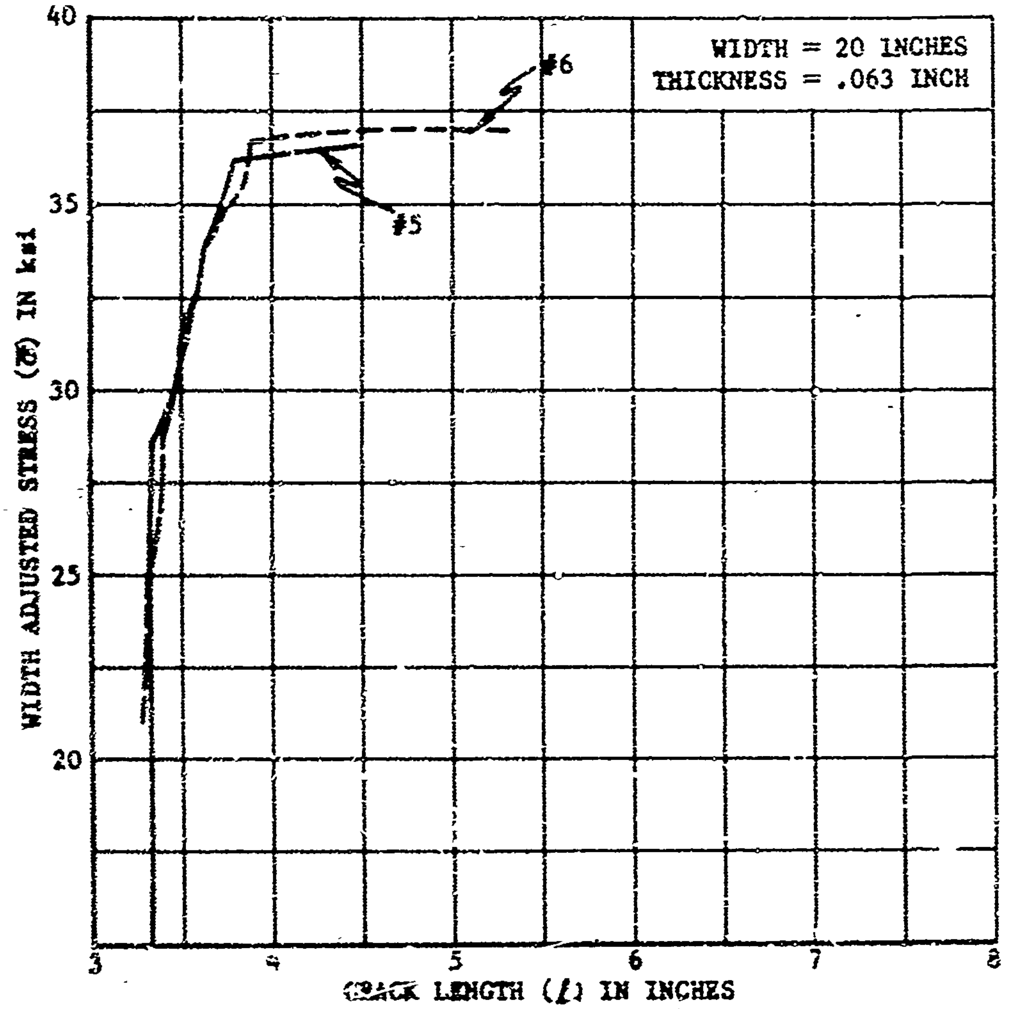

FIGURE 44 COMPARISON OF INCREMENTAL AND CONTINUOUS LOADING 2024-T3 ALUMINUM

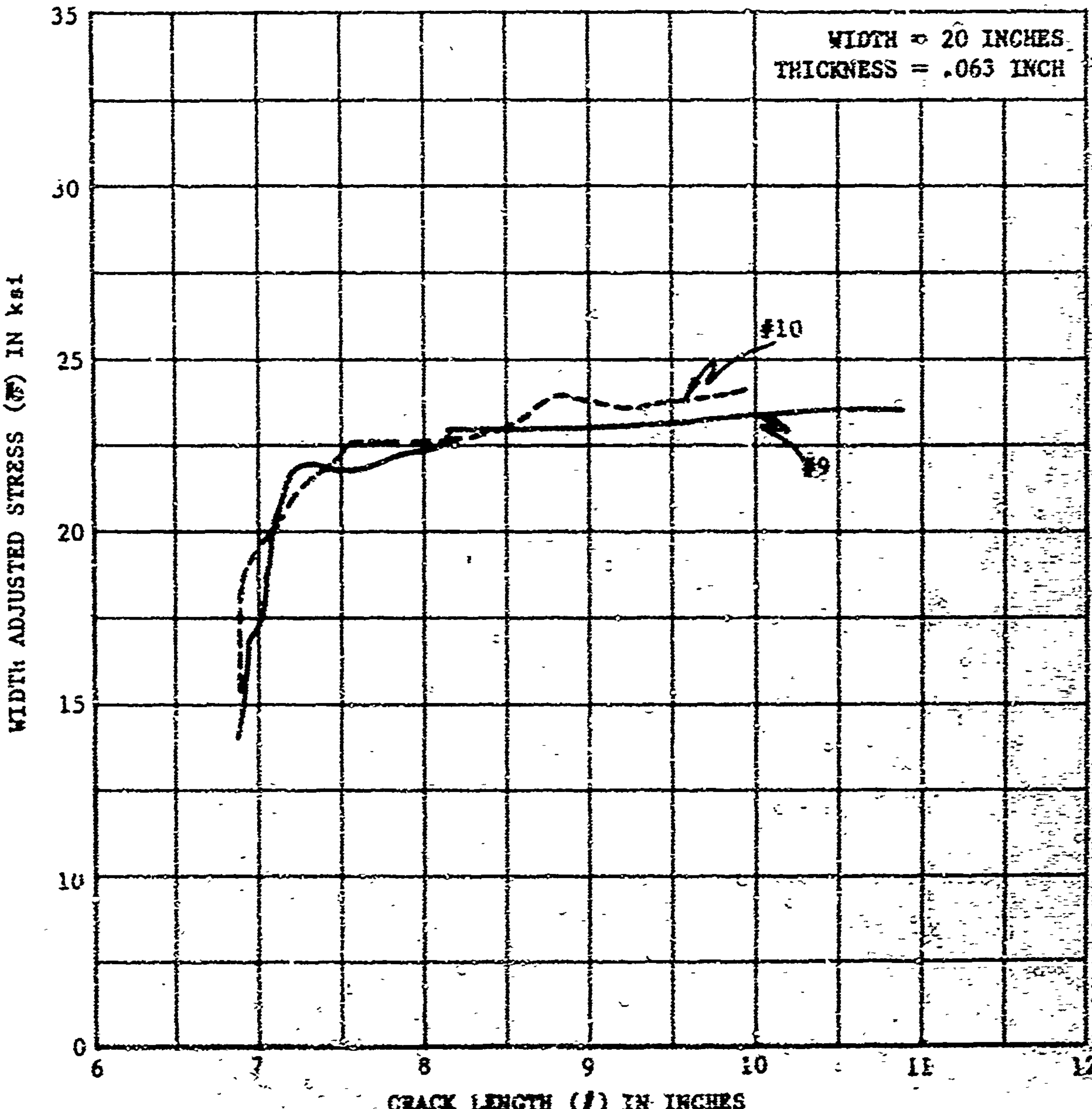

FIGURE 45 COMPARISON OF INCREMENTAL AND CONTINUOUS LOADING 2024-T3 ALUMINUM.

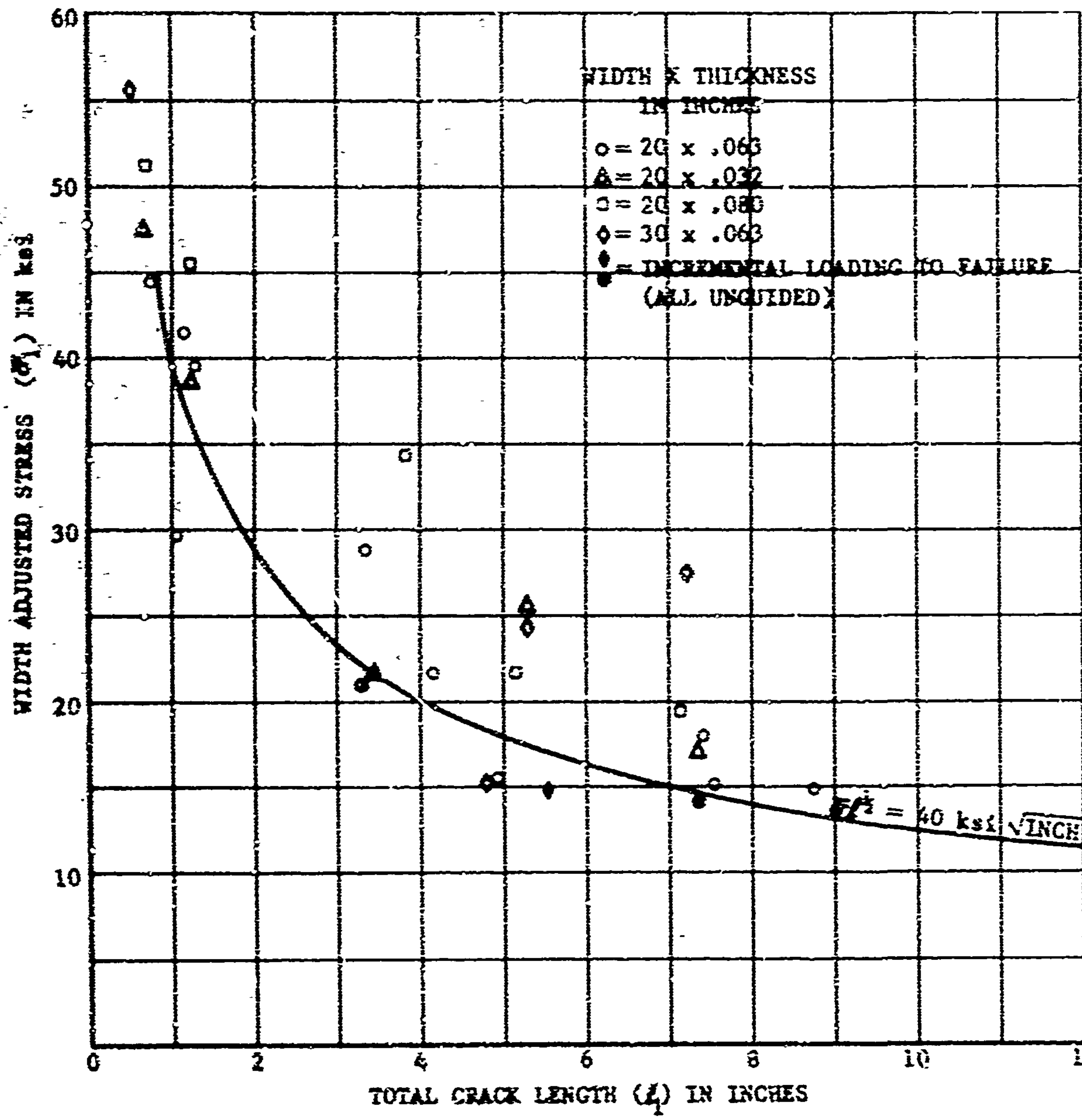

FIGURE 46 STRESS VS. CRACK LENGTH FOR START OF SLOW TEAR IN UNGUIDED PANELS 2024-T3 ALUMINUM

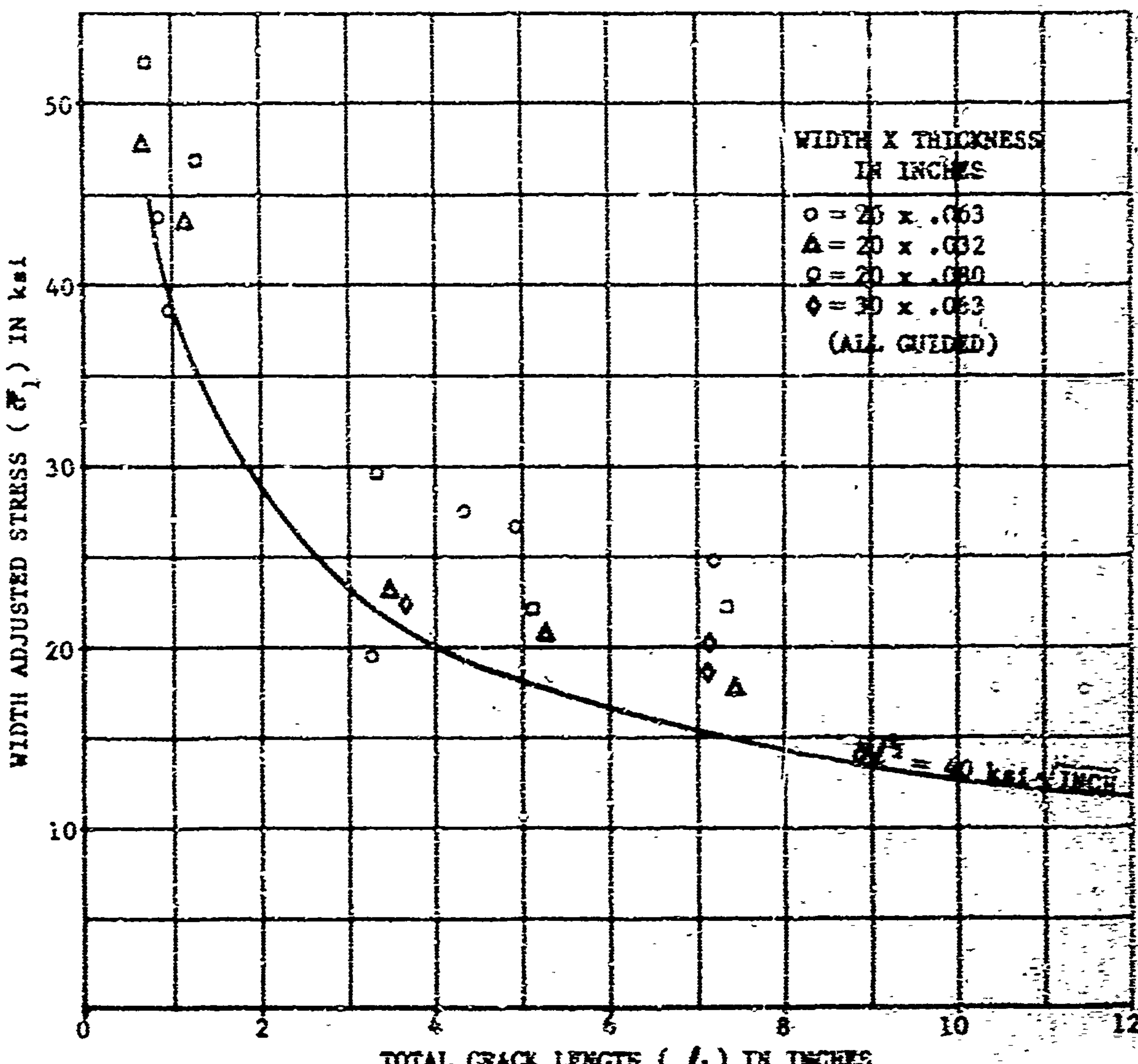

FIGURE 47 STRESS VS. CRACK LENGTH FOR START OF SLOW TEAR IN GUIDED PANELS 2024-T3 ALUMINUM

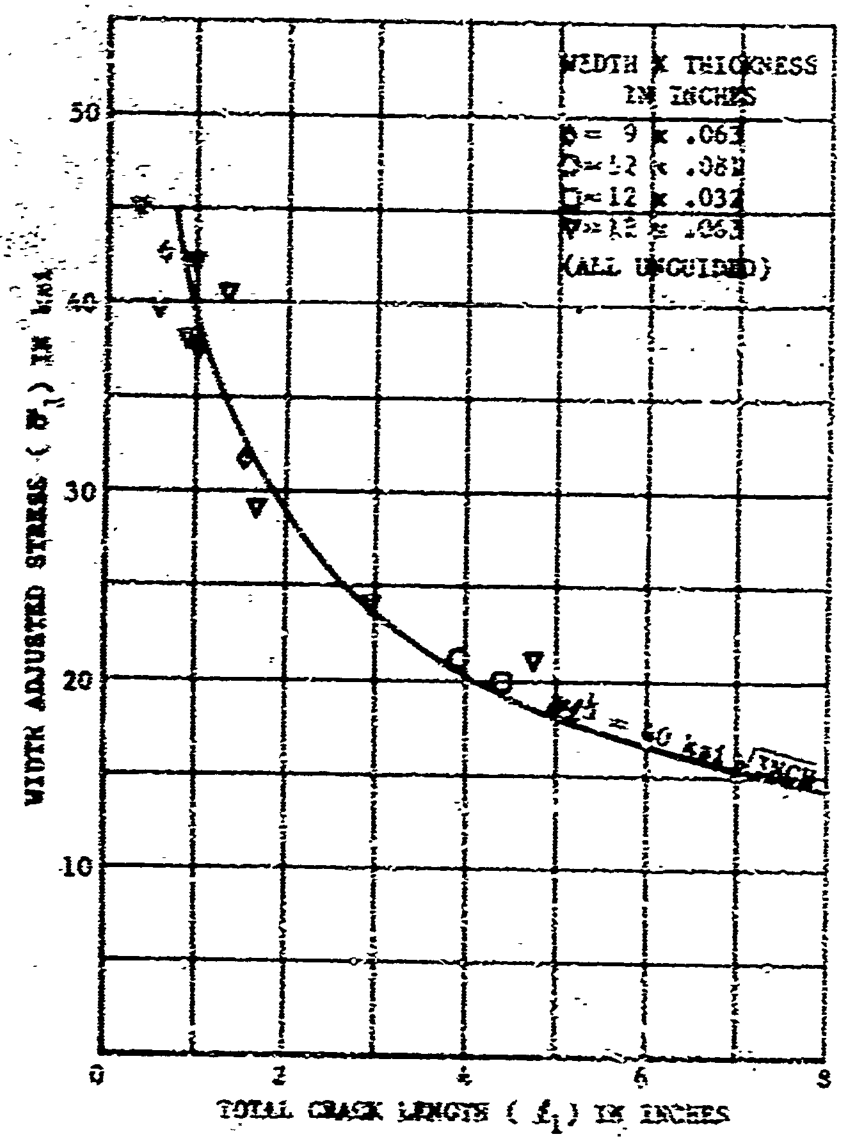

FIGURE 45 STRESS VS. CRACK LENGTH FOR START OF SLOW TEAR IN UNGUIDED PANELS 2024-T3 ALUMINUM

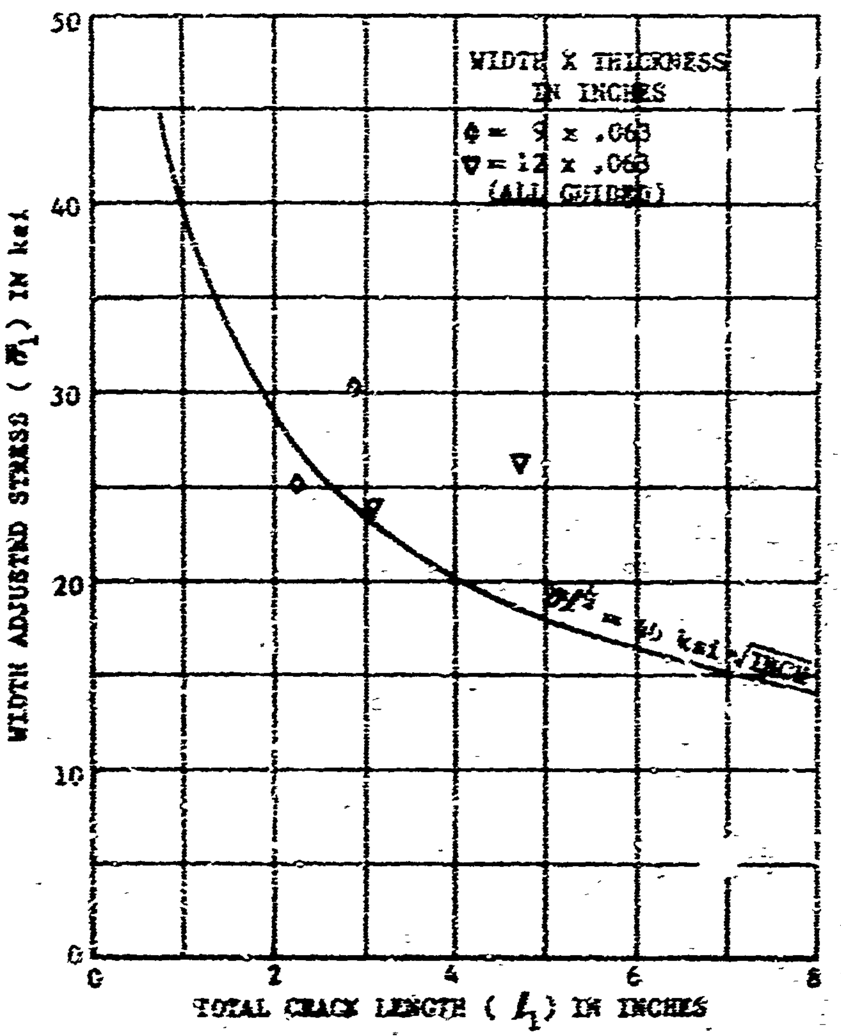

FIGURE 49 STRESS VS. CRACK LENGTH FOR START OF SLOW TEAR
IN GUIDED PANELS 2024-T3 ALUMINUM

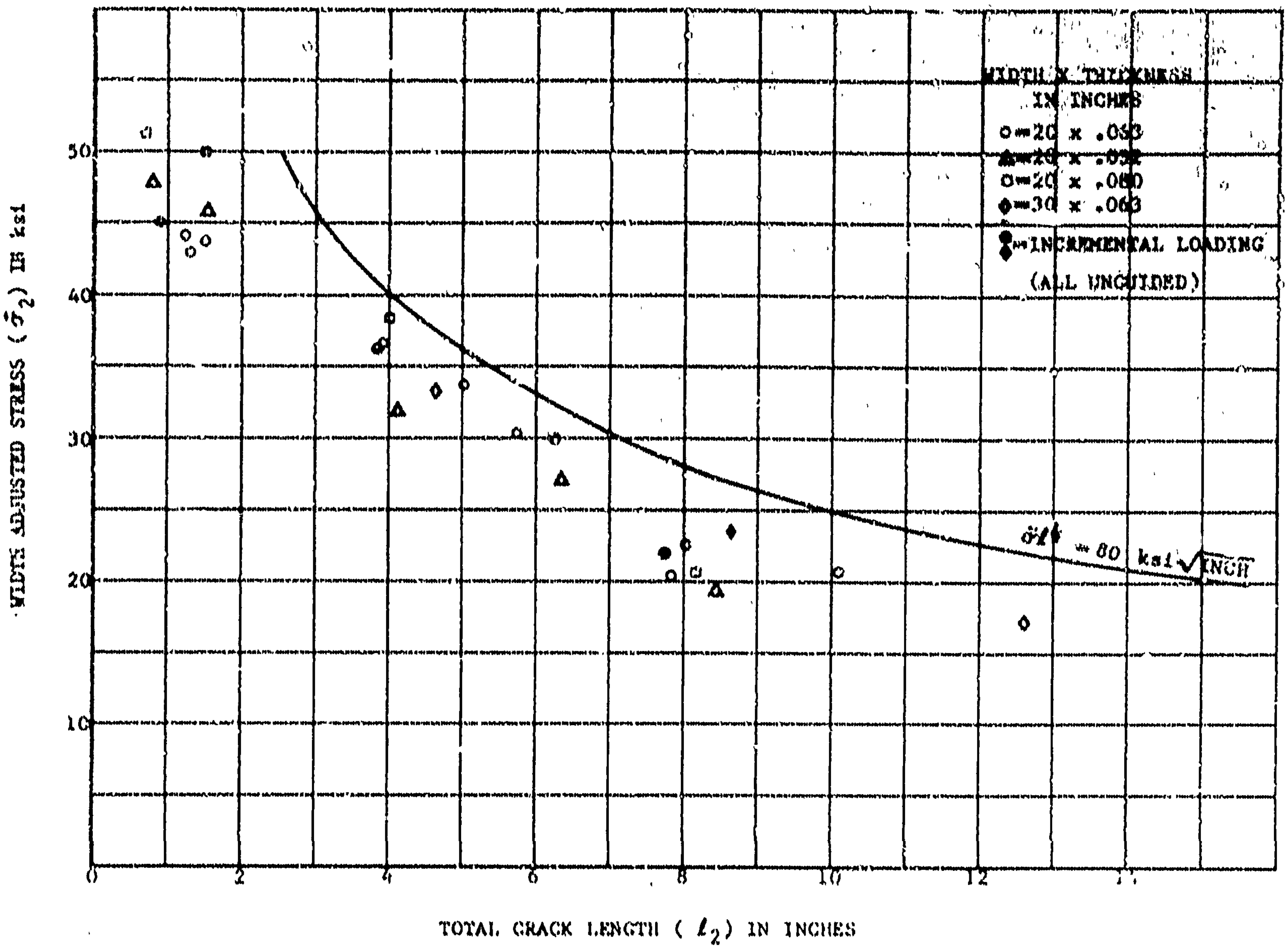

FIGURE 50 STRESS VS. CRACK LENGTH FOR CONSTANT LOAD IN UNGUIDED PANELS 2024-T3 ALUMINUM

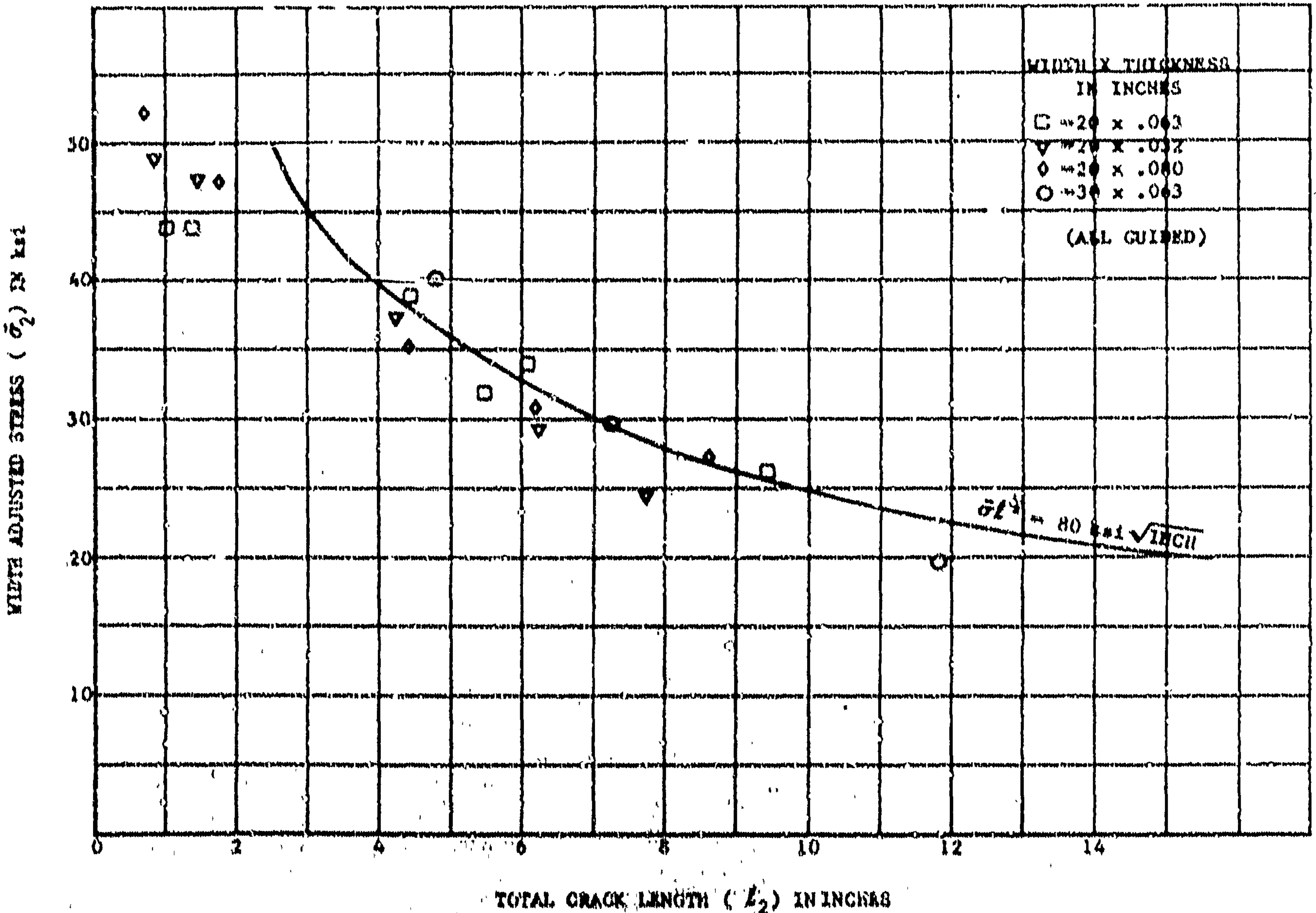

FIGURE 51 STRESS VS. CRACK LENGTH FOR CONSTANT LOAD IN GUIDED PANELS 2024-T3 ALUMINUM

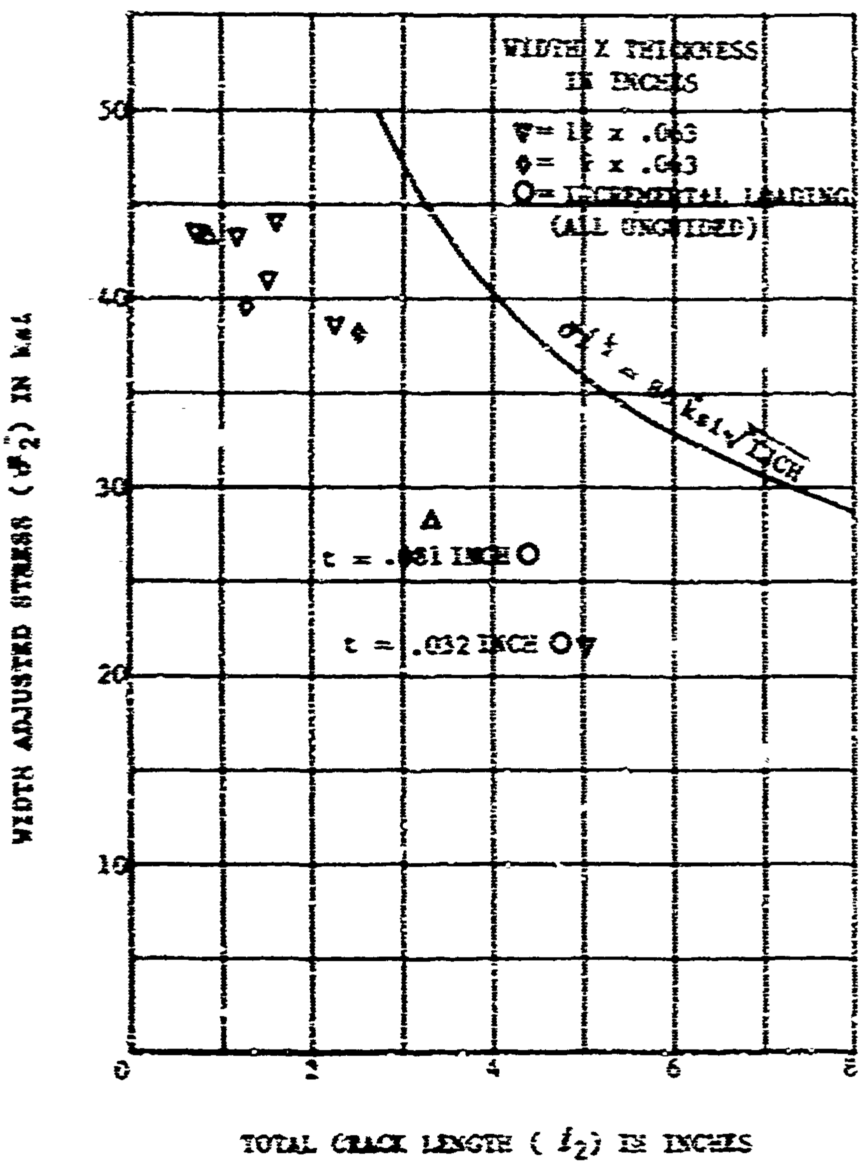

FIGURE 52 STRESS VS. CRACK LENGTH FOR CONSTANT LOAD IN UNGUIDED PANELS 2024-T3 ALUMINUM

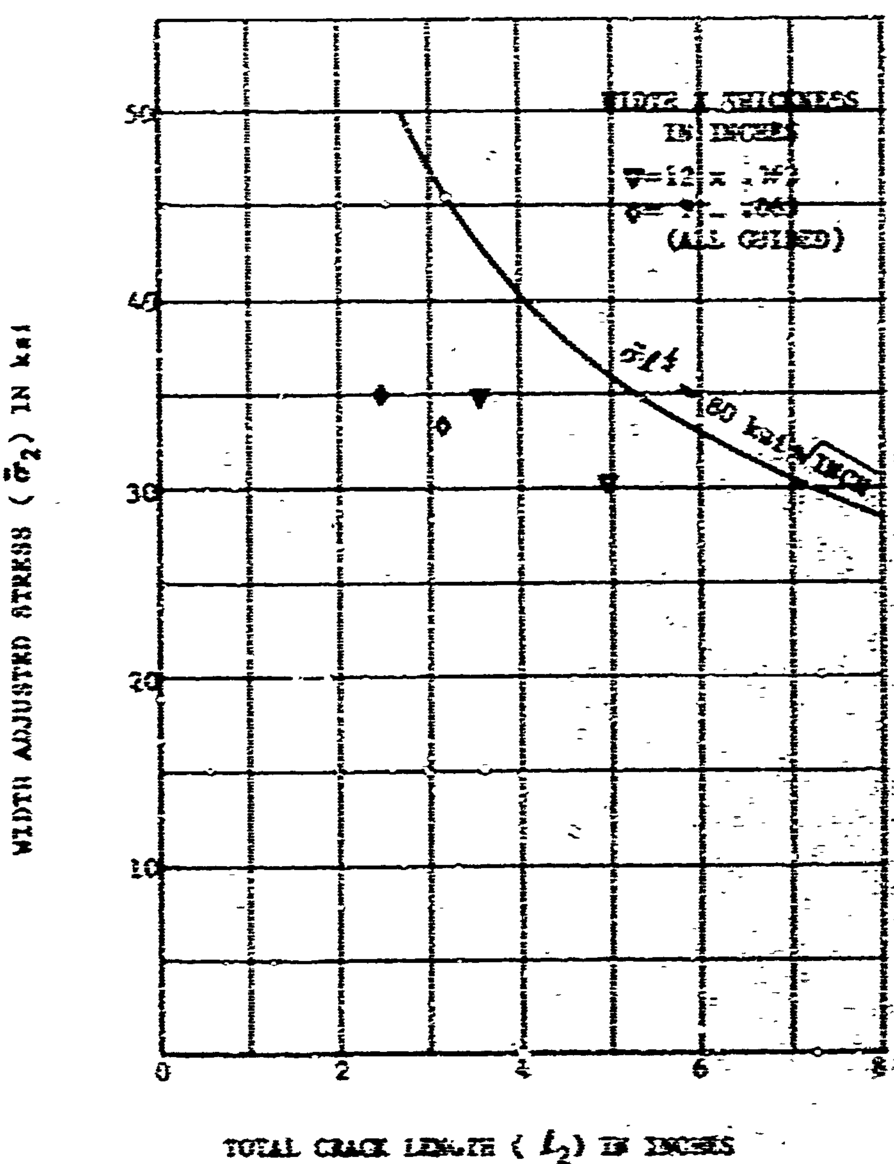

FIGURE 53 STRESS VS. CRACK LENGTH FOR CONSTANT LOAD IN GUIDED PANELS 2024-T3 ALUMINUM

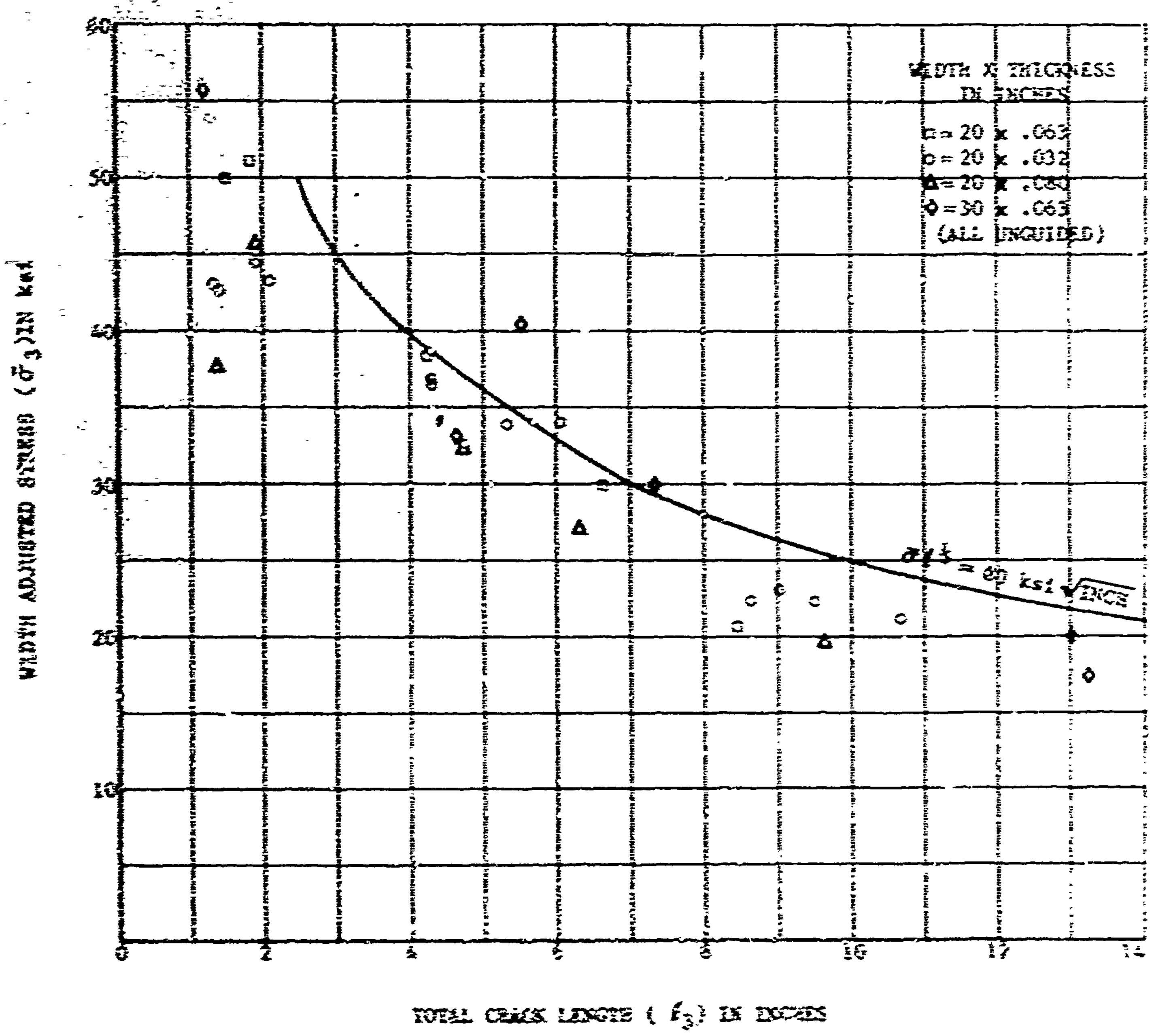

FIGURE 54 STRESS VS. CRACK LENGTH FOR CONSTANT CRACK VELOCITY OF ONE INCH PER SECOND IN UNGUIDED PANELS 2024-T3 ALUMINUM

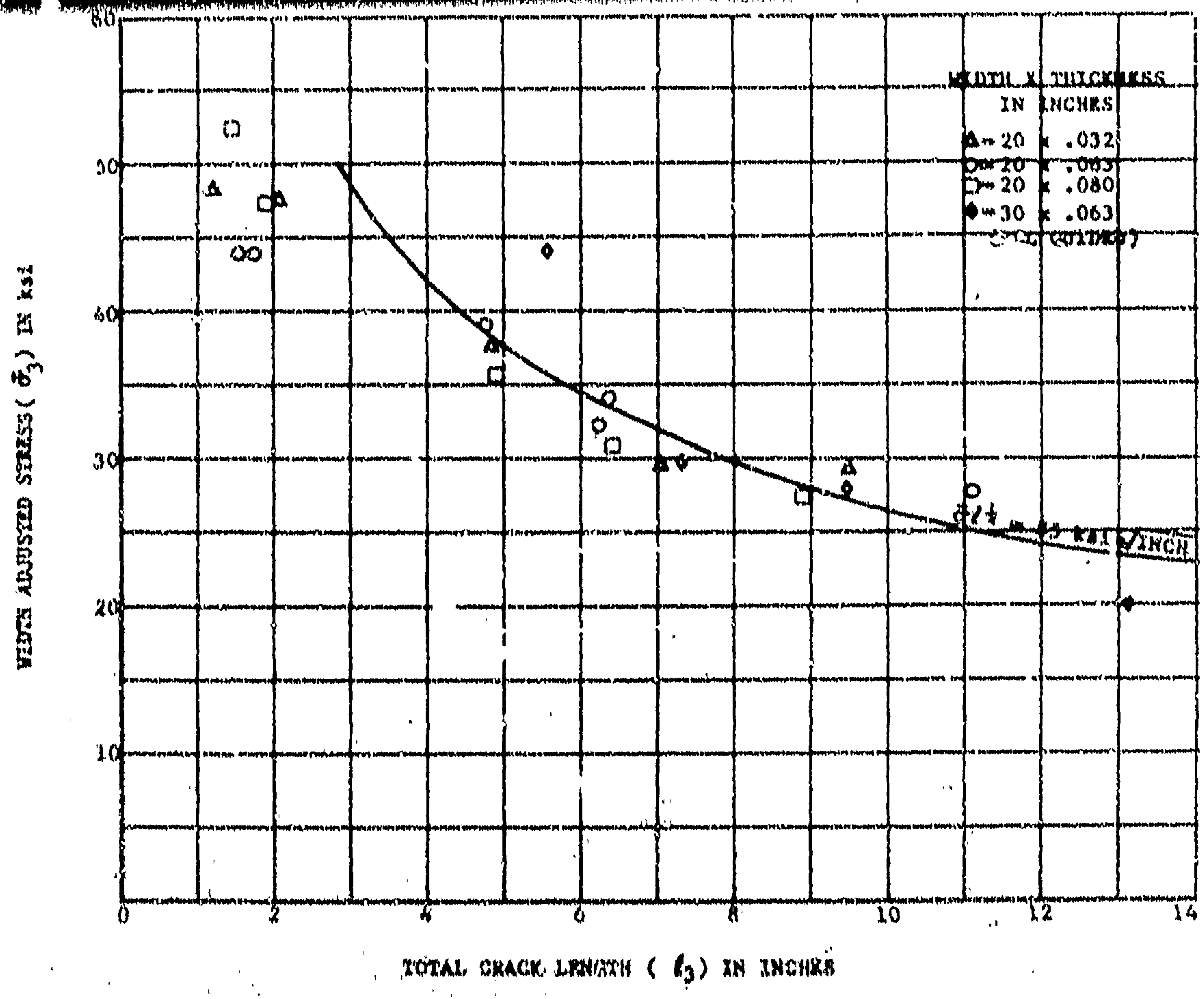

FIGURE 53 STRESS VS. CRACK LENGTH FOR CONSTANT CRACK VELOCITY OF ONE INCH PER SECOND IN GUIDED PANELS 2024-T3 ALUMINUM

and the unstable crack extension at constant load was recorded. A comparison of the results of this procedure with the results of the continuous loading procedure showed little difference (Figures 44 and 45). Because of the convenience afforded in loading and in recording subsequent unstable crack behavior, the majority of panels were loaded at 30,000 pounds-per-minute. The panels which were incrementally loaded are indicated in the data summary contained within this report.

The fact that the load reached a maximum value and held nearly constant after an unstable crack length had been attained must be attributed to the response characteristics of the load system. The fact that the recorded behavior was not sensitive to the above differences in procedure was encouraging and should indicate the general usefulness of the data obtained.

During the testing of panels with gross and net sections near the yield stress, the question of whether the point of constant load could still be associated with crack extension needed further resolution. Since the constant load point on the tear curve is actually dependent upon the response of the load system to the rate of travel of the test grips, it was reasoned that in the range of behavior where gross and net section yielding accompanied fracture, the maximum load point could possibly be reached without an accompanying change in crack extension. Figures 56 through 60 show the load-crack length-elongation versus film frames at 16/sec. for 12 inch wide panels near failure. It can be seen that tear velocity decreases with increasing crack length and in the longer crack lengths the point of peak load has only moderate significance. In the shorter cracks, good correlation between peak load and significant increase in tear rate were obtained.

Buckling studies were conducted on 12 inch, 20 inch and 30 inch wide panels of each thickness. These studies were conducted for the purpose of determining whether the beginning of significant buckling displacements could be correlated with the observed drop off in strength at longer crack lengths for unguided panels. The results of this study showed that this was not the case. Deflection of the panels started at shorter crack lengths than the observed drop in strength. A summary of buckling deflections is given in Table 19. These measurements were taken using a tool makers microscope from photographs taken parallel to the load direction and as close to the panel as possible. The results of other buckling studies are shown on Figures 19 through 23.

Figure 61 was taken an instant before the failure of panel 43 to show the extent of plastic deformation near the crack tip. The grid on the panel was applied using a silk screen process. The lack of a large visible plastic zone is of interest when considering the possible use of a plastic zone correction.

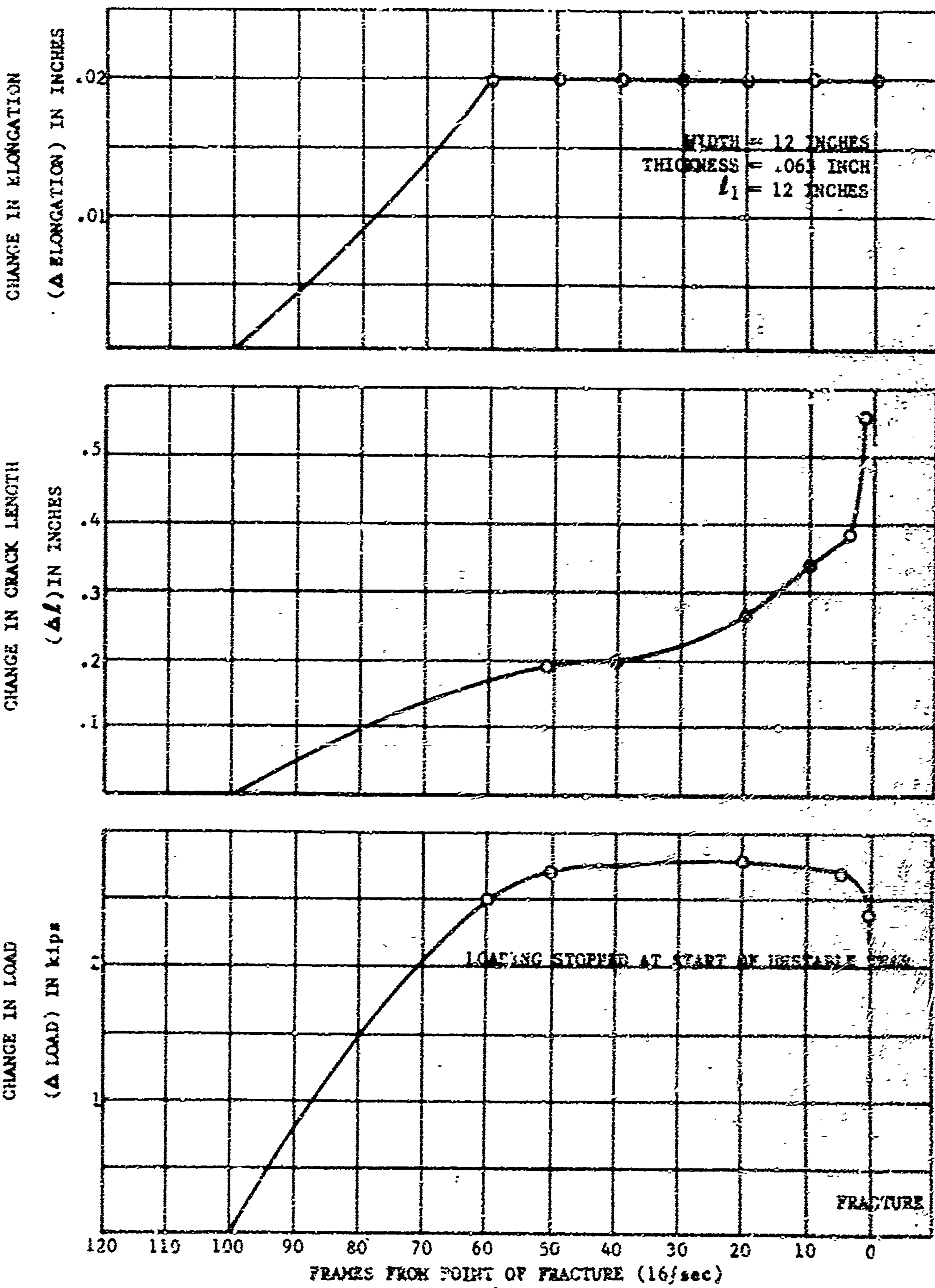

FIGURE 56 LOAD - CRACK LENGTH-ELONGATION VS. FRAMES FROM FRACTURE FOR TEST PANEL 49, UNGUIDED 2024-T3 ALUMINUM

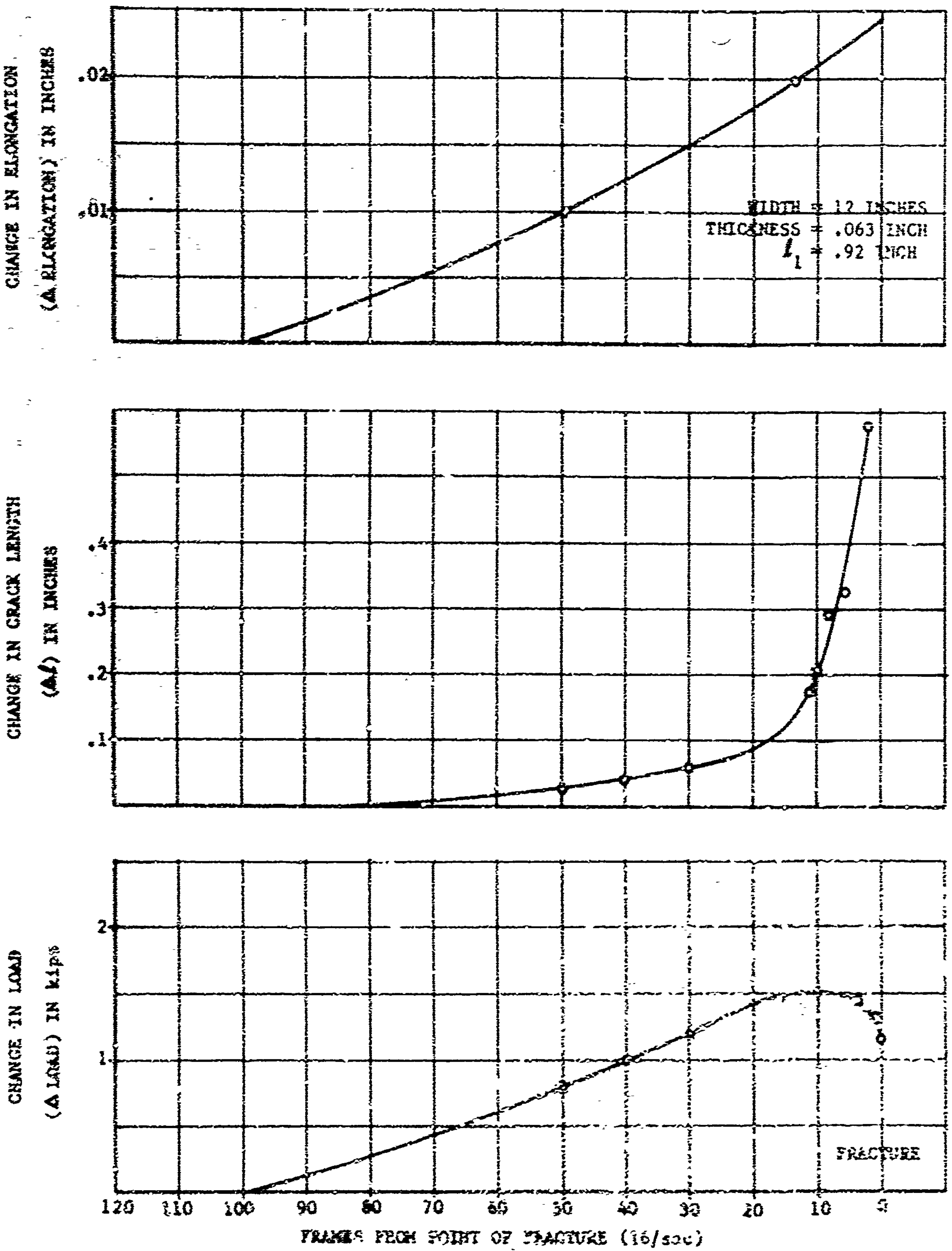

FIGURE 57 LOAD - CRACK LENGTH-ELONGATION VS. FRAMES FROM FRACTURE FOR TEST PANEL 50, UNGUIDED 2024-T3 ALUMINUM

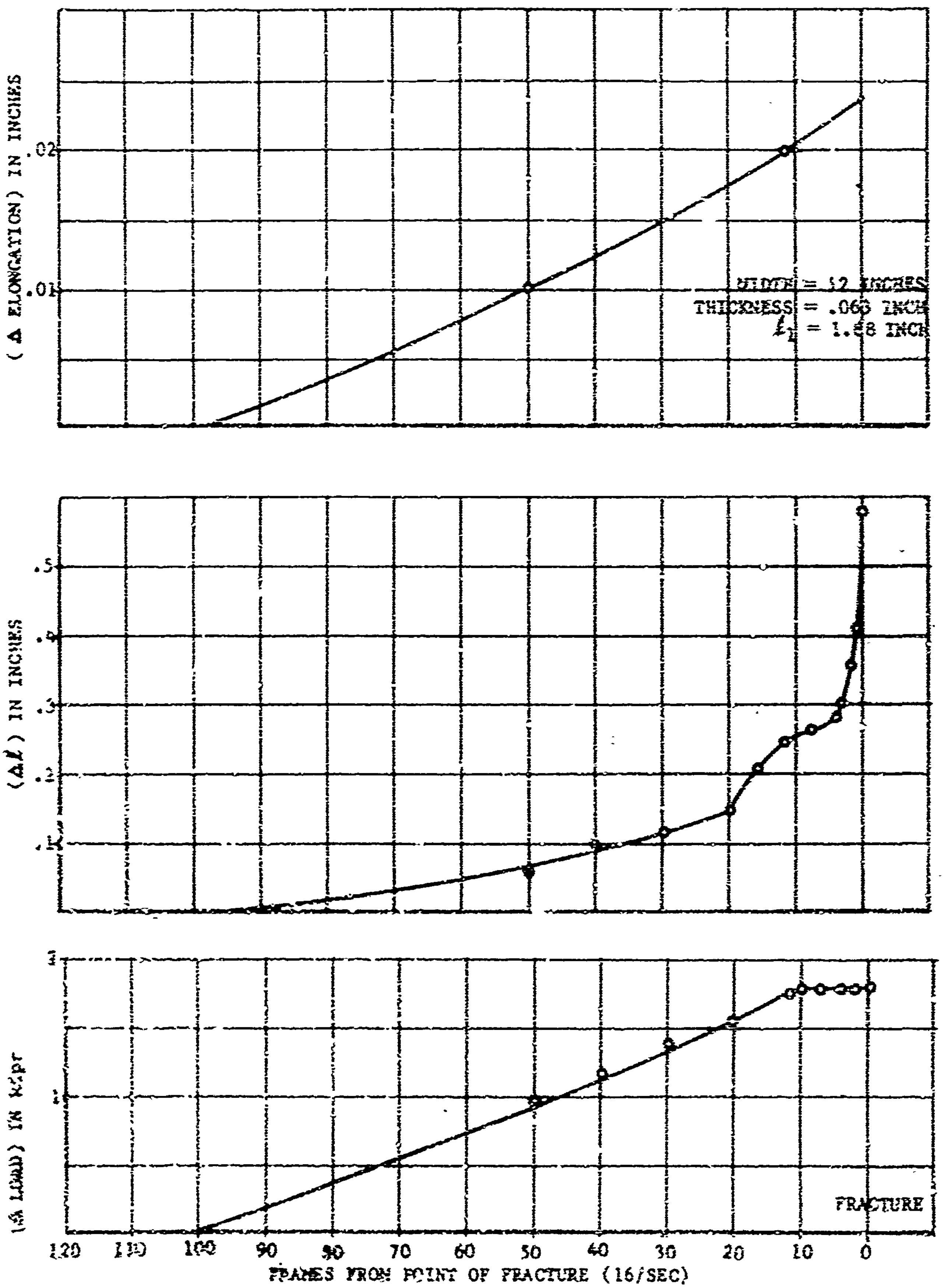

FIGURE 56 LOAD - CRACK LENGTH-ELONGATION VS. FRAMES FROM FRACTURE FOR TEST PANEL 53, UNGUIDED 2024-T3 ALUMINUM

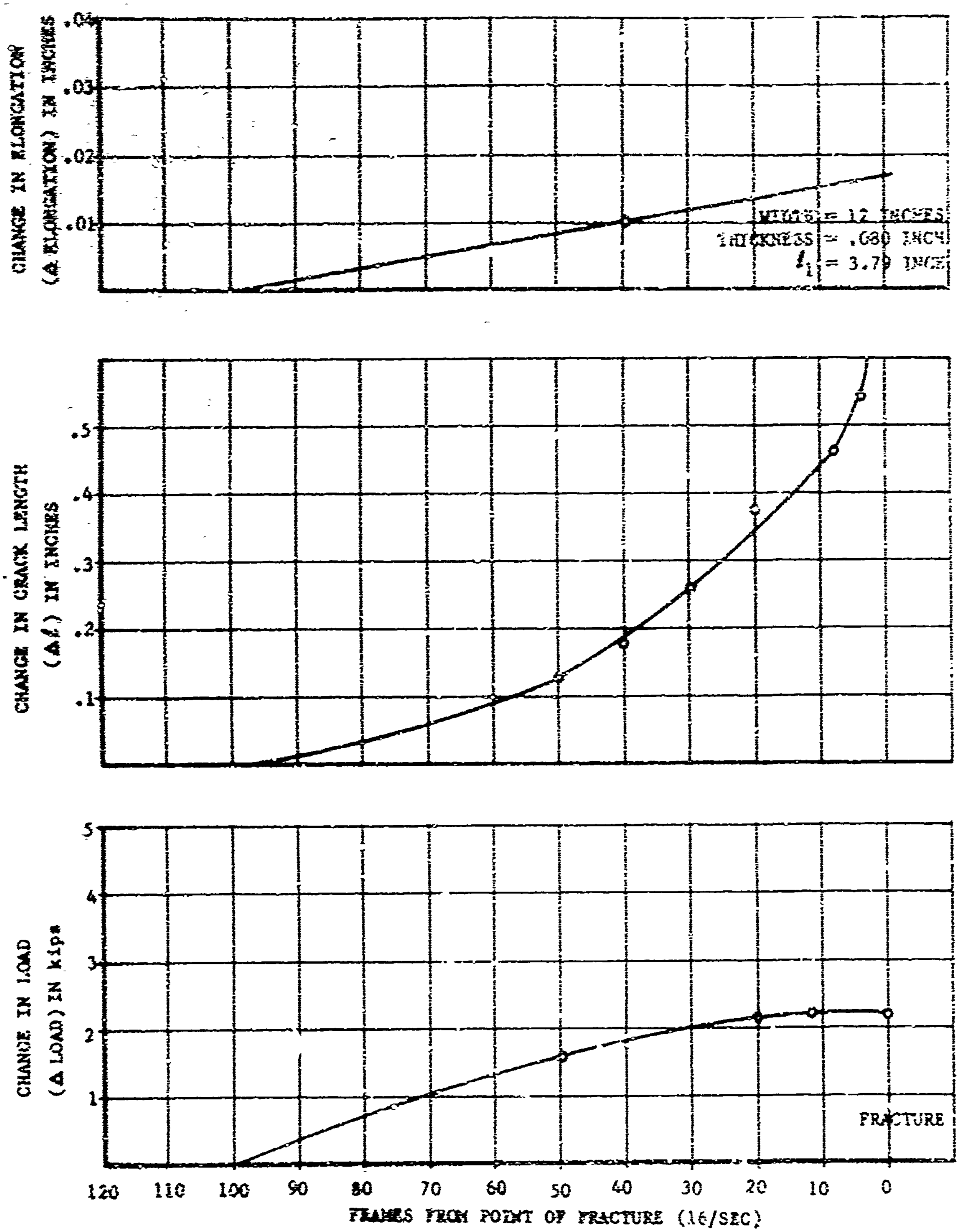

FIGURE 59 LOAD - CRACK LENGTH-ELONGATION VS. FRAMES FROM FRACTURE FOR TEST PANEL 54, UNGUIDED 2024-T3 ALUMINUM

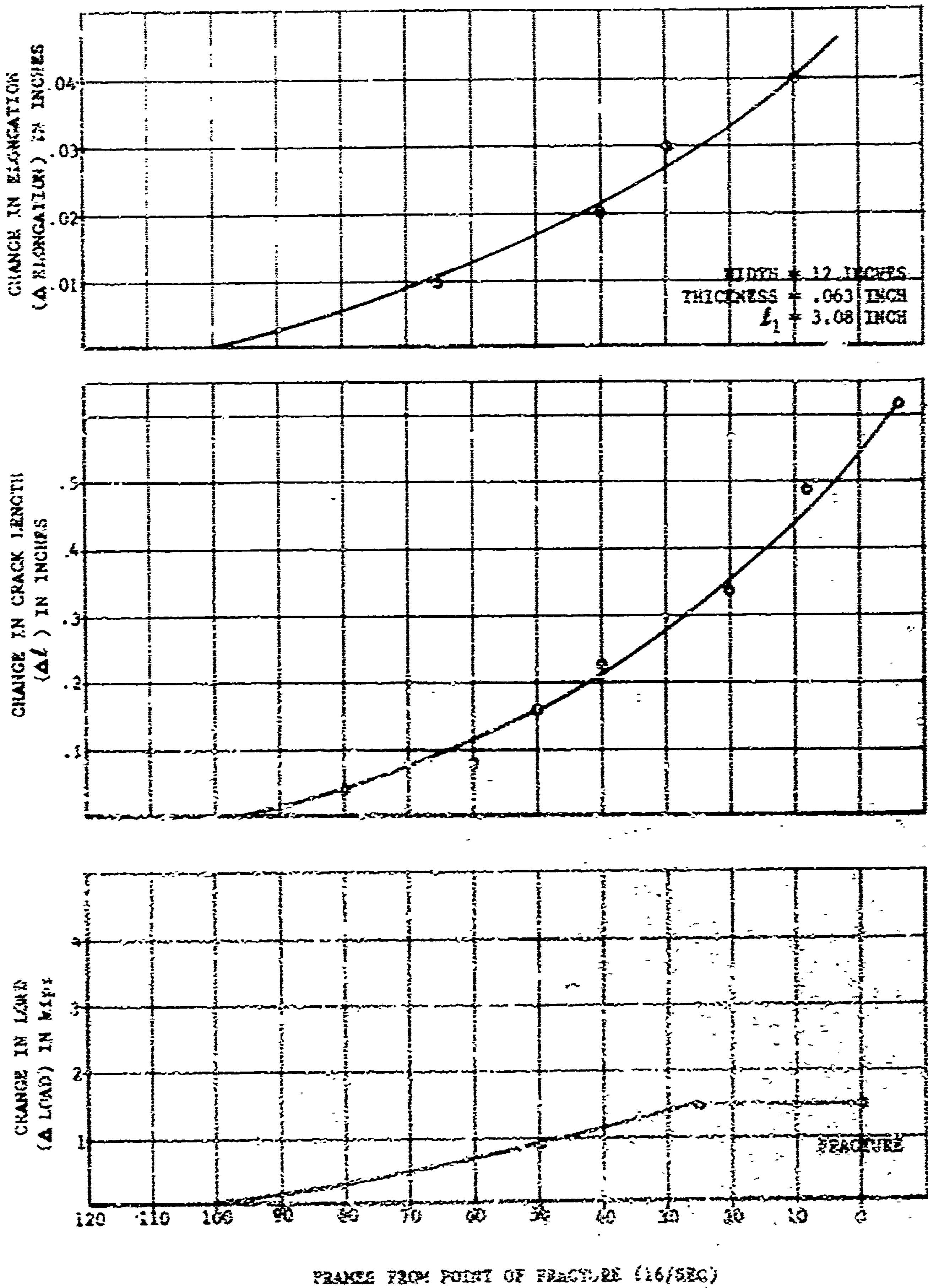

FIGURE 60 LOAD - CRACK LENGTH-ELONGATION VS. FRAMES FROM FRACTURE FOR TEST PANEL 57, GUIDED 2024-T3 ALUMINUM

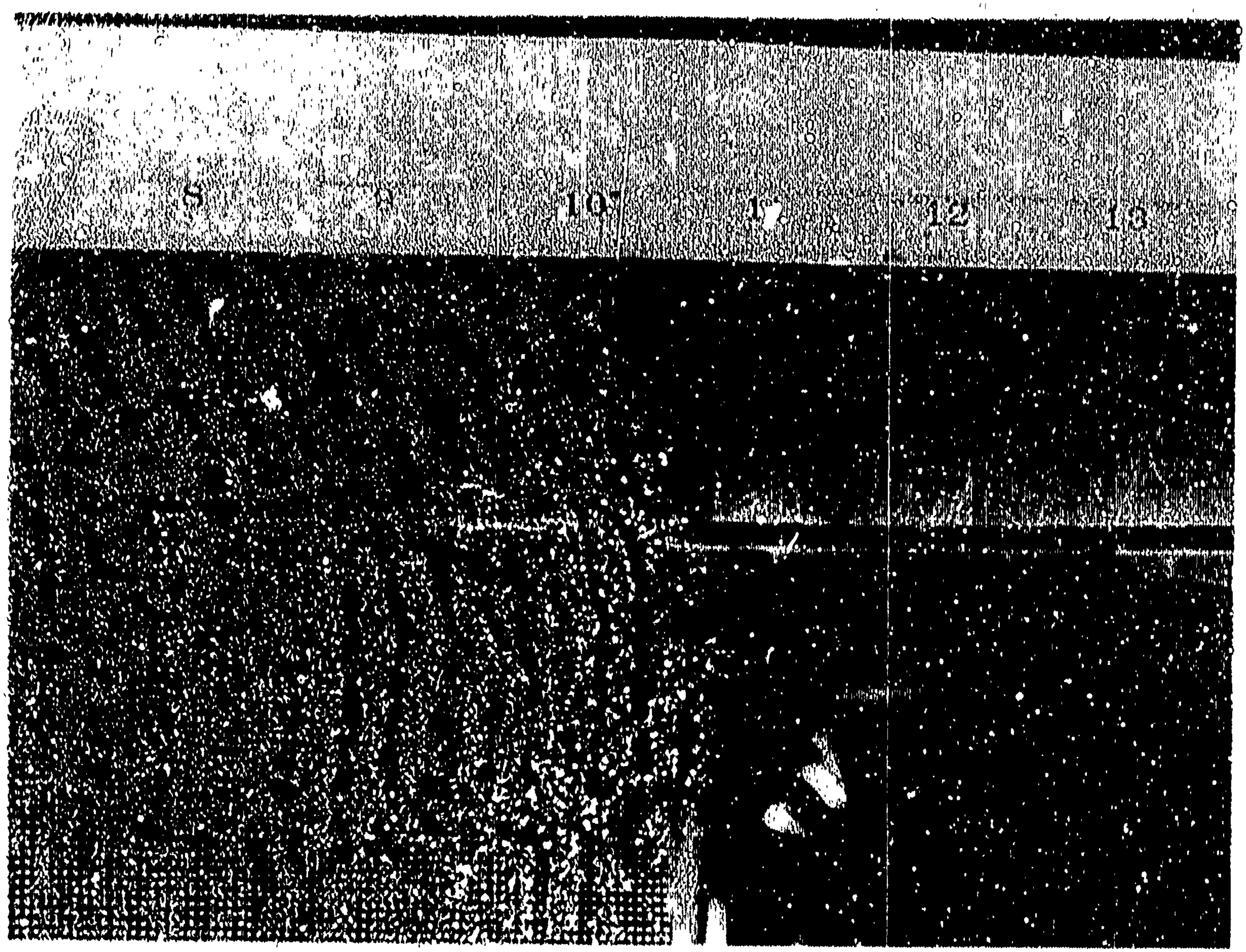

FIGURE 61 DEFORMATION NEAR CRACK TIP IN 2024-T3 ALUMINUM PANEL

TABLE 13
CALCULATED DATA SUMMARY
WIDTH = 20 INCHES, THICKNESS = .032 INCH

PANEL NUMBER	$\frac{\ell_1}{w}$	$\frac{\ell_2}{w}$	$\frac{\ell_3}{w}$	$\frac{\ell_4}{w}$	σ_{o1} (ksi)	σ_{o2} (ksi)	σ_{o3} (ksi)	σ_{o4} (ksi)	$\bar{\sigma}_1$ (ksi)	$\bar{\sigma}_2$ (ksi)	$\bar{\sigma}_3$ (ksi)	$\bar{\sigma}_4$ (ksi)	σ_{n1} (ksi)	σ_{n2} (ksi)	σ_{n3} (ksi)	σ_{n4} (ksi)
19	.032	.039	.069	.069	47.4	47.6	47.4	47.4	47.5	47.8	47.6	47.6	48.9	49.6	51.0	51.0
20	.062	.077	.095	.095	38.5	45.6	45.4	45.4	38.7	45.8	45.7	45.7	41.1	49.5	50.4	50.4
21	.172	.205	.236	.272	21.4	31.3	31.3	30.2	21.7	31.9	32.2	31.4	25.8	39.4	40.9	41.7
22	.262	.319	.318	.393	24.6	25.6	25.6	25.3	25.6	27.0	27.0	27.4	33.2	37.8	37.8	41.9
23	.405	.423	.483	.610	15.7	17.7	17.2	15.7	17.1	19.4	19.7	20.0	26.4	30.8	33.4	40.3
24	.032	.043	.060	.072	47.7	48.5	48.0	48.0	47.8	48.7	48.2	48.2	48.0	50.5	51.4	51.6
25	.056	.071	.103	.378	43.2	47.0	46.9	46.9	43.3	47.2	47.4	50.5	45.3	50.5	52.1	75.0
26	.172	.210	.243	.316	22.8	36.4	36.4	35.5	23.1	37.2	37.6	37.4	27.6	46.6	48.8	52.0
27	.263	.314	.353	.539	20.0	27.7	27.7	26.6	20.8	29.2	29.6	31.3	27.3	40.6	43.0	56.6
28	.373	.387	.475	.610	16.3	22.4	22.4	20.3	17.6	24.3	29.4	25.8	26.1	36.8	43.0	52.1

TABLE 14
CALCULATED DATA SUMMARY
WIDTH = 20 INCHES, THICKNESS = .063 INCH

PANEL NUMBER	$\frac{l_1}{w}$	$\frac{l_2}{w}$	$\frac{l_3}{w}$	$\frac{l_4}{w}$	σ_{o1} (ksi)	σ_{o2} (ksi)	σ_{o3} (ksi)	σ_{o4} (ksi)	$\bar{\sigma}_1$ (ksi)	$\bar{\sigma}_2$ (ksi)	$\bar{\sigma}_3$ (ksi)	$\bar{\sigma}_4$ (ksi)	σ_{n1} (ksi)	σ_{n2} (ksi)	σ_{n3} (ksi)	σ_{n4} (ksi)
1	.037	.045	.071	.098	44.4	44.9	44.9	44.9	44.5	45.1	45.3	45.4	46.2	47.2	48.3	49.9
2	.053	.062	.095	.108	29.7	44.0	44.0	44.0	29.8	44.3	44.4	44.5	31.2	46.5	47.5	49.6
3	.064	.078	.105	.133	39.6	43.6	42.8	42.8	39.7	43.8	43.2	43.3	42.4	47.5	48.0	49.6
4	.064	.066	.068	.068	41.2	42.8	42.8	42.8	41.4	43.0	43.1	43.1	44.1	45.9	46.2	46.2
5	.165	.190	.216	.222	20.8	35.6	35.6	35.6	21.0	36.2	36.5	36.7	25.0	43.9	45.4	45.8
6	.167	.196	.216	.241	28.5	36.0	36.0	36.0	28.8	36.7	36.9	37.1	34.2	44.7	45.7	47.4
7	.209	.251	.267	.279	21.2	32.5	32.5	32.5	21.7	33.8	33.9	34.1	26.9	43.5	44.5	45.4
8	.247	.287	.304	.409	15.1	28.9	28.9	28.9	15.6	30.3	30.4	31.6	20.0	40.5	41.8	49.2
9	.370	.389	.432	.590	13.2	20.3	20.3	19.3	14.1	21.9	22.3	23.6	21.0	33.3	35.6	47.1
10	.370	402	.453	.524	16.8	20.7	20.7	20.7	18.1	22.6	23.1	24.2	26.8	34.5	37.6	43.5
11	.379	.392	.477	.555	14.1	19.7	19.7	19.7	15.2	21.3	22.3	23.7	22.9	32.5	37.5	46.1
12	.440	.507	.535	.643	13.5	17.9	17.9	17.4	15.0	20.7	21.2	24.0	24.1	[illegible]	38.5	49.6
13	.043	.051	.079	.110	43.7	43.7	43.7	43.7	43.8	43.8	43.9	44.0	45.9	46.0	47.5	48.9
14	048	.069	.089	.130	38.5	43.7	43.7	43.7	38.6	43.8	43.9	44.1	40.6	47.0	48.0	50.2
15	.164	.221	.239	.252	19.2	37.7	37.7	37.7	19.4	38.8	38.9	39.0	23.0	48.2	49.6	50.1
16	.216	.277	.312	.390	26.7	30.7	30.7	30.7	27.4	31.9	32.2	33.1	34.0	42.4	46.6	50.4
17	.247	.304	.319	.345	25.7	32.3	32.3	32.3	26.6	33.9	34.1	34.4	33.9	46.5	47.9	49.4
18	.360	.472	.555	.675	23.2	23.2	23.2	22.0	24.8	26.2	27.8	31.0	36.4	42.9	52.1	67.5

TABLE 15
CALCULATED DATA SUMMARY
WIDTH = 20 INCHES, THICKNESS = .080 INCH

PANEL NUMBER	$\frac{\ell_1}{w}$	$\frac{\ell_2}{w}$	$\frac{\ell_3}{w}$	$\frac{\ell_4}{w}$	σ_{c1} (ksi)	σ_{c2} (ksi)	σ_{c3} (ksi)	σ_{c4} (ksi)	$\bar{\sigma}_1$ (ksi)	$\bar{\sigma}_2$ (ksi)	$\bar{\sigma}_3$ (ksi)	$\bar{\sigma}_4$ (ksi)	σ_{n1} (ksi)	σ_{n2} (ksi)	σ_{n3} (ksi)	σ_{n4} (ksi)
29	.034	.034	.091	.117	51.0	51.0	50.5	49.5	51.2	51.2	51.0	50.0	52.0	52.0	55.5	56.0
30	.060	.073	.076	.122	44.5	49.6	49.6	49.6	45.6	50.0	50.0	50.1	47.6	53.4	53.4	56.6
31	.190	.208	.212	.212	24.0	37.5	37.5	37.5	24.4	38.3	38.4	38.4	29.6	46.4	47.5	47.3
32	.258	.312	.331	.410	21.1	28.4	28.1	28.1	21.8	29.9	29.8	30.6	28.5	41.4	42.1	47.6
33	.356	.409	.424	.498	18.2	18.9	18.7	18.7	19.5	20.6	20.6	21.0	28.6	32.1	32.6	34.6
34	.032	.035	.033	.119	32.0	52.0	52.0	51.0	32.2	52.2	52.7	52.5	54.1	54.1	55.9	59.4
35	.083	.089	.095	.139	46.7	46.8	46.8	46.8	46.9	47.1	47.3	47.4	50.0	51.5	52.0	54.4
36	.169	.221	.248	.254	29.2	34.3	34.3	34.3	29.5	35.2	35.4	35.5	35.6	43.5	43.6	46.0
37	.254	.309	.322	.344	21.3	26.1	29.1	29.1	22.1	30.7	30.8	32.0	28.6	42.4	43.3	44.5
38	.367	.430	.446	.486	20.8	24.8	24.8	24.8	33.2	27.2	27.5	26.0	32.9	43.5	44.6	47.5

TABLE 16
CALCULATED DATA SUMMARY
WIDTH = 30 INCHES, THICKNESS = .063 INCH

PANEL NUMBER	$\frac{l_1}{w}$	$\frac{l_2}{w}$	$\frac{l_3}{w}$	$\frac{l_4}{w}$	σ_{o1} (ksi)	σ_{o2} (ksi)	σ_{o3} (ksi)	σ_{o4} (ksi)	$\bar{\sigma}_1$ (ksi)	$\bar{\sigma}_2$ (ksi)	$\bar{\sigma}_3$ (ksi)	$\bar{\sigma}_4$ (ksi)	σ_{n1} (ksi)	σ_{n2} (ksi)	σ_{n3} (ksi)	σ_{n4} (ksi)
30	.017	.037	.040	.046	55.7	57.3	57.3	57.3	55.7	55.8	55.8	55.9	56.9	57.4	57.6	58.0
40	.055	.087	.091	.091	33.8	41.3	41.3	41.3	33.8	41.5	41.5	41.5	35.4	44.8	45.0	45.0
41	.118	.154	.155	.155	24.5	32.8	32.8	32.8	24.6	33.2	33.2	33.2	27.6	38.7	38.7	38.7
42	.167	.197	.207	.218	20.6	29.2	29.2	29.2	20.8	29.8	30.0	30.0	24.8	[illegible]	35.8	37.4
43*	.240	.288	-	-	14.5	22.4	-	-	14.9	23.4	-	-	19.1	31.4	-	-
44	.360	.420	.441	.621	14.4	15.6	15.6	15.0	15.4	17.2	17.3	19.4	22.7	26.8	27.8	29.6
45	.122	.160	.185	.224	27.5	39.7	39.7	39.7	27.7	40.1	40.4	40.9	31.2	47.3	48.9	51.2
46	.238	.283	.318	.321	19.8	26.4	26.4	26.4	20.2	27.6	27.8	28.0	27.0	37.0	38.7	38.8
47	.191	.241	.244	.259	22.0	28.8	28.8	28.8	22.4	29.7	29.8	30.0	27.1	38.0	38.2	39.6
48	.361	.395	.436	.480	17.5	18.0	18.0	18.0	18.7	19.6	20.0	20.6	27.4	29.8	31.9	34.6

* Incremental loading to failure.

TABLE 17
CALCULATED DATA SUMMARY
WIDTH = 12 INCHES, THICKNESS = .063 INCH
(UNLESS NOTED)

PANEL NUMBER	$\frac{\ell_1}{w}$	$\frac{\ell_2}{w}$	$\frac{\ell_3}{w}$	$\frac{\ell_4}{w}$	σ_{o1} (ksi)	σ_{o2} (ksi)	σ_{o3} (ksi)	σ_{o4} (ksi)	$\overline{\sigma}_1$ (ksi)	$\overline{\sigma}_2$ (ksi)	$\overline{\sigma}_3$ (ksi)	$\overline{\sigma}_4$ (ksi)	σ_{n1} (ksi)	σ_{n2} (ksi)	σ_{n3} (ksi)	σ_{n4} (ksi)
49	.049	.056	.116	.131	39.7	43.4	43.0	42.7	39.8	43.6	43.4	43.1	41.6	45.9	48.6	49.2
50	.076	.097	.122	.140	38.2	43.0	42.9	42.5	38.4	43.4	43.4	43.0	41.2	47.5	48.9	49.4
51	.081	.131	.086	.172	42.4	44.2	43.6	44.2	42.5	44.1	43.9	44.5	45.8	52.0	47.6	53.0
52	.110	.124	.147	.171	40.3	40.5	40.5	40.2	40.7	40.9	40.9	40.7	44.8	46.1	47.4	48.5
53	.137	.182	.171	.205	28.9	38.0	38.0	38.0	29.2	38.6	38.4	38.8	33.3	46.4	45.6	47.9
54*	.319	.359	.390	.394	20.0	24.6	24.6	24.5	21.1	26.3	26.6	26.7	31.4	38.4	40.4	40.6
55**	.362	.390	.416	.596	18.3	20.0	20.0	20.0	19.5	21.7	22.0	23.0	28.5	32.8	34.2	75.0
56	.391	.412	.455	.609	19.0	19.8	19.3	18.8	11.2	21.6	21.6	23.8	32.2	32.5	35.3	48.2
57	.252	.292	.311	.323	23.3	33.2	33.0	33.0	23.9	34.8	34.9	35.0	30.8	47.5	48.4	48.9
58	.386	.406	.443	.501	24.4	27.4	27.0	27.0	26.3	30.2	30.1	31.1	39.7	46.4	48.6	54.0

* Thickness = .080 INCHES
** Thickness = .032 INCH

TABLE 18
CALCULATED DATA SUMMARY
WIDTH = 9 INCHES, THICKNESS = .063 INCH

PANEL NUMBER	$\frac{\ell_1}{w}$	$\frac{\ell_2}{w}$	$\frac{\ell_3}{w}$	$\frac{\ell_4}{w}$	σ_{o1} (ksi)	σ_{o2} (ksi)	σ_{o3} (ksi)	σ_{o4} (ksi)	$\bar{\sigma}_1$ (ksi)	$\bar{\sigma}_2$ (ksi)	$\bar{\sigma}_3$ (ksi)	$\bar{\sigma}_4$ (ksi)	σ_{n1} (ksi)	σ_{n2} (ksi)	σ_{n3} (ksi)	σ_{n4} (ksi)
59	.070	.092	.115	.149	42.5	43.2	42.9	42.9	42.8	43.4	43.2	43.4	47.6	47.5	48.5	50.6
60	.113	.140	.156	.156	37.4	39.4	39.3	39.3	37.8	39.8	39.7	39.7	42.2	44.9	46.4	46.4
61	.174	.277	.304	.300	31.1	36.6	36.5	36.5	31.6	38.1	38.4	38.4	37.7	50.5	52.2	52.2
62	.328	.364	.395	.410	22.6	26.1	26.1	26.1	23.9	28.1	28.3	28.4	33.6	41.0	43.1	44.4
63	.251	.373	.307	.307	24.3	33.5	33.2	33.2	25.1	36.2	35.2	35.2	32.1	53.5	48.5	48.5
64	.318	.351	.375	.408	28.6	31.0	30.9	30.5	30.2	33.2	33.4	33.2	42.1	47.9	49.5	51.5

TABLE 18
CALCULATED DATA SUMMARY
WIDTH = 9 INCHES, THICKNESS = .063 INCH

PANEL NUMBER	$\frac{\ell_1}{w}$	$\frac{\ell_2}{w}$	$\frac{\ell_3}{w}$	$\frac{\ell_4}{w}$	σ_{o1} (ksi)	σ_{o2} (ksi)	σ_{o3} (ksi)	σ_{o4} (ksi)	$\bar{\sigma}_1$ (ksi)	$\bar{\sigma}_2$ (ksi)	$\bar{\sigma}_3$ (ksi)	$\bar{\sigma}_4$ (ksi)	σ_{n1} (ksi)	σ_{n2} (ksi)	σ_{n3} (ksi)	σ_{n4} (ksi)
59	.070	.092	.115	.149	42.5	43.2	42.9	42.9	42.8	43.4	43.2	43.4	47.6	47.5	48.5	50.6
60	.113	.140	.156	.156	37.4	39.4	39.3	39.3	37.8	39.8	39.7	39.7	42.2	44.9	46.4	46.4
61	.174	.277	.304	.300	31.1	36.6	36.5	36.5	31.6	38.1	38.4	38.4	37.7	50.5	52.2	52.2
62	.328	.364	.395	.410	22.6	26.1	26.1	26.1	23.9	28.1	28.3	28.4	33.6	41.0	43.1	44.4
63	.251	.373	.307	.307	24.3	33.3	33.2	33.2	25.1	36.2	35.2	35.2	32.1	53.5	48.5	48.3
64	.318	.351	.375	.408	28.6	31.0	30.9	30.5	30.2	33.2	33.4	33.2	42.1	47.9	49.5	51.5

TABLE 19
MEASUREMENTS OF BUCKLED PANELS
2024-T3 ALUMINUM

PANEL WIDTH w (INCHES)	PANEL THICKNESS (INCHES)	CRACK LENGTH ℓ (INCHES)	BUCKLE LOAD P (kips	BUCKLE STRESS σ_c ksi)	TOTAL LENGTH OF BUCKLE PARALLEL TO CRACK (INCHES)	LENGTHS BETWEEN POINTS OF INFLECTION (INCHES)	DISPLACEMENT AT ℄ OF CRACK (INCHES)	NOTES
30	.032	3	4.25	4.69	5.5	2.0	.10	
30	.032	4	9.6	10.0	6.[illegible]	2.8	.12	
30	.032	5	8.[illegible]	9.0	7.6	3.8	.15	
30	.032	5	11.4	11.9	7.6	3.8	.20	
30	.032	5	17.1	17.8	7.5	3.8	.25	
30	.032	5	20.0	20.8	7.6	3.8	.28	
30	.032	5	24.0	25.0	8.8	4.0	.36	Start of tear 0.16 inches crack = 1/2 crack extension
30	.063	3	44.5	23.5	6.5	1.6	.07	
30	.063	4	35.2	18.6	8.5	2.6	.12	
30	.063	5	19.4	10.3	10.5	2.3	.20	Buckled section non-symmetrical
30	.063	5	38.9	20.6	11.5	3.6	.23	Start of tear
30	.080	5	26.2	10.9	10.7	-	.07	
30	.080	5	42.5	17.7	10.5	3.2	.19	
30	.080	5	50.5	21.0	10.9	3.5	.22	
30	.080	5	62.5	26.5	10.7	4.0	.28	Start of tear
20	.032	2	10.0	15.7				
20	.032	3	4.8	7.5				
20	.032	4	2.8	4.4				
20	.032	5	1.6	2.5				
20	.032	6	1.2	1.88				
20	.063	2.75	26.8	21.3				
20	.063	3	24.8	19.6				
20	.063	4	18.2	14.4				
20	.063	5	11.6	9.2				
20	.063	6	8.4	6.6				
20	.063	7	6.0	4.8				
20	.063	8	4.0	3.2				
20	.08	3	50.8	31.8				
20	.08	3.25	47.6	29.8				
20	.08	4	39.6	24.8				
20	.08	5	26.0	16.2				
20	.08	6	21.2	13.2				
20	.08	7	15.6	9.8				
20	.08	8	12.0	9.8				
12	.032	2	4	10.4				
12	.032	3	2	5.2				
12	.032	4	1	2.6				
12	.063	2	26	33.8				No buckling
12	.063	2.5	22.6	29.4				
12	.063	3	16.6	21.7				
12	.063	4	10.8	14.1				
12	.063	5	6.2	8.1				
12	.08	3.25	21.2	20.4				
12	.08	4	16	15.4				
12	.08	5	10.2	9.5				

APPENDIX REFERENCES

(1) Dixon, J. R., Stress Distribution Around Edge Slits in a Plate Loaded in Tension - The Effect of Finite Width of Plate. Journal of the Royal Aeronautical Society (T.N.), Vol. 66, No. 617, May 1962.

(2) Lorenz, P. M., Some Parameters Affecting Measured Fracture Toughness of High-Strength Steel, Transactions of ASM, Vol. [illegible], 1961.

UNCLASSIFIED
Security Classification

DOCUMENT CONTROL DATA - R&D

(Security classification of title, body of abstract and indexing annotation must be entered when the overall report is classified)

1. ORIGINATING ACTIVITY (Corporate author) Northrop Corporation, Norair Division, Hawthorne, California 90250	2a. REPORT SECURITY CLASSIFICATION: UNCLASSIFIED
	2b. GROUP
3. REPORT TITLE	A STUDY OF THE INFLUENCE OF GEOMETRY ON THE STRENGTH OF FATIGUE CRACKED PANELS
4. DESCRIPTIVE NOTES (Type of report and inclusive dates)	Final Report - June 1965 to May 1966
5. AUTHOR(S) (Last name, first name, initial)	Walker, E. K.
6. REPORT DATE: June 1966	7a. TOTAL NO. OF PAGES: 130 — 7b. NO. OF REFS: 20
8a. CONTRACT OR GRANT NO.: AF 33(615)-2522	9a. ORIGINATOR'S REPORT NUMBER(S): NOR 66-131
b. PROJECT NO.: 1467	
c.	9b. OTHER REPORT NO(S) (Any other numbers that may be assigned this report)
d.	AFFDL-TR-66-92
10. AVAILABILITY/LIMITATION NOTICES	This document is subject to special export controls and each transmittal to foreign governments or foreign nationals may be made only with prior approval of the Air Force Flight Dynamics Laboratory (FDTR), Research and Technology Division, Wright-Patterson AFB, Ohio 45433.
11. SUPPLEMENTARY NOTES	12. SPONSORING MILITARY ACTIVITY: Air Force Flight Dynamics Laboratory, Wright-Patterson Air Force Base, Ohio, FDTR

13. ABSTRACT The objectives of the study program were to define and verify a synthesis of strength-limiting parameters for fatigue cracked panels which would be applicable to the wide range of conditions of interest in the engineering problem of strength analysis and to present this synthesis in a form that would lead to a better conceptual understanding of the interaction between parameters.

The program consisted of an analytical study and a supporting experimental study. The analytical study, governed by the above objectives, considered fracture in the elastic range with buckling restraint provided, fracture combined with net section and gross section yielding, and fracture in the elastic range for unrestrained panels. The design problem involving appreciable amounts of slow tear was also considered. The experimental program provided supporting information on the behavior of fatigue cracks for bare 2024-T3 aluminum. Limited test data were also obtained for duplex annealed titanium 8Al-1Mo-1V. The aluminum alloy crack lengths ranged from .5 inch to over 10 inches. Panel widths were thirty, twenty, twelve and nine inches, and nominal panel thicknesses were .080 inch, .063 inch, and .032 inch. The titanium alloy panel widths were twelve and nine inches, and thicknesses were .045 inch and .020 inch. Buckling restraints were used for approximately half of the panels tested.

Test information from other sources was used to illustrate specific points in theory and to show the generality of conclusions.

DD FORM 1 JAN 64 1473

UNCLASSIFIED
Security Classification

14. KEY WORDS	LINK A		LINK B		LINK C	
	ROLE	WT	ROLE	WT	ROLE	WT

INSTRUCTIONS

1. ORIGINATING ACTIVITY: Enter the name and address of the contractor, subcontractor, grantee, Department of Defense activity or other organization (corporate author) issuing the report.

2a. REPORT SECURITY CLASSIFICATION: Enter the overall security classification of the report. Indicate whether "Restricted Data" is included. Marking is to be in accordance with appropriate security regulations.

2b. GROUP: Automatic downgrading is specified in DoD Directive 5200.10 and Armed Forces Industrial Manual. Enter the group number. Also, when applicable, show that optional markings have been used for Group 3 and Group 4 as authorized.

3. REPORT TITLE: Enter the complete report title in all capital letters. Titles in all cases should be unclassified. If a meaningful title cannot be selected without classification, show title classification in all capitals in parenthesis immediately following the title.

4. DESCRIPTIVE NOTES: If appropriate, enter the type of report, e.g., interim, progress, summary, annual, or final. Give the inclusive dates when a specific reporting period is covered.

5. AUTHOR(S): Enter the name(s) of author(s) as shown on or in the report. Enter last name, first name, middle initial. If military, show rank and branch of service. The name of the principal author is an absolute minimum requirement.

6. REPORT DATE: Enter the date of the report as day, month, year; or month, year. If more than one date appears on the report, use date of publication.

7a. TOTAL NUMBER OF PAGES: The total page count should follow normal pagination procedures, i.e., enter the number of pages containing information.

7b. NUMBER OF REFERENCES: Enter the total number of references cited in the report.

8a. CONTRACT OR GRANT NUMBER: If appropriate, enter the applicable number of the contract or grant under which the report was written.

8b, 8c, & 8d. PROJECT NUMBER: Enter the appropriate military department identification, such as project number, subproject number, system numbers, task number, etc.

9a. ORIGINATOR'S REPORT NUMBER(S): Enter the official report number by which the document will be identified and controlled by the originating activity. This number must be unique to this report.

9b. OTHER REPORT NUMBER(S): If the report has been assigned any other report numbers (either by the originator or by the sponsor), also enter this number(s).

10. AVAILABILITY/LIMITATION NOTICES: Enter any limitations on further dissemination of the report, other than those imposed by security classification, using standard statements such as:

(1) "Qualified requesters may obtain copies of this report from DDC."

(2) "Foreign announcement and dissemination of this report by DDC is not authorized."

(3) "U. S. Government agencies may obtain copies of this report directly from DDC. Other qualified DDC users shall request through
_______________________________."

(4) "U. S. military agencies may obtain copies of this report directly from DDC. Other qualified users shall request through
_______________________________."

(5) "All distribution of this report is controlled. Qualified DDC users shall request through
_______________________________."

If the report has been furnished to the Office of Technical Services, Department of Commerce, for sale to the public, indicate this fact and enter the price, if known.

11. SUPPLEMENTARY NOTES: Use for additional explanatory notes.

12. SPONSORING MILITARY ACTIVITY: Enter the name of the departmental project office or laboratory sponsoring (paying for) the research and development. Include address.

13. ABSTRACT: Enter an abstract giving a brief and factual summary of the document indicative of the report, even though it may also appear elsewhere in the body of the technical report. If additional space is required, a continuation sheet shall be attached.

It is highly desirable that the abstract of classified reports be unclassified. Each paragraph of the abstract shall end with an indication of the military security classification of the information in the paragraph, represented as (TS), (S), (C), or (U).

There is no limitation on the length of the abstract. However, the suggested length is from 150 to 225 words.

14. KEY WORDS: Key words are technically meaningful terms or short phrases that characterize a report and may be used as index entries for cataloging the report. Key words must be selected so that no security classification is required. Identifiers, such as equipment model designation, trade name, military project code name, geographic location, may be used as key words but will be followed by an indication of technical context. The assignment of links, rules, and weights is optional.